Cooperation of Basolateral Amino Acid Transporters in Mouse and Cell Culture Models

---

Dissertation

zur

Erlangung der naturwissenschaftlichen Doktorwürde

(Dr. sc. nat.)

vorgelegt der

Mathematisch-naturwissenschaftlichen Fakultät

der

Universität Zürich

von

Adriano Antonio Doriano Guetg

von

Savognin GR

Promotionskomitee

Prof. Dr. François Verrey (Vorsitz)

Prof. Dr. Olivier Devuyst

Prof. Dr. Bernard Thorens

Zürich, 2014

To my grandmother Elvira

Table of contents

1. Summary

Amino acids have central roles in every living organism as structural units for proteins, metabolic precursors, osmolytes and signaling molecules. In some heterotrophic organisms, such as humans and mice, some amino acids cannot be synthesized *de novo* through other metabolic pathways and need to be constantly provided from the diet. This important evolutionary constraint led to the important classification of the 20 known proteinogenic amino acids into nutritionally essential and non-essential ones.

In order to achieve all their biological functions, amino acids need to cross cell membranes and because of their chemical partial charges they cannot freely diffuse across the lipid bilayer. To overcome this hurdle, cell membranes are endowed with transmembrane carrier proteins called amino acid transporters. In (re)absorptive epithelia, cells are in a differentiated state with an apical membrane, which is facing an organ-specific lumen, and a basolateral membrane, which is in contact with the extracellular matrix and the blood vessels. In contrast to the apical transport, the mechanism of amino acid transport across the basolateral membrane still remains elusive. The best characterized basolateral amino acid transporters in the small intestine and kidney, i.e. y^+LAT1-4F2hc (*Slc7a7-Slc3a2)* and LAT2-4F2hc (*Slc7a8-Slc3a2)*, are obligatory antiporters and therefore cannot mediate alone the net vectorial amino acid efflux. In order to achieve this task, additional amino acid transporters capable of transporting amino acids unidirectionally, such as the uniporters TAT1 (*Slc16a10*) and/or LAT4 (*Slc43a2*), need to be present. TAT1 transports aromatic amino acids and has been recently shown to be important in the regulation of amino acid homestasis *in vivo*. On the other hand, LAT4 has been shown to transport branched-chain amino acids, phenylalanine and methionine, but information about its potential role *in vivo* is still missing. Therefore, with the present work we aimed at providing new information about the physiological role of this transporter by characterizing a newly established constitutive *Slc43a2*$^{-/-}$ knock-out mouse.

The *Slc43a2*$^{-/-}$ mice were born at the expected Mendelian ratio and without any phenotypic difference compared with wild type littermates but showed an early severe phenotype with

malnutrition, altered glucose homeostasis, altered hepatic gene expression and premature death. Moreover, by using these Lat4-deficient mice as negative control, we gathered new information about the localization of Lat4 in kidney, small intestine, liver and skeletal muscle. Specifically, we observed a major expression of Lat4 in the basolateral membrane of kidney proximal tubule, thick ascending limb and a minor expression in the distal convoluted tubule. In the small intestine, Lat4 expression was confined to the basolateral membrane of enterocytes with no expression in the intestinal crypts. On the other hand, skeletal muscle and liver did not show any Lat4 expression.

In addition to the aforementioned work *in vivo*, we aimed at deepening the understanding of LAT4 regulation and cooperation in the MDCK cell model. We therefore reconstituted the essential machinery for neutral amino acid transport and validated its function with uptake of radiolabeled amino acids. Moreover, using the *Xenopus laevis* oocytes expression system we addressed the effect of a predicted serine phosphorylation site on LAT4 function. In both *in vitro* systems, we provided preliminary information indicating that this phosphorylation downregulates LAT4 function by cellular mechanisms that still need to be investigated in more details.

In conclusions, the major achievements of the present thesis consist in the first characterization of a newly generated constitutive *Slc43a2*$^{-/-}$ knock-out mouse with which we demonstrated that Lat4 is essential for early postnatal development. Moreover, findings obtained using the MDCK cell model and the *Xenopus laevis* oocytes expression system provided new preliminary information about a potential functional regulation of LAT4 by phosphorylation.

2. Zusammenfassung

Aminosäuren haben zentrale Rollen in jedem lebenden Organismus als strukturelle Einheiten für Proteine, metabolische Vorläufermoleküle, Osmolyte und Signalmoleküle. In einigen heterotrophen Organismen, solchen wie Menschen und Mäusen, können manche Aminosäuren nicht *de novo* über andere metabolische Wege synthetisiert werden und müssen konstant über die Nahrung aufgenommen werden. Diese wichtige evolutionäre Beeinträchtigung führte zu der wichtigen Klassifizierung der 20 bekannten proteinogenen Aminosäuren in essentielle und nicht-essentielle Aminosäuren. Um all ihre biologischen Funktionen zu erzielen, müssen Aminosäuren Zellmembranen überqueren und können wegen ihrer chemischen partiellen Ladungen nicht frei über die Lipid-Doppelschicht diffundieren. Um diese Hürde zu überwinden sind Zellmembranen mit Transmembran-Trägerproteinen ausgestattet, auch Aminosäuretransporter genannt. In (re)absorbierendem Epithel sind Zellen in einem differenzierten Zustand, mit einer apikalen Membran, welcher das organspezifische Lumen gegenübersteht, und einer basolateralen Membran, welche in Kontakt mit der extrazellulären Matrix und den Blutgefäßen ist. Im Gegensatz zum apikalen Transport bleibt der Mechanismus des Aminosäuretransports über die basolaterale Membran noch undefiniert. Die am besten charakterisierten basolateralen Aminosäuretransporter im Dünndarm und der Niere, z. B. y^+LAT1-4F2hc (*Slc7a7-Slc3a2)* and LAT2-4F2hc (*Slc7a8-Slc3a2),* sind obligatorische Antiporter und können daher nicht allein den Netto-vektoriellen Aminosäure-Efflux vermitteln. Um diese Aufgabe zu erzielen, müssen zusätzliche Aminosäuretransporter die fähig sind Aminosäuren unidirektional zu transportieren, wie die Uniporter TAT1 (*Slc16a10*) und/oder LAT4 (*Slc43a2*), präsent sein. TAT1 transportiert aromatische Aminosäuren und wie kürzlich gezeigt wurde, scheint es für die Regulation der Aminosäure-Homöstasis *in vivo* wichtig zu sein. Andererseits wurde gezeigt, dass LAT4 verzweigt-kettige Aminoäuren, sowie Phenylalanin und Methionin transportiert, allerdings gibt es noch keine Informationen über seine potentielle Rolle *in vivo*. Daher haben wir mittels der vorliegenden Arbeit durch Charakterisierung einer neu generierten konstitutiven *Slc43a2*$^{-/-}$ knock-out Maus darauf abgezielt neue Informationen über die physiologische Rolle dieses Transporters zu bekommen. Die *Slc43a2*$^{-/-}$ Mäuse

wurden im erwarteten Mendelschen Verhältnis geboren ohne irgendwelchen phänotypischen Unterschied verglichen mit den Wildtyp-Wurfgeschwistern; allerdings zeigten sie einen frühen akuten Phänotyp mit Mangelernährung, veränderter Glucose Homöostasis, veränderter hepatischer Genexpression und vorzeitigem Tod. Des Weiteren sammelten wir durch die Nutzung dieser Lat4-defizienten Mäuse als Negativkontrolle neue Informationen über die Lokalisation von Lat4 in der Niere, dem Dünndarm, der Leber und des Skelettmuskels. Besonders in der basolateralen Membran der proximalen Tubuli der Niere und der dicken, aufsteigenden Henle'schen-Schleife beobachteten wir eine starke Expression von Lat4 und auch eine etwas geringere Expression in den distalen verschlungenen Tubuli. Im Dünndarm war die Lat4-Expression auf die basolaterale Membranen der Enterozyten beschränkt, ohne Expression in den intestinalen Krypten. Andererseits zeigte sich keine Lat4 Expression im Skelettmuskel und der Leber.

Zusätzlich zu der oben erwähnten *in vivo* Arbeit, versuchten wir das Verständnis über die LAT4 Regulation und Kooperation im MDCK Zellmodel zu vertiefen. Daher stellten wir die essentielle Maschinerie des neutralen Aminosäuretransports wieder her und bestätigten seine Funktion mittels der Aufnahme von radiomarkierten Aminosäuren. Des Weiteren untersuchten wir den Effekt von vorhergesagten Serin-Phosphorylierungsstellen auf die LAT4 Funktion im *Xenopus laevis* Oozyten Expressionssystems. In beiden *in vitro* Systemen erhielten wir vorläufige Informationen die darauf hinweisen, dass diese Phosphorylierung die LAT4 Funktion durch einen zellulären Mechanismus, der noch im Detail untersucht werden muss, runter reguliert.

Zusammenfassend bestehen die Haupterrungenschaften der vorliegenden Arbeit in der ersten Charakterisierung einer neu generierten, konstitutiven *Slc43a2*$^{-/-}$knock-out Maus, in welcher wir zeigten dass Lat4 essentiell für die frühe postnatale Entwicklung ist. Weiterhin lieferten Ergebnisse, die durch die Nutzung des MDCK Zellmodels und des *Xenopus laevis* Oozyten Expressionssystems erzielt wurden, neue vorläufige Informationen über die potentielle funktionelle Regulation von LAT4 durch Phosphorylierung.

3. Introduction

3.1 General anatomical organization and functions of the kidney

The human kidneys are paired and bean-shaped organs located in the retroperitoneal space. The right kidney localizes posterior to the liver and right below the diaphragm; whereas, the left is as well right below the diaphragm but posterior to the spleen. Two layers of adipose tissue within the retroperitoneal space, i.e. the perinephric and the paranephric fat, surround the kidneys providing a certain degree of mechanical protection. The kidney is itself surrounded by a fibrous layer known as the renal capsule (Fig. 3.1A). Each kidney weighs approximately between 125 and 170 g in adult human males and between 115 and 155 g (Boron & Boulpaep, 2005).

The kidney parenchyma can be divided anatomically in repetitive cone-shaped structures known as the renal pyramids (or pyramids of Malpighi). These structures span a part of the internal region of the kidney (renal medulla) and face with their distal part the external region of the kidney (renal cortex), which projects into the renal medulla at specific locations known as the columns of Bertin (Fig. 3.1A). The proximal part of each renal pyramid faces the renal pelvis, which conveys the urine (see below) out of the kidney via the ureter (Boron & Boulpaep, 2005).

The renal arteries are the vessels branching directly from the abdominal aorta and delivering the blood supply to the kidney, which receives at rest about 20% of the cardiac output. The renal artery undergoes many divisions and ends up finally in the interlobar arteries that spray the renal tissue at the border between cortex and medulla. From there, these interlobar arteries spread in an arc-like fashion and are therefore named arcuate arteries (Fig. 3.1B). These blood vessels give in turn rise to the interlobular arteries that spray within the cortical labyrinth to generate the afferent arterioles. These vessels finally end up in a bundle-shaped capillary network known as the glomerulus, which links the blood circulation with the functional unit of the kidney: the nephron (Boron & Boulpaep, 2005; Alpern *et al.*, 2013).

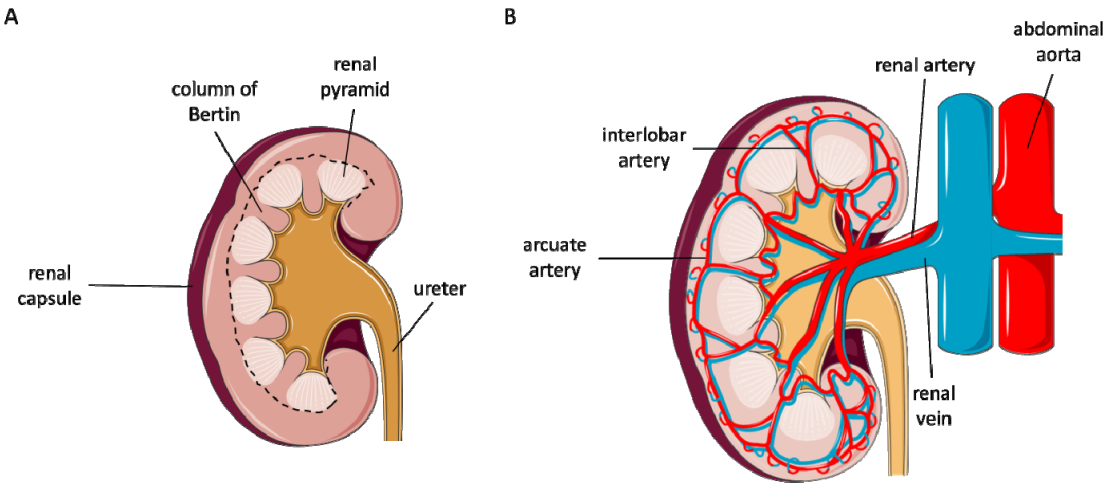

Figure 3.1 General anatomy of the kidney and its major blood supply. (**A**) The kidney is divided into an inner region (renal medulla) and an outer region (renal cortex), which in the figure are outlined by the dashed black line. (**B**) The major arteries and veins supplying the kidney. For simplification, the interlobular arteries and the afferent arterioles are not represented.(Figure adapted from www.servier.com).

The human kidneys are estimated to have each about 1 million nephrons (Fig. 3.2), although great interindividual variances have been reported. The nephron is composed of a renal corpuscle surrounding the glomerulus and connected to a twisted tubule draining into the final collecting duct. This tubular part consists basically of a proximal part and a more distal part connected via a particular looping segment known as the loop of Henle. Based on the length of this loop, two different types of nephrons can be identified in the human kidney: nephrons with short loops that turn back at the level of the outer medulla and nephrons with long loops that proceed deeply into the inner medulla before turning back. The tubular part before and after the loop of Henle can be further divided into tubular subdivisions (Fig 3.2), with each of these having a characteristic cellular composition and function.

The functional role of the nephron consists primarily in the selective clearance of the blood from waste products, such as catabolic end-products, pharmacological agents and toxic products. Via this filtering function, the kidney has the possibility to have an important influence on different physiological parameters such as blood pressure, degree of bone mineralization, acid-base regulation, erythropoiesis and aging processes. In the next

paragraph, a brief overview of how the kidney achieves its main filtering function will be outlined.

The clearance of the blood starts with the production of a primary ultrafiltrate in the Bowman's capsule (about 180 L/day). This ultrafiltrate contains, in addition to the waste products, also important molecules, such as glucose, amino acids and ions that would get excreted together with the undesired products. In order to counteract this constant loss of important molecules, evolution has endowed the kidney with the characteristic to selectively refine the composition of the primary ultrafiltrate along the tubule. This reabsorption of important solutes is mainly achieved at the level of the proximal convoluted tubule (PCT) and proximal straight tubule (PST), where the bulk expression of membrane transporters (see paragraph "Membrane transport") enables the reabsorption of different important solutes and water. From the proximal segments, the tubular fluid reaches the loop of the Henle, whose primary role is to concentrate the urea in the urine. The loop can be anatomically divided into a thin descending limb (tDLH), a thin ascending limb (tALH) and a thick ascending limb (TAL). Depending on the type of nephron, the tDLH can extend deep into the renal medulla, where the osmotic gradient between tubule lumen and interstitium can drive water out of the tubule. The ascending part of the loop of Henle, i.e. tALH and TAL, has other characteristics: it is impermeable to water but actively transports solutes; specifically, the TAL reabsorbs Na^+, Cl^- and K^+ via the membrane transporter Na-K-Cl cotransporter 2 (NKCC2). This results in the generation of hyposmotic tubular fluid. After the loop of Henle, the next nephron segments are the distal convoluted tubule (DCT), the connecting tubule (CNT) and the collecting duct (CD), which are responsible for the fine regulation of salt and water excretion in the urine. The collectin duct descends across the renal medulla and conveys the urine to the renal pelvis, where it is finally excreted via the ureter. The collecting duct plays a major role in the fine regulation of urine osmolarity upon regulation by the antidiuretic hormone (ADH) and aldosterone. In a situation of reduced water intake, ADH is indeed released from the posterior pituitary gland and binds to V2 receptors at the level of the collecting duct resulting via a secondary message cascade in an increased reabsorption of water and thus compensating for the diminished fluid intake (Boron & Boulpaep, 2005; Alpern *et al.*, 2013).

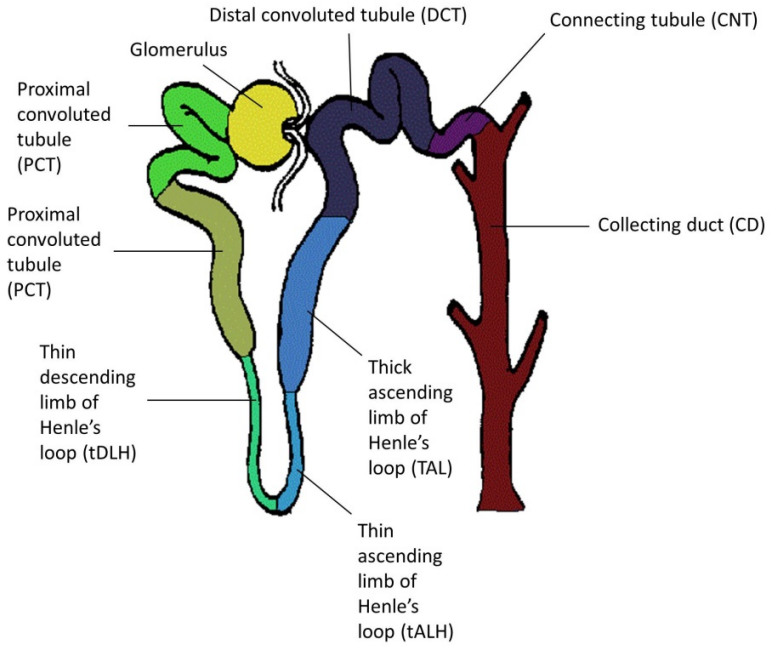

Figure 3.2 Schematic representation of the different nephron segments. (Figure adapted from http://kobiljak.msu.edu/cai/psl501/50197f1e.htm)

3.2 General anatomical organization and functions of the digestive system

The digestive system is composed of a hollow tube going from mouth to anus, where the ingested nutrients are progressively processed, and of accessory organs responsible for the productions of digestive secretions that are ultimately delivered into the lumen of the digestive tract to aid the digestive and absorptive process (Fig. 3.3).

Digestion starts in the oral cavity, where food is mainly mechanically broken down and mixed with saliva released from three different salivary glands. This secretion has the primary role to dissolve and physically modify the food into a convenient form for the swallowing and subsequent digestion. Enzymes, such as α-amylase and lipase, present in the saliva help the initial digestion process of starch and lipids. From the mouth, the bolus is then delivered via the esophagus into the stomach, where the bolus gets mixed with the

stomach secretion. Different epithelial cells laying the mucosa of the stomach are responsible for the production and the chemical characteristics of the gastric juice: the chief cells produce pepsinogen, the parietal cells secrete hydrochloric acid and the intrinsic factor, which is important for vitamin B_{12} absorption, the neck cells are responsible for the mucus secretion and the enteroendocrine cells secrete a variety of hormones involved in gastric secretion regulation. The bulk secretion of hydrochloric acid lowers the pH of the stomach denaturing the ingesting ingested proteins and killing many potential harmful bacteria ingested together with the food. Moreover, the low pH activates the enzymes pepsinogen to its active form pepsin, which hydrolyzes the denatured proteins rendering them suitable for the absorption process. Despite the presence of digestive enzymes, the major digestion process is actually performed at the level of the small intestine; however, the stomach makes an important chemical contribution in the initial digestion of proteins and also in the absorption of water, alcohols and some drugs.

After being processed in the stomach, the chyme reaches the small intestine by passing through the pyloric sphincter. The small intestine is the main site of nutrient digestion and absorption and can be anatomically divided in three portions: the duodenum, the jejunum and the ileum. The small intestinal mucosa is characterized by anatomical features aimed at maximizing the absorption efficiency: the mucosal surface is in fact largely increased by multiple folds (Kerckring's folds) protruding in the lumen of the small intestine. Moreover, these folds have themselves fingerlike projections, known as villi, which consist of many enterocytes having in turn hair-like membrane projections called microvilli. With these particular anatomical features, the small intestine is able to achieve a surface area of about 300 m^2. Small pockets in between the villi, known as the crypts of Lieberkühn, do not have a direct role in the absorption process; instead, intestinal stem cells are located in these crypts that are regenerating the small intestine mucosa. Moreover, the crypts host additional important cells such as the Paneth cells and the enterochromaffin cells that have an important role in the immunological and endocrine function of the small intestine, respectively (Fig. 3.4).

The major food digestion in the small intestine is performed with the aid of accessory organs such as the pancreas and the liver that deliver their secretions in the duodenum and by specific enzymes present at the membrane of the microvilli. Pancreatic acinar cells

secrete the pancreatic juice into small ducts that then converge into the main Wirsung duct. This secretion joins the bile secreted by the liver at the level of the duodenal papilla of Vater and gets in contact with the small intestinal lumen. At this point, pancreatic enzymes with different substrate affinities process the macromolecules within the chyme, e.g. carbohydrates, peptides and lipids, to their final monomeric constituents that can be easily absorbed though the small intestine. On the other hand, the bile coming from the liver contains different conjugated fatty acids that emulsify the ingested lipids rendering them suitable for enzymatic hydrolysis and subsequent absorption.

The absorption process starts at the level of duodenum and continues throughout the jejunum and ileum. Small digestion products like fatty acids, monosaccharides, amino acids and oligopeptides, and different ions are absorbed mostly in the jejunum. The absorption is then continued at the level of the ileum, in particular for ions and different vitamins. The unabsorbed intestinal contents travel from the ileum through the ileocecal valve into the large intestine. This last intestinal segment has an important role in the reabsorption of water and sodium; moreover, the intestinal bacteria have pivotal roles in the production of short-chain fatty acids and vitamin K, which is required for the posttranslational modification of some blood clotting factors.

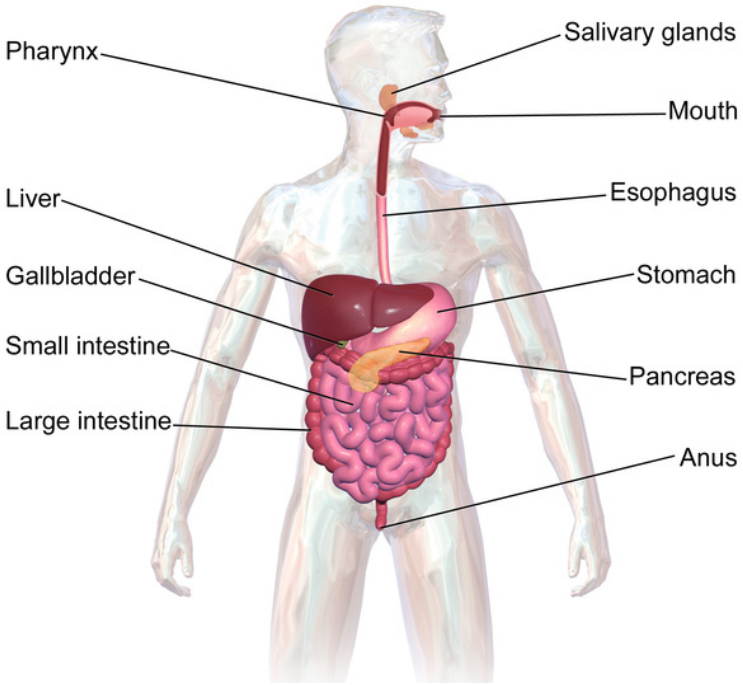

Figure 3.3 The gastrointestinal tract with the accessory organs. The digestive system consists of a hollow tube extending from mouth to anus, where ingested food is progressively processed and absorbed (from Wikipedia, The Free Encyclopedia).

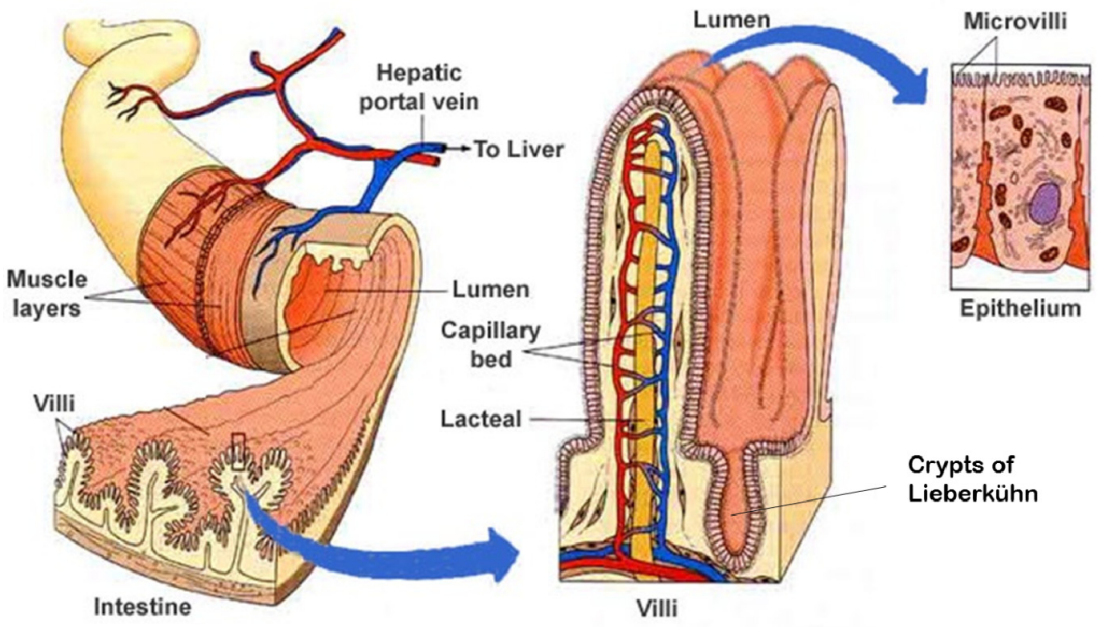

Figure 3.4 Anatomical structure of the small intestine. The surface are of the small intestine lumen is enlarged by the Kerckring's folds that are composed by small fingerlike structures called the villi. The crypts of Lieberkühn are found at the epithelial lining of the mucosa and are the site where stem cells constantly divide and differentiate to regenerate the small intestine epithelium (Modified from www.edoctoronline.com).

3.3 The epithelial structure

The tight regulation of internal fluid composition represents a central important goal for proper body homeostasis. This task is achieved by a sheet of cells, known as the epithelium, which lines body surfaces in contact with the external milieu and provides a tight barrier regulating the solute exchange with the external environment. To achieve this goal, the epithelium is endowed with particular macromolecular complexes that are going to be briefly mentioned in the following paragraphs.

Tight junctions (*zonula occludens*) are complex structures that connect epithelial cells to each other and limit the free diffusion of solutes and water between the cells (paracellular diffusion). The principal components of tight junctions are the claudins and, interestingly, their arrangement differs between epithelia of different organs and is responsible for the different degree of tight junction permeability. In the kidney proximal tubule for example,

the tight junctions are relatively cation-leaky and permit the paracellular flow and reabsorption of Na^+; whereas, in the thick ascending limb, the tight junctions are impermeable to most ions, besides divalent cations, and to water.

Adherens junctions (*zonula adherens*) are complexes of proteins localized usually just below the tight junctions. The structural feature of these junctions is their linkage to the intracellular actin cytoskeleton via a complex of different proteins, e.g. catenins and cadherins, thereby, providing a continuous bridge of actin filaments along the epithelium.

Desmosomes (*macula adherens*) interconnect adjacent cells via cadherin proteins anchored to the intracellular intermediate filaments. They have an important role in withstanding the shearing forces in epithelia subjected to physical stress.

Gap junctions are channels interconnecting the cytosol between different cells. They enable the free diffusion of small molecules, such as ions, between interconnected cells resulting in a sheet of cells that are electrically coupled. This feature is of particular importance for example in the cardiac muscle, where the synchronous contraction of cardiomyocytes is required for proper heart function.

In addition to the structural features outlined above, the epithelium is characterized by two functionally distinct membrane regions with different protein and lipid composition: the apical membrane and the basolateral membranes. The apical membrane is facing the external environment and its surface area is typically amplified by the presence of finger-like membrane infoldings known as brush border, which increases the transport efficiency of solutes. On the other hand, the basolateral membrane faces the extracellular space adjacent to the blood capillaries. In analogy to the apical membrane, infoldings amplifying the surface area are also present, but the extent of surface area amplification is less important than at the apical membrane. In addition to the cytological differences, the epithelial polarization endows the apical and basolateral membranes with characteristic protein compositions. The ubiquitously expressed Na^+/K^+-ATPase, for example, is restricted to the basolateral membrane; whereas, digestive disaccharidases are expressed at the apical membrane of small intestine, where they come in contact with their substrates in the intestinal lumen. The maintenance of a proper cellular polarity is an essential feature for the functionality of the epithelium: disruption of tight junction and consequently of cell

polarity results in misdistribution of membrane transporters with compromised transepithelial trafficking of solutes and macromolecules.

3.4 Amino acids

3.4.1 Amino acid structure and classification

The general chemical structure of amino acids (Fig. 3.5A) is characterized by a central carbon atom (C_α) bound to a carboxylic acid group (-COOH),a primary amino group (-NH_2) (in the case of L-proline a secondary amino group (-NH-)) and a variable side chain (R group) that differentiates the different amino acids and determines all the different biochemical properties between them (Table 3.1). With the exception of glycine, where the R group is another hydrogen carbon, the C_α is chiral and exhibit therefore optical activity. Therefore, two different optical isomers (enantiomers) can be distinguished that are conventionally named as either D- or L-isoform with reference to glyceraldehyde. The amino and carboxylic groups ionize at physiological pH (i.e. pH 7.4): the carboxylic group is deprotonated and bears a partial negative charge, while the amino group is protonated and bears a partial positive charge. This particular chemical form of the amino acid, where both a positive and a negative charge is present, is known as the "zwitterionic" form (Fig. 3.5B). Depending on the ionization status of the side chain (the pK_R listed in Table 1), amino acids might bear an additional charge resulting in a net positive or negative charged amino acid (Voet *et al.*, 2006). In nature, more than 300 amino acids are known, but in humans only 20 of them possess a structural role as being building blocks for proteins and the polarity of the R group represent an important criterion to classify these proteinogenic amino acids (Voet *et al.*, 2006; Wu, 2009). In ribosomal-dependent protein synthesis only the L-isoforms are incorporated; however, in some microorganisms as well as multicellular organisms there are examples of peptides and proteins bearing D-amino acids. In microorganisms, this is achieved mainly via a parallel ribosome-independent peptide-synthesizing system, which utilizes D-amino acids as substrates (Konz & Marahiel, 1999; Clugston *et al.*, 2003); whereas in multicellular organisms, this is mainly achieved via

specific enzymes that epimerize the L-amino acid into the D-isoform (Heck *et al.*, 1996). Although they are not part of proteins, it is important to mention that nonproteinogenic amino acids (e.g. citrulline) do indeed possess pivotal metabolic roles within the organism (Wu, 2009).

According to the current classification scheme proteinogenic amino acids are categorized in three different groups according to the chemical characteristics of the R group: nonpolar amino acids, uncharged polar amino acids and charged amino acids (Voet *et al.*, 2006).

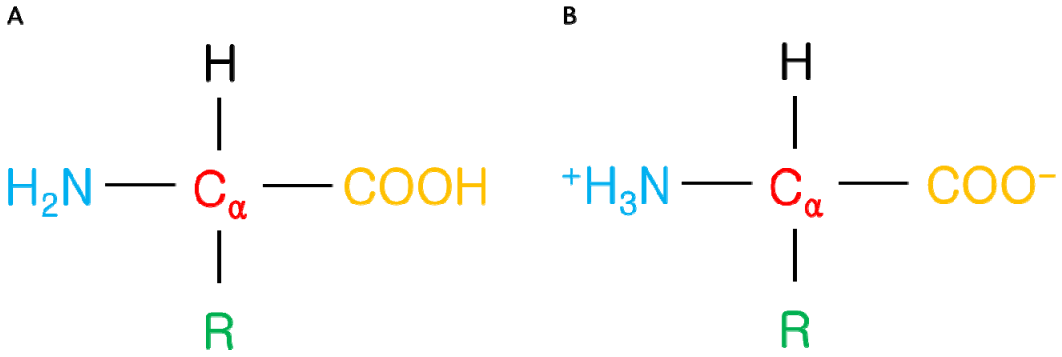

Figure 3.5 General structure of amino acid (A) and the zwitterionic form (B). The R group represents the variable side chain and differs between all the amino acids.

Group	Subgroups	Full name	Three letter abbreviation	One letter abbreviation
Nonpolar	small residual group	Glycine	Gly	G
		Alanine	Ala	A
	branched-chain	Valine	Val	V
		Leucine	Leu	L
		Isoleucine	Ile	I
	aromatic	Phenylalanine	Phe	F
		Tyrosine	Tyr	Y
		Tryptophan	Trp	W
		Proline	Pro	P
		Methionine	Met	M
uncharged polar	hydroxylic	Serine	Ser	S
		Threonine	Thr	T
	acidic	Asparagine	Asn	N
		Glutamine	Gln	Q
		Cysteine	Cys	C
charged	negative	Glutamate	Glu	E
		Aspartate	Asp	D
	positive	Lysine	Lys	K
		Arginine	Arg	R
		Histidine	His	H

Table 3.1 The proteinogenic amino acids grouped according to the chemical characteristics of the R group. Amino acids are conventionally abbreviated with a three-letter name and as well a one-letter name. (Modified from Kessel & Ben-Tat, 2011).

3.4.2 The nutritional role of amino acids

Amino acids represent central metabolic molecules for every living organism and need to be constantly supplied via the metabolism. However, with the emergence and the spreading of heterotrophy, the selective pressure on metabolic genes involved in amino acid synthesis dropped leading to the evolutionary loss of particular metabolic pathways involved in amino acid synthesis. This evolutionary constraint rendered some organisms totally dependent on a dietary protein intake to guarantee their entire pool of amino acids. In adult humans, 9 amino acids are not synthesized at all *de novo* or the rate of synthesis does not meet the optimal body requirements and therefore need to be supplemented within the diet (Table 3.2). These amino acids are collectively defined essential amino acids (EAAs) (Gropper *et al.*, 2009).

The dietary source of essential amino acids is represented by the exogenous proteins and also by endogenous proteins that are catabolized in the stomach and the small intestine. Exogenous proteins are ingested in the form of animal products (e.g. meat) or plant products (e.g. grain products); whereas the endogenous proteins originate mainly from the

mucosal cells that deliver about 50 g of protein per day, or from digestive proteins that are responsible for delivering about 17 g of protein per day.

The optimal protein intake to meet optimal amino acid requirements varies with body size, age and the general physiological state. For healthy adult human beings, it is estimated that the recommended dietary allowance (RDA) is 0.8/kg of body weight/day; whereas, the RDA for EAAs in adults are listed in Table 1.2. However, lactating and pregnant females, for example, require about 54% more of gram protein per day compared to what normally recommended to adult females with the same body size. Moreover, athletes such as body builders are known to ingest a significantly higher amount of recommended proteins per day (Gleeson, 2005).

If the protein intake does not balance the body requirements a particular status of protein deficiency or malnutrition state develops. Kwashiorkor, for example, represents a particular form of protein malnutrition, which is widely diffused in developing countries. Kwashiorkor patients are characterized by a reduced total protein concentration in the blood, which leads to dramatic changes in the oncotic pressure and the consequent formation of edemas in the different parts of the body. Additional symptoms include skin depigmentation, enlarged and fatty liver, loss of teeth and anorexia (Dewji, 1969; Williams *et al.*, 2003). An additional syndrome of protein is malnutrition is marasmus. Individuals suffering from this syndrome are typically emaciated and exhibit clear signs of muscle and adipose tissue wasting that are due to a prolonged time of inadequate energy and protein intakes (Gropper *et al.*, 2009).

Essential amino acids (EAAs)	RDA (mg/kg of body weight/day)
Phenylalanine	33
Methionine	19
Isoleucine	19
Valine	24
Tryptophan	5
Leucine	42
Threonine	20
Histidine	14
Lysine	38

Table 3.2 The 9 amino acids known as essential in human adults. RDA: Recommended Dietary Allowance. Adapted from Gropper *et al.* 2009.

3.4.3 Interorgan amino acid metabolism

Protein-containing meals are known to elicit a rise in plasma amino acid concentration with the branched-chain amino acids having the biggest increase in concentration due to their relative low degree of catabolism by the liver. Upon absorption from the small intestine, the liver takes up about 50-65% of the amino acid from the portal vein and catabolizes them for the synthesis of proteins and other nitrogen-containing compounds (Schimassek & Gerok, 1965; Brosnan, 2003), but for the branched-chain amino acids the liver plays a minor catabolic role. The elicited rise in plasma amino acid concentration can last for hours until it declines to a basal level, which can be specifically modified upon specific hormonal and physiological stimuli. Plasma amino acids, for example, can be oxidize to generate energy if the nutrient intake does not meet the optimal requirements and these concentration changes involve usually catabolic amino acid pathways that are organ-specific and are going to be briefly described in the next paragraphs.

Amino acid catabolism by enterocytes. Not the entire pool of amino acids is transported outside the intestinal cell and diffuses into the portal vein circulation. The intestinal cells need in fact as well a part of the transported amino acids for energy balance and protein synthesis. It is estimated that the intestine uses about one third of the absorbed amino acids for metabolic purposes. Glutamine, in particular, is known to be an important energy resource for the small intestine cells (Matthews *et al.*, 1993; Wu, 2009). This involves its deamination to glutamate and the transamination reactions with α-ketoglutarate to yield alanine and pyruvate. However, the generated glutamate can also be alternatively catabolized to generate other amino acids, such as proline, citrulline or ornithine that are then released into the portal vein. In analogy to glutamine, aspartate undergoes as well extensive catabolism in the small intestine cells such that very little aspartate is actually released from the enterocytes. Methionine and arginine are as well to a large extend taken up and modified by the small intestine cells: it is in fact estimated that about half of the methionine intake in the enterocyte is devoted to produce cysteine and other nitrogen-containing products (Shoveller *et al.*, 2005); whereas, for the absorbed arginine, it is known that about 40% is oxidized by the enterocyte to yield citrulline and urea (Morris, 2006).

Metabolic interplay between skeletal muscle and liver in alanine metabolism. As outlined in the previous section, glutamine represents an important energy source for intestinal cells and immune cells. In addition to this amino acid, also alanine has an important metabolic role in the liver and skeletal muscle. Alanine can be generated for example in the skeletal muscle from the branched-chain amino acids via transamination reactions and can be delivered via the bloodstream to the liver, which can convert alanine to glucose (Fig 3.6). These reactions are collectively known as the alanine-glucose cycle and have an important role in maintaining the proper blood glucose concentration, when glycogen stores in the liver are diminished. Hormones such as glucagon, epinephrine and cortisol are known to stimulate the alanine-glucose cycle (Gropper *et al.*, 2009).

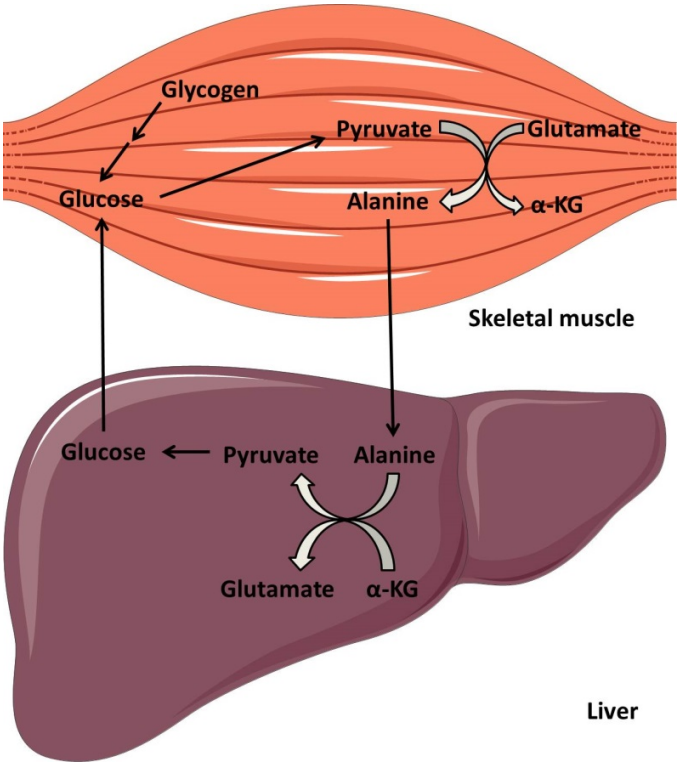

Figure 3.6 The alanine-glucose cycle. The alanine generated in the muscle is converted back to glucose in the liver. α-KG: α-ketoglutarate. (Figure adapted from Gropper *et al.* 2009).

Amino acid metabolism in skeletal muscle. The skeletal muscle represents about 43% of the body mass and contains about 40% of the total proteins found in the body. Upon

ingestion of protein-containing meal, amino acids are taken up by the skeletal muscle to synthesize proteins. Moreover, aspartate, asparagine, glutamate and the branched-chain amino acids are known to be extensively catabolized in the skeletal muscle.

The branched-chain amino acids are catabolized by the branched-chain aminotransferases that are as well present in other tissues such as kidney and the adipose tissue. This first transamination step leads to the production of α-keto acids that can be retained within the muscle or can be exported to other peripheral tissue for further metabolic reactions. After transamination, the subsequent catabolic step is the decarboxylation of the α-keto acids by the multienzyme complex branched-chain α-keto acids dehydrogenase (BCKAD), which is found in the mitochondria of different tissues such as liver, kidney, intestine, brain and heart. Genetic defects in the BCKAD are known to cause the maple syrup urine disease (MSUD), which is an autosomal recessive metabolic disorder characterized by the toxic accumulation of branched-chain amino acids and their byproducts in the blood and urine. This leads in turn to a characteristic change in the urine odor, which is similar to the maple syrup. If left untreated, the disease might cause severe brain damage and lead to death (Strauss *et al.*, 1993; Ogier de Baulny & Saudubray, 2002).

Leucine has an important role in the context of skeletal muscle physiology. This amino acid accounts for about 20% of the dietary protein intake and plays a prominent role in the regulation of protein turnover in the skeletal muscle (Layman & Walker, 2006). Leucine is in fact known to inhibit the proteosomal-dependent protein degradation pathway and stimulates the anabolic mTORC1-depedent pathways, which results in an increased muscle protein synthesis with the consequent increase in muscle mass (Nagasawa *et al.*, 2002; Drummond *et al.*, 2009). In addition, in the skeletal muscle leucine is as well extensively oxidized to produce acetyl-CoA and acetoacetate and this process has been shown to increase for example during fasting conditions (Lynch, 2001; Garlick, 2005).

The skeletal muscle represents as well an important source of glutamine, which can be generated via the transamination of branched-chain amino acids with α-ketoglutarate to produce branched-chain α-keto acids and glutamate. Ammonia combines in a subsequent step with the generated glutamate to yield glutamine, which is released into the blood and used by other organs as energy resource especially during conditions of starvation (Gropper *et al.*, 2009).

Kidney amino acid metabolism. The kidney-mediated catabolism of amino acids represents an important pathway for the regulation of acid-base balance especially during fasting conditions, where the increased catabolism of lipids and consequent release of ketone bodies might result in acidotic status. To counteract this metabolic phenomenon, the kidney increases its glutamine uptake and generates ammonia, which can combine with the H^+ ions in the urine and gets excreted. This urinary loss of H^+ ions in the urine during acidotic states contributes to the reestablishment of a proper blood pH.

Moreover, the kidney represents an important site of synthesis of the amino acid arginine, tyrosine and serine. Arginine is synthesized from citrulline and subsequently released into the bloodstream. It is estimated that the daily uptake of citrulline in the kidney is about 1.5 g; whereas, the released arginine ranges from 2 to 4 g per day (van de Poll *et al.*, 2004). The daily tyrosine production in the kidney from phenylalanine is about 1 g a day; whereas, serine is produced mainly in the kidney proximal tubule from estimated 1.5 g of glycine taken up by the kidney every day (van de Poll *et al.*, 2004).

3.5 Membrane transport

3.5.1 Membrane protein-independent transport

The peculiar chemical structure of the cellular lipid bilayer imposes obvious constraints to the molecular diffusion across it. The presence of phospholipids renders indeed the cellular membrane impermeable to most hydrophilic molecules such as amino acids, glucose and ions. Transport of such substrates is however guaranteed by the presence of membrane transport proteins that will be discussed more in the detail in the next section. On the other hand, small uncharged molecules can cross freely cellular membrane by passive diffusion without the specific need of membrane proteins. The diffusion rate of a specific substance involves different factors and can be described by a modified version of Fick's law:

$$\frac{\partial m}{\partial t} = D \cdot \frac{A}{x} \cdot \Delta C$$

The quotient $\boldsymbol{\partial m/\partial t}$ represents the molar diffusion per unit of time, which is directly proportional to the diffusion coefficient (D), the diffusion area (A), the concentration difference across the membrane (ΔC) and inversely proportional to the membrane thickness (x). The diffusion coefficient depends on the hydrophobicity of the molecule and of its size: small uncharged molecules, such as CO_2 and O_2, will diffuse better across the cellular membrane compared to ions and charged molecules, such as amino acids or glucose. However, the latter molecules represent key molecules necessary for the proper cellular homeostasis and therefore, to enable their movement across the cellular membrane, the evolution has endowed the cell with membrane proteins known as transporters (Alberts *et al.*, 2002; Boron & Boulpaep, 2005; Lodish *et al.*, 2008).

3.5.2 Membrane transporters

As mentioned in the previous sections, the transport of ions and charged macromolecules is fulfilled by integral membrane proteins, known as membrane transporters that are embedded in the plasma membrane and composed of multiple transmembrane amphipathic α-helical domains with about 3.6 amino acids per helix turn. Clustering of these helices with both hydrophobic and hydrophilic amino acid residues establishes a protein-lined pathway though which specific hydrophilic substances can cross the plasma membrane. Depending on the type of transport and the biochemical structure, membrane transporters are conventionally classified as pores, channels, ATP-powered pumps and carriers (Fig. 3.7) (Alberts *et al.*, 2002; Boron & Boulpaep, 2005; Lodish *et al.*, 2008).

The biochemical features of pores and channels involve the establishment of a hydrophilic pore interacting only weakly with the transported solute, which needs to have an appropriate size and charge. Pores and channels usually transport specific ions, small hydrophilic molecules and water down their electrochemical concentration gradient via a process known as facilitated diffusion. An important difference between pores and channels is that pores are constantly open structures allowing a very high number of solutes to cross the membrane. As constantly open structures, pores cannot dynamically modulate the influx of their substrate once docked to the membrane. Therefore, if the solute transport needs to be regulated, this is achieved by modulating the amount pores expressed at the

plasma membrane. AQP2 for example, is a pore responsible for the facilitated diffusion of water from the primary ultrafiltrate into the collecting duct cells. The tertiary protein structure of AQP2 is not endowed with the possibility of modulating water transit across its hydrophilic pore, but the tight regulation of AQP2 membrane expression upon vasopressin stimulation enables a precise control of primary ultrafiltrate osmolarity depending on the whole-body water balance. Channels are diffusion pathways that have the additional possibility of controlling the solute transport by gating. This dynamic structural feature consists in a specific conformational change of the membrane protein upon a predetermined physical or chemical trigger, which enables the opening and closing of the channel. The most prevalent types of gated channels are voltage-gated and ligand-gated, but other gating possibility such as light-stimulated gating and mechanostimulated-gating are also present. Voltage-gated channels are activated upon a change in the transmembrane electrical potential (Catterall, 1995), whereas ligand-gated channels respond to specific molecules binding to an allosteric site (Sheng & Pak, 2000). Both stimuli result in an influx or efflux of ions, which in turn modify the cell membrane potential.

Carriers, in contrast with pores and channels, provide to specific solutes a structural conduit, which is never continuous between the two sides of the membrane. The carrier-mediated transport involves a conformational change upon binding of a substrate on one side of the membrane and its subsequent release on the other side. The involvement of a dynamic structural change in the transport process imposes to carriers a lower rate of transport compared to pores and channels.

The type of transport performed by carriers can be classified depending on the involvement of more substrates and the directionality of the transport. Uniporters mediate the facilitated diffusion of one molecule at a time. GLUT1 for example is a uniporter mediating the transport of glucose down its concentration gradient across the plasma membrane of different cells in the human body (Olson & Pessin, 1996). In contrast, cotransporters couple the active transport of one substrate to the movement of another substrate down its concentration gradient. If the energetically favorable movement of one substrate is coupled to the movement of an additional substrate in the same direction, the cotransporter is classified as a symporter; whereas, if the direction of the two transported substrates is antipodal, the cotransporter is called exchanger and classified as an antiporter. This

coupling reaction relies on the proper establishment of electrochemical gradients via ATP hydrolysis (primary active transport) by ATP-powered pumps. The ubiquitous expressed Na^+/K^+-ATPase establishes a pivotal electrochemical gradient of Na^+ and K^+ by actively transporting these ions out and into the cell, respectively. The resulting gradients can then be coupled by a cotransporter to enable the transmembrane movement of another substrate against its concentration gradient (secondary active transport). The symporter SGLT1 for example couples the Na^+ gradient to the import of the D-glucose inside the enterocytes (Turk *et al.*, 1994). In an analogous way, tertiary active transporters couple the gradient generated by a secondary active transporter to the transport of another solute. The apical transporter OAT4 represent an example of a tertiary active transporter where the gradient of dicarboxylate molecules established by the NaDC1 transporter is coupled to the import of urate (Boron & Boulpaep, 2005).

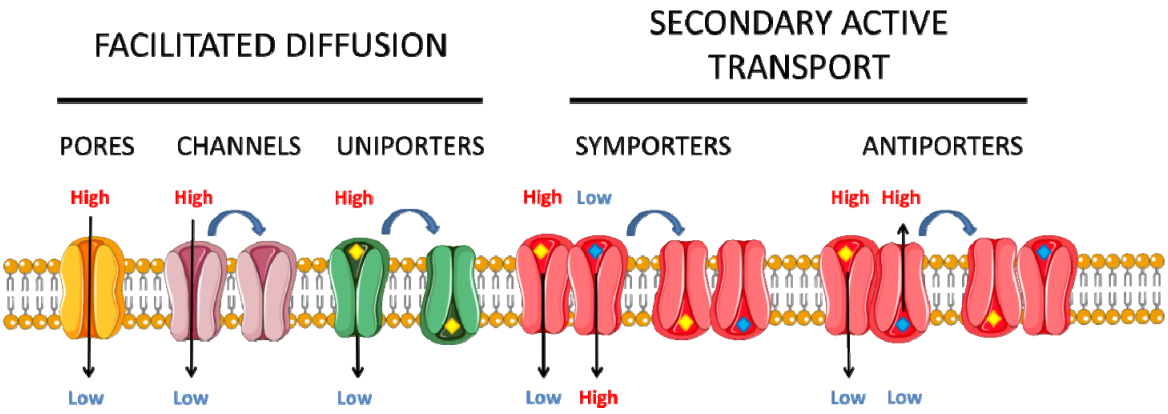

Figure 3.7 Schematic representation of membrane transport protein classification. Membrane proteins are divided depending on the Gibbs free energy involved in the transport. Pores, channels and uniporters transport their respective substrates down to their concentration gradient (indicated by the words "high" and "low" in the pictures) and therefore classified as "facilitated diffusion" transporters. Symporters and antiporters, on the other hand, mediate the transmembrane movement of a specific substrate against its concentration gradient by coupling to an energetically favorable transport of another substrate. Representative substrates are indicated by yellow and blue rhombi. Curved arrows indicate conformational changes of membrane proteins. (Figure adapted from www.servier.com).

3.5.3 Modeling the membrane transport with Michaelis-Menten kinetics

The carrier-mediated transport of a specific solute can be modeled in analogy with an enzyme-substrate binding reaction. The rate of substrate transport (V) by a carrier, varies namely with the substrate concentration [S] and can be graphically represented as in Fig. 3.8A. At a constant concentration of enzyme and when [S] is small V is linearly proportional to the substrate concentration; whereas, if [S] increases until a certain level the conformational changes of the enzyme becomes a limiting factor and V gets nearly independent of [S]. The interdependence of rate of catalysis (V) and concentration of [S] can be algebraically expressed with the Michaelis-Menten equation:

$$V = V_{max} \frac{[S]}{[S] + K_m}$$

K_m is known as the Michaelis-Menten constant and represents the substrate concentration required to achieve half the maximum velocity of the enzyme; therefore, in the case of membrane transport, the Michaelis-Menten constant represents the concentration of the substrate at half-maximal rate of transport (Voet *et al.*, 2006).

For analysis purpose, the Michaelis-Menten equation can be transformed into the Eadie-Hofstee equation:

$$V = -K_m \frac{V}{[S]} + V_{max}$$

If we plot the reaction rate (V) against $V/[S]$ we obtain a linear graph with the y-intercept being the V_{max} and K_m as the negative slope (Fig. 3.8B).

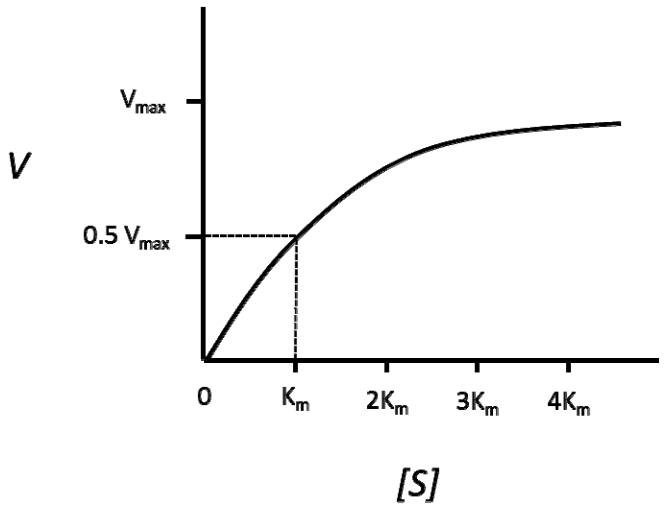

Figure 3.8 Michaelis-Menten plot and Eadi-Hofstee transformation. In case of membrane protein-mediated transport the V_{max} represents the maximal transport rate, whereas the K_m, which is known as Michaelis-Menten constant, represents the substrate concentration at a half-maximal transport rate.. (Figure adapted from Voet, 2006).

The K_m gives useful indications about the transporter's affinity: conventionally, transporters are classified as high affinity (K_m < 100 µM), medium affinity (100 µM < K_m < 1 mM) or low affinity (K_m > 1 mM). If a transporter has a high affinity transport it will reach saturation at lower substrate concentrations compared to a low affinity transporters; therefore, its transport capacity will be reduced (low capacity). On the other hand, a low affinity transport will reach saturation at much higher substrate concentrations and therefore will have a higher transport capacity (high capacity). The apical glucose transporter SGLT2, for example, is localized in the early part of the kidney proximal tubule (S1 segment) and has a low-affinity/high-capacity transport kinetics; whereas, SGLT1, which is localized in the later part of the kidney proximal tubule segment (S3 segment) is a high-affinity/low capacity transporter. This serial arrangement of secondary active glucose transporter with different characteristics enables the proximal tubule to reabsorb nearly the entire load of ultrafiltrated glucose within the first segment part (S1); whereas the rest is reabsorbed by more distal segments.

3.6 Amino acid transporters

3.6.1 Transport systems and the Solute Carrier families

The first reports about amino acid transport in human cell starts at the beginning of 20th century: Van Slyke and Meyer could in fact show that upon intravenous infusion of casein in dogs there was a significant accumulation of amino nitrogen in the tissue compared to the blood (Van Slyke & Meyer, 1913). Further studies of amino acid transport performed in different cell types, e.g. hepatocytes, fibroblasts and erythrocytes (Christensen & Oxender, 1960; Kilberg *et al.*, 1980), together with the work performed on membrane vesicles by Evers *et al.* (Evers *et al.*, 1976) and the contribution of Stevens in 1980 (Stevens *et al.*, 1982) enabled the detailed classification of so-called amino acid transport systems. The classification system categorizes different amino acid transporters into transport systems according to different factors (e.g. sodium- and pH-dependency, stereospecificity and inhibition by amino acid analogs (Christensen, 1989)) that are orthographically transposed according to described conventions (see Table 3.3) (Oxender & Christensen, 1963; Bannai *et al.*, 1984; Christensen, 1990). The use of upper or lower case indicates for example the dependence or independence respectively from sodium for the transport; the use of "+" and "-" symbols as superscripts on the other hand indicates the preference for cationic or anionic amino acid respectively (e.g. x^- or y^+); whereas the superscript 0, indicates transport of amino acids with no net charge in their variable chains. Moreover, the system classification is based on the first or main substrate preference for the specific transport system, e.g. system L is a sodium-independent system which has preference for amino acid like leucine and therefore the designation "L); whereas, system A mediates the sodium-dependent uptake of amino acid substrates like alanine. On the same line, the system ASC derives its name by the capacity to transport alanine, serine and cysteine in a sodium-dependent way (Bannai *et al.*, 1984). In the case of the system B, however, (e.g. B^0, $B^{0,+}$ or $b^{0,+}$) the "B" stands for "broad" indicating the remarkable number of different amino acids that this system can transport.

From the characterization of the different types of transport systems introduced in the previous section, it was clear that amino acid transport was performed via different types of

transporters such as symporters, antiporters (exchangers) and uniporters. Symporters usually couple a primary established gradient to the transport of specific amino acids providing therefore the possibility to enrich specific substrates within the cells (concentrative amino acid transport). The apical transport system B° for example couples the sodium-gradient established by the Na^+/K^+-ATPase to the import of neutral amino acids into the cells, thereby establishing a tertiary gradient of amino acids, which can then be used by a tertiary active amino transporter, i.e. amino acid antiporters (obligatory exchangers). Actually antiporters play an important role in mammalian tissues and in many cases, it appears that they preferentially exchange essential amino acids against nonessential ones, thus thereby not changing the total intracellular and extracellular amino acid concentrations. One important additional characteristic of antiporters is their possibility to display asymmetric transport: for instance, LAT1-4F2hc has been reported to show higher extracellular substrate affinity than intracellular, which might imply a difference between the intracellular and extracellular concentrations for specific amino acids (Meier *et al.*, 2002). Uniporters appear to be less numerous based on current information on transporter identification by cDNA cloning and investigation of their function in expression systems (see below). Indeed, the only uniporters identified so far are the ones corresponding to system y^+, T and L (two out of four). As already stated in the previous section, amino acid uniporters cannot concentrate specific amino acids inside or outside of the cells, but are facilitated diffusion pathways across which the transmembrane concentration gradient determines the direction of the net solute flux.

Transport system	Transport type	Transporters
A	Symport	SNAT1 (*SLC38A1*); SNAT2 (*SLC38A2*); SNAT4 (*SLC38A4*)
ASC	Antiport	ASCT1 (*SLC1A4*); ASCT2 (*SLC1A5*)
asc	Antiport	Asc1-4F2hc (*SLC7A10-SLC3A2*)§
B^0	Symport	B^0AT1-Coll (*SLC6A19-TMEM27*); B^0AT2 (*SLC6A15*); B°AT3-Coll (*SLC6A18-TMEM27*) ; NTT5 (*SLC6A16*); NTT4 (*SLC6A17*)
$B^{0,+}$	Symport	$ATB^{0,+}$ (*SLC6A14*)
$b^{0,+}$	Antiport	$b^{0,+}$-rBAT (*SLC7A9-SLC3A1*)
β	Symport	GAT1 (*SLC6A1*); TAUT (*SLC6A6*); GAT3 (*SLC6A11*); BGT1 (*SLC6A12*); GAT2 (*SLC6A13*)
Gly	Symport	GlyT2 (*SLC6A5*); GlyT1 (*SLC6A9*)
IMINO	Symport	SIT1-Coll (*SLC6A20-TMEM27*); PROT (*SLC6A7*)
L	Antiport	LAT1-4F2hc (*SLC7A5-SLC3A2*); LAT2-4F2hc (*SLC7A8-SLC3A2*);
	Uniport	LAT3 (*SLC43A1*); LAT4 (*SLC43A2*)
N	Symport	SNAT3 (*SLC38A3*); SNAT5 (*SLC38A5*); SNAT7 (*SLC38A7*)
PAT	Symport	PAT1 (*SLC36A1*); PAT2 (*SLC36A2*); PAT3 (*SLC36A3*); PAT4 (*SLC36A4*)
T	Uniport	TAT1 (*SLC16A10*)
X^-_{AG}	Symport	EAAT3 (*SLC1A1*); EAAT2 (*SLC1A2*); EAAT1 (*SLC1A3*); EAAT4 (*SLC1A6*); EAAT5 (*SLC1A7*)
x^-_c	Antiport	xCT-4F2hc (*SLC7A11-SLC3A2*); AGT-1 (*SLC7A13*)
y^+	Uniport	CAT1 (*SLC7A1*); CAT2 (*SLC7A2*); CAT3 (*SLC7A3*); CAT4 (*SLC7A4*)
y^+L	Antiport	y^+LAT1-4F2hc (*SLC7A7-SLC3A2*); y^+LAT2-4F2hc (*SLC7A6-SLC3A2*

Table 3.3 Amino acid transport systems. The different amino acid transporters are listed according to the transport system they correspond and their gene names are indicated in brackets. 4F2hc, Coll (collectrin) and rBAT represent accessory proteins. (Adapted from Broer, 2002, 2008).

Advances in molecular cloning techniques in the late 1980's enabled the genetic identification of transporters by use of cDNA cloning and heterologous expression in cell systems such as *Xenopus laevis* oocytes (Kanai & Hediger, 1992; Palacin *et al.*, 1998; Verrey *et al.*, 1999; Hediger *et al.*, 2004; Broer, 2008). The new classification system based on gene homology was pioneered by the human genome organization (HUGO), which categorized genes encoding for membrane transporters as "Solute Carriers" (SLC). This resulted in the establishment of 52 families (http://slc.bioparadigms.org), of which about 50 encode membrane transport proteins localized either on intracellular organelles or at the plasma membrane and that transport oligopeptides, neurotransmitters or amino acids.

3.6.2 B°AT1 (SLC6A19)

B°AT1 (SLC6A19) belongs to the SLC6 family, which represents the largest family of solute transporters and includes sodium- and chloride-dependent amino acid and neurotransmitter transporters. B°AT1 is a luminal amino acid symporter, which couples the Na^+-gradient to the import of a broad range of neutral amino acids (Bohmer *et al.*, 2005; Camargo *et al.*, 2005). In contrast with other SLC6 family members, B°AT1 does not depend on Cl^- for the transport and does not transport any chemically related non-amino acid substrates (Broer *et al.*, 2004). It is highly expressed at the mRNA level in the small intestine and the kidney proximal tubule, but for its proper membrane expression in these two organs B°AT1 requires the interaction with accessory proteins. In the kidney proximal tubule, this accessory protein is represented by Collectrin (*TMEM27*), which is a type I transmembrane protein able to regulate via non-covalent interactions the localization and expression of B°AT1 (Danilczyk *et al.*, 2006). In the small intestine, B°AT1 has been shown to have as interacting partner the angiotensin-converting enzyme 2 (ACE2), which shares about 40% sequence identity with the angiotensin-converting enzyme (ACE) and has been shown to act as a receptor for the coronavirus responsible for Severe Acute Respiratory Syndrome (SARS) (Imai *et al.*, 2005; Kuba *et al.*, 2005; Camargo *et al.*, 2009). Disruption of B°AT1 expression has been shown to cause in humans Hartnup disorder (OMIM #234500) (Kleta *et al.*, 2004), which is mainly characterized by an abnormal loss of neutral amino acids in the urine. In the majority of affected subjects the disease is asymptomatic despite the aminoaciduria, but it is important to mention that other major

clinical manifestations such as intermittent cerebellar ataxia, pellagra-like dermatitis and psychosis-like dysfunctions might be present in some individuals, especially in conditions of stress or protein-restricted diet.

3.6.3 LAT2

LAT2 (SLC7A8) belongs to the SLC7 family of amino acid transporters. This family can be functionally and structurally subdivided into two distinct subfamilies: the first four family members (SLC7A1-4) are glycosylated membrane proteins with 14 putative transmembrane segments; whereas, other 6 members of the family (SLC7A5-11) have only 12 transmembrane segments and require the association of a glycoprotein from the SLC3 family. Because of this peculiarity, these transporters are also collectively known as glycoprotein-associated amino acid transporters (gpaATs). As a gpaAT, LAT2 depends for its proper surface expression on the accessory protein 4F2hc (described in more details in the next section) and transports large and small neutral amino acids across the plasma membrane (Pineda *et al.*, 1999; Rossier *et al.*, 1999). It functions as an antiporter and therefore the transport depends on the presence of amino acid substrates on both sides of the plasma membrane (Rossier *et al.*, 1999) that are transported with a 1:1 stoichiometry and with asymmetric apparent affinities: the extracellular apparent affinity is in fact about 200 times higher than the intracellular one (Meier *et al.*, 2002). LAT2 is expressed at the basolateral membrane of small intestine, kidney proximal tubule (S1 and S2 segments), muscle, brain, pancreas, bladder and lungs (Dave *et al.*, 2004; Nishimura & Naito, 2005). No inherited disease has been clearly associated to LAT2 yet; however, LAT2 has been proposed as a potential candidate responsible for isolated cystinuria (OMIM 238200). *Slc7a8*$^{-/-}$ knock-out (KO) mice was reported to display a mild phenotype with elevated urinary levels of glycine, threonine, glutamine, leucine, valine and glutamine most probably due to the increased concentration of these amino acids in the plasma.

3.6.4 4F2hc

4F2hc belongs to the SLC3 family and analogous with rBAT (*SLC3A2)* associates with amino acid transporters of the SLC7 family via a disulfide bridge for proper membrane expression (Verrey *et al.*, 1999). Currently, rBAT is known to associate only with the SLC7

family member $b^{0,+}$AT (*SLC7A9)*, whereas many interacting amino acid transporters have been identified that associate with 4F2hc, i.e. LAT1 (*SLC7A5*), y^+LAT1 (*SLC7A7*), LAT2 (*SLC7A8*), y^+LAT2 (*SLC7A6*), xCT (*SLC7A11*), ASC1 (*SLC7A10*). 4F2hc, which is also known as CD98, was first identified as interesting protein in the context of immunological activation of lymphocytes and upregulation in tumor cells (Kanai & Hediger, 1992; Nakamura *et al.*, 1999). The involvement of 4F2hc in the context of amino acid transport was discovered using the *Xenopus laevis* oocytes expression system. 4F2hc expression resulted in fact in an amino acid transport activity compatible with the y^+L system (Bertran *et al.*, 1992; Wells *et al.*, 1992) and also with system L (Broer *et al.*, 1995). The associated amino acid transporters responsible for this observation were identified later as component of the endogenous transport system of oocytes (Mastroberardino *et al.*, 1998).

4F2hc is a ubiquitously expressed protein with highest expression levels in brain, lung, kidney, testis and spleen (Parmacek *et al.*, 1989). Total deletion of 4F2hc in mouse models leads to embryonic lethality (Tsumura *et al.*, 2003), which is most probably due to the disruption of 4F2hc-mediated signaling pathway involving β1 and β3 integrins rather than its accessory role in amino acid transport.

3.6.5 TAT1

TAT1 (SLC16A10) belongs to the monocarboxylate transporter family SLC16 (Halestrap & Meredith, 2004). It corresponds to the T-type system of of amino acid transport, which has been originally first described in erythrocytes as a Na^+-independent transport system for aromatic amino acids (Fincham *et al.*, 1985). TAT1 is a 12 transmembrane protein of 534 amino acids, which is highly expressed in small intestine, kidney, colon, liver, stomach, heart, muscle and testis (Kim *et al.*, 2001). The highest expression in kidney has been reported in the proximal segments, i.e. S1 and S2 segments. TAT1 function as a low-affinity facilitated-diffusion transporter for aromatic amino acids, L-dopa and iodothyronines with symmetric apparent affinities of about 30 mM (Ramadan *et al.*, 2006). TAT1 has been proposed as a potential candidate for the blue diaper syndrome (OMIM 211000); however, recent data obtained from *Slc16a10*$^{-/-}$ knock-out mice challenged this hypothesis (Mariotta *et al.*, 2012). Interestingly, upon coexpression with the exchanger LAT2-4F2hc in the *X. laevis* oocytes expression, TAT1 has been shown to functionally

cooperate with the exchanger and enhance the efflux of intracellular LAT2-4F2hc substrates (Ramadan *et al.*, 2007). The importance of this functional cooperation has been clearly demonstrated in the case of Tat1 deficiency. In fact, when *Slc16a10*$^{-/-}$ knock-out mice fed a high protein diet, they did not only develop a major aromatic aminoaciduria, but they also presented a minor urinary loss of Lat2-4F2hc neutral amino acid substrates highlighting the physiological importance of the cooperation between Tat1 and Lat2-4F2hc (Mariotta *et al.*, 2012). In addition to this, the characterization of Tat1-deficient mice highlighted the importance of Tat1 for the equilibration of aromatic amino acids between hepatocytes and plasma and its pivotal role in the physiological role in the regulation of aromatic amino acid concentration in the plasma (Mariotta *et al.*, 2012).

3.6.6 LAT4

LAT4 (SLC43A2) belongs to the SLC43 family of transporters together with two other members, LAT3 and EEG1, with whom it shares about 57% and 27% identity, respectively. LAT4 is a uniporter and has been shown to mediate the facilitated-diffusion of branched-chain amino acids, methionine and phenylalanine in a Cl^--independent and Na^+-independent way. In contrast with other system L transporter, e.g. LAT2 and LAT1, it does not require the association of a partner protein from the SLC3 family for its proper expression at the plasma membrane. *In situ* hybridization data reported high LAT4 expression in peripheral blood leucocytes, placenta and kidney; whereas, only a minor expression could be reported in spleen, skeletal muscle, heart, lung and brain (Bodoy *et al.*, 2005; Bodoy *et al.*, 2013). A more detailed analysis of LAT4 expression in kidney and small intestine reported this uniporter to be expressed in the more distal parts of the kidney nephron and in the crypts of the small intestine (Bodoy *et al.*, 2005). A recent characterization of genes expressed along the kidney confirmed the expression of LAT4 in the late part of the nephron, but reported as well a significant degree of expression in the TAL and the S1 segment of the PT (Cheval *et al.*, 2011).

In analogy to what was already reported in the case LAT3, LAT4 was proposed to display a peculiar uptake kinetics with the coexistence of one high (i.e. K_m of about 180 µM) and low apparent affinities (i.e. K_m of about 5 mM) for phenylalanine. Moreover, LAT4 was shown

to be inactivated by the thiol reagent N-ethylmaleimide (NEM) (Babu *et al.*, 2003; Bodoy *et al.*, 2005; Fukuhara *et al.*, 2007).

3.7 Cooperation of amino acid transporters

The epithelial amino acid transporter machinery mediates the flow of amino acids from a particular lumen (e.g. the small intestine lumen or kidney proximal tubule lumen) first into the epithelial cells by crossing the apical membrane and finally across the basolateral membrane into the extracellular space from where the amino acids may diffuse into the bloodstream. In this context, the presence at the basolateral membrane of an amino acid antiporter, such as LAT2, which mediates a symmetric exchange of amino acids between outside and inside of the cell, challenges the view of a net transcellular flow. To disentangle this issue, hypothesis of specific substrate cooperation between antiporters and parallel expressed uniporters have been proposed (Bauch *et al.*, 2003; Ramadan *et al.*, 2007; Mariotta *et al.*, 2012). A parallel expressed uniporter could as efflux pathway provide, in fact, a constant supply of amino acid substrates to the antiporter that would then recycle them into the cell in exchange for intracellular ones. In this way, the coexpression of uniporters together with antiporters would enable antiporters to mediate the efflux of their substrate amino acids (Fig. 3.9).

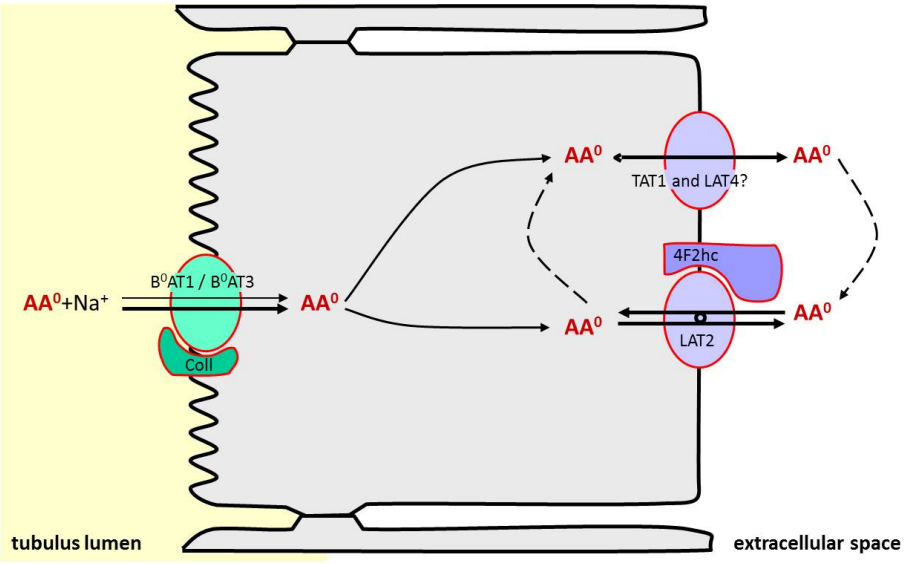

Figure 3.9 Cooperation of uniporters and exchangers for the efflux of intracellular amino acid substrates. The intracellular concentration of neutral amino acids imported by the symporter B°AT1 is equilibrated by the uniporters (either TAT1 or LAT4). This provides extracellular amino acid substrates for the exchanger LAT2 that are then recycled into the cytosol in exchange to intracellular amino acid substrates. AA°: neutral amino acids, Coll: collectrin. (Adapted from Verrey *et al.* 2009).

Evidence for this statement come from different experiments: Ramadan *et al.* for example, showed that the LAT2-mediated glutamine efflux was significantly increased upon coexpression of the uniporter TAT1 in the *Xenopus laevis* oocytes expression system (Ramadan *et al.*, 2007); moreover, Cleal *et al.* postulated an analogous cooperation with uniporters (i.e. TAT1, LAT3 and LAT4) and exchangers to be responsible for the net amino acid transfer across the placenta to the fetus (Cleal *et al.*). The cooperation of amino acid transporters has been shown to have an important impact also on the intracellular mTORC1 signaling cascade and cellular growth: the import of leucine, which is a known activator of mTORC1, via LAT1 was namely reported to be dependent on the parallel import of non-essential amino acids, such as glutamine, via ASCT2. The imported glutamine is thought to act as intracellular substrate for LAT1 and to be exported by this antiporter in exchange for leucine (Fuchs & Bode, 2005; Nicklin *et al.*, 2009). In conclusion, the outlined data provide evidence that the cooperation of amino acid symporters and antiporters represents an important way to achieve a directional flow of a specific intracellular amino acid substrate across the plasma membrane. This directional flow can then result in specific activation of

downstream intracellular signaling cascade or simply in an enhanced efflux across the epithelial basolateral membrane.

3.8 *In vitro* models to investigate amino acid transporters

3.8.1 The *Xenopus laevis* oocyte expression system

The use of *Xenopus laevis* oocytes as an expression system started at the beginning of the 1970's with the observation by John B. Gurdon that the injection of mRNA into oocytes resulted in protein translation (Gurdon *et al.*, 1971). Pioneering work using the oocytes as expression systems to investigate the acetylcholine receptor was however performed only about 10 years later (Mishina *et al.*, 1984) by Miledis, which further contributed to the spreading of oocytes as a conventional and widely recognized expression system for the investigation of membrane transporters and channels.

Xenopus laevis oocytes are derived from the South African clawed frog upon induction of ovulation and oviposition by the administration of human chorionic gonadotropins (HCG) (Wallace & Dumont, 1968). This hormonal-mediated stimulation starts a series of particular physiological reactions, among which the large accumulation of yolk protein within the oocyte represents the most important one. This accumulation delineates the beginning of a particular stage of oogenesis known as vitellogenesis (Wallace & Jared, 1969). This developmental stage can be divided according to Dumont (Dumont, 1972) into 4 different substages (stage II – V), with stage IV being the first one where the differential polarization between an animal and a vegetal pole becomes evident. Postvitellogenic oocytes, i.e. classified as stage VI, are fully developed cells with a diameter ranging from 1200 µm to 1300 µm and represent the most conventionally used for heterologous protein expression. A single female frog is able to provide in fact several thousands of these oocytes that can be developmentally arrested at the diplotene phase of the first meiotic prophase by keeping them at 16°C in a saline solution supplemented with antibiotics. Moreover, stage IV oocytes can sustain an impressive amount of protein synthesis (i.e. between 200 and 400 ng of protein per day) and therefore represent a convenient single-cell

expression system also for conventional protein analysis technique such as Western blotting (Ferrell & Machleder, 1998). Due to the high amount of yolk protein stored during vitellogenesis, oocytes do not depend strictly on extracellular nutrients for their metabolic homeostasis; therefore, the amount of endogenous membrane transporters expressed is usually very limited. This peculiarity renders the oocytes a convenient system to functionally investigate membrane transporters due to the low interference with the background transport rate of the endogenous transporters, which might represent a limiting factor in other expression systems such as cell culture models.

In addition to its numerous positive points as heterologous expression system, *Xenopus laevis* oocytes maintain a proper expression of signaling pathways that can be investigated in the context of membrane transporter regulation. In particular, signaling pathways such as G-protein coupled receptor (GPCR) signaling (Maller *et al.*, 1979; Uezono *et al.*, 1993) and tyrosine kinase receptor kinases (Ferrell, 1999; Wagner *et al.*, 2001) have been described. It is anyway important to mention that the regulation in oocytes might differ markedly from other cell type. Therefore, a potential regulatory effect on membrane transporters should be further addressed and confirmed in an additional expression system such as a specific primary cell line, where the membrane transporter is endogenously expressed.

3.8.2 The Madin-Darby Canine Kidney cells

The Madin-Darby Canine Kidney (MDCK) cell lines represent a widely used model to investigate molecular and cellular aspects of epithelia. Apico-basolateral polarity, well-structured cell junctions and rapid growth render these cells a convenient *in vitro* system for various studies about epithelial cell trafficking and cell polarity (Steed *et al.*, 2010; Datta *et al.*, 2011; Pieczynski & Margolis, 2011). Moreover, the MDCK cell line has been shown to represent a useful *in vitro* system to investigate viral assembly and propagation as it is permissive to the growth of several different viral strains. On the other hand, a clear technical disadvantage of the MDCK cells is the canine origin. Several common molecular biology tools, such as siRNA vectors or antibodies, are targeted to mouse or human protein orthologs that sometimes might differ significantly from the canine ortholog. This might limit the possibility to visualize a specific endogenously expressed protein by immunofluorescence or Western blotting.

MDCK cells were originally established in 1958 by Madin and Darby and these parental cell line was first used to investigate particular aspects of viral infection (Green, 1962). In 1966, Gaush *et al.* published the first detailed characterization of this established cell lines, which marked the entry of MDCK cells at the beginning of 1980s among the common used *in vitro* models to investigate epithelial development and function (Simmons, 1982). The originally established MDCK cell line, from which several other strains of MDCK cells were derived (see Table 3.4), is commonly referred as "NBL-2", which represents a mixture of heterogeneous cells (Simmons, 1982). This factor needs to be considered while performing experiments as particular manipulations could lead to the selection of a subpopulation of cells, which might in turn complicate the reproducibility of the obtained results (Husted *et al.*, 1986). From the NBL-2 parental cell line, two subtypes of MDCK cells, i.e. MDCK I and II cells, were isolated and represent currently the most commonly used cell lines (Barker & Simmons, 1981; Richardson *et al.*, 1981).

MDCK I cells were isolated from the "NBL-2" parental strain at a low passage and are characterized by a very high transepithelial resistance (TER), i.e. > 4000 $\Omega \cdot cm^2$. The TER is inversely correlated with the degree of "epithelial leakiness" and consequent paracellular flow of solutes: cells with a low TER will be more "leaky" compared to cells with a higher TER. In contrast with MDCK I cells, MDCK II were derived from a higher passage "NBL-2" parental strain and display significant lower TER values, i.e. < 300 $\Omega \cdot cm^2$. This difference can be explained by the structural composition of the tight junctions. MDCK II cells express namely in addition the tight junction protein claudin-2, which is known to have pore-forming capacities and might therefore be responsible for the lower TER in MDCK II cells (Furuse *et al.*, 2001).

The TER does not represent the only difference between the two MDCK strains: many differences regarding the plasma membrane protein and lipid composition, i.e. alkaline phosphatase and Na^+/K^+-ATPase expression as well as glycosphingolipid content, have been namely outlined in different publications (Hansson *et al.*, 1986; Zimmer *et al.*, 1997). Moreover, MDCK II cells have been reported to be on average bigger and taller than the other strain type (Barker & Simmons, 1981).

Strain	Characteristics	Supplier
MDCK (NBL-2)	Original parental cell line from which type I and type II MDCK cells are derived. This cell line represents a mixture of different cells.	ATCC, JCRB, ECACC
MDCK I	Cell line derived from NBL-2 at a low passage. Type I MDCK cells have high TER and do not express claudin-2. They have gap junctions.	ECAAC
MDCK II	Cell line isolated from NBL-2 at a high passage. Type II MDCK cells have low TER and express claudin-2. They are taller and larger compared to type I strain and do not expressed gap junctions.	ECACC

Table 3.4 MDCK strains most commonly used in research. (Table adapted from Dukes *et al.* 2011).

4. Materials and Methods

4.1 Cell culture

Madin-Darby Canine Kidney strain I (MDCK I) cells were cultured according to standard cell culture protocols at 37°C and 5% CO_2 in Dulbecco-modified Eagle's Medium (PAA Laboratories GmbH, Cat. No. E15-843, Austria) supplemented with 2 mM L-glutamine (PAA Laboratories GmbH, Cat. No. M11-0044, Austria), 10% heat-inactivated fetal bovine serum (FBS) (Sigma-Aldrich, Cat. No. F7524, Germany), 1% MEM non-essential amino acids (PAA Laboratories GmbH, Cat. No. M11-003, Austria) and 1x Penicillin/Streptomycin (PAA Laboratories GmbH, Cat. No. P11-010, Austria). The growth medium was changed every 2 days and cells were split at a ratio of 1:10 to 1:20 two times per week. In order to allow cell polarization, MDCK cells were seeded at confluent density ($1.7 \cdot 10^5$ cells/cm^2) and grown on polycarbonate filters (Cat. No. 3412, Corning, USA) for 6 days in standard medium.

Human embryonic kidney cells (HEK293T) were kindly provided by the lab of prof. D. Schümperli (University of Bern) and Phoenix amphotropic retrovirus-producing cells were provided by the American Type Culture Collection (ATCC) with the permission of G. Nolan (Stanford University). Both cell lines were grown in DMEM supplemented with 10% heat-inactivated FBS, 2 mM L-Glutamine and 1% NEAA at standard cell culture conditions (37°C, 95% relative humidity and 5% CO_2). Upon reaching a subconfluency of about 80-90%, cells were trypsinized and passaged at a ratio of 1:10.

4.2 cDNA constructs and retroviral transduction

The human B^0AT1 cDNA sequence was cloned in the multiple cloning site of pIRES-EGFP (kindly provided by Thierry Hennet – University of Zurich), upstream of the internal ribosomal entry site (IRES) and the EGFP reporter gene. Human TMEM27 cDNA sequence was subcloned in the aforementioned vector in place of the EGFP sequence. The resulting bicistronic construct containing B^0AT1 and TMEM27 upstream and downstream

of IRES, respectively, was then excised from the plasmid and inserted in the retroviral vector pLPCX.

Cloning of the human LAT2 and human 4F2hc fusion cDNA constructs was performed by first introducing a *SmaI* restriction site in the pSDeasy-hLAT2 vector described in (Rossier *et al.*, 1999) with the following primers: 5'-GCA GCC CCA GCC CGG GGG ACC ACC ATT CC-3' (for) and 5'-GGA ATG GTG GTC CCC CGG GCT GGG GCT GC-3' (rev). The human LAT2 cDNA sequence was subcloned using *EcoRI / SmaI* restriction sites in the vector pSDeasy-XT3-4F2hc in place of the XT3 cDNA sequence. The human LAT2-4F2hc fusion cDNA constructs was then cloned into the pSC-B vector (Agilent Technologies, USA) with the following primers: 5'-TCG AGA GGA AGC TGG TGA AG-3' (for) and 5'-GGT TTC AGA GGG AAG ACT TCA C-3' (rev) and according to manufacturer's instructions. Finally, the fusion construct was subcloned into a retroviral pLHCX vector.

The human TAT1 cDNA sequence was cloned by adding an *Eco47III* and a *SalI* restriction sites via the following primer: 5'-AAT CAT AGC GCT TCG GGC CAT GGT G-3' (for) and 5'-AAT CTA GTC GAC GAT TAC GCC CAA GCT C-3' (rev). The PCR product was then purified and cloned into a pLenti6-EGFP vector (Invitrogen) in place of the EGFP cDNA using *Eco47III* and *SalI* restriction sites.

The pTLN vector with the human LAT4 cDNA sequence was kindly provided by Manuel Palacin. The cDNA was cloned in a pLenti6-EGFP vector (Invitrogen) in place of the EGFP cDNA using *NruI* / *MluI* restriction sites. For FLAG-tagging the human LAT4 insert, the cDNA was cloned with the following primers: 5'-CAT GGC GCC CAC CCT GGC CAC TG-3' (for) and 5'-CTA CAC GAA GGC CTC CTG GTT G-3' (rev) into a FastBac-FLAG(C) vector, which was kindly provided by Thierry Hennet. The hLAT4-FLAG(C) insert was subsequently cloned into a pSDeasy vector using *XbaI / NotI* restriction sites. To mutagenize the serine 274 of the human LAT4 insert into alanine, the following primers were used: 5'-GGC CGG CGC CTG GCT GTG GGC AGC TC-3' (for) and 5'- GAG CTG CCC ACA GCC AGG CGC CGG CC-3'; whereas, the following primers were used to mutagenize serine into glutamate: 5'-GTG GGC CGG CGC CTG GAA GTG GGC AGC TCC ATG-3' (for) and 5'-CAT GGA GCT GCC CAC TTC CAG GCG CCG GCC CAC-3' (rev). For the studies performed in MDCK cells, the human

LAT4 cDNA was further subcloned from the pSDeasy vector, which has been previously described (Puoti *et al.*, 1997), into a pLPCX vector using *HindIII / NotI* restriction sites.

HEK293T (below passage 20) were cultured according to the cell culture protocol. For transfection procedure, 4-5·10^6 HEK293T cells were seeded on 10 cm dishes and allowed to adhere overnight. The following day, medium was changed two hours before transfection. The transfection mixture was prepared as follows: 5 µg of pMD2.G, 10 µg of pCMV-pR8.91 and 15 µg of the vector of interest. Volume was adjusted to 450 µl with 0.1x TE buffer pH 8.8. 50 µL of 2.5 M $CaCl_2$ were given drop-wise to the DNA mixture and the volume was subsequently adjusted to 500 µL with 2x HBS. After appropriate mixing, the solution was incubated for at least 20 min at RT. DNA transfection mixture was added dropwise to the cell culture dish and medium was exchanged the next morning. The supernatant was collected from transfected HEK293T cells 48 hours post transfection, filtered through 0.45 µm filters and centrifuged at 25000 rpm (Sorvall® Ultraspeed Centrifuge/Rotor TH64I) for 90 min at 4°C. Supernatant was aspirated almost completely and pellet of viral complexes was re-suspended in approx. 1 mL of the same medium. The same day of virus harvesting, MDCK cells were trypsinized, counted and 1·10^6 cells were resuspended with the virus containing medium and plated on a 35 mm petri dish. After overnight incubation, the medium was replaced with MDCK standard medium and the cells were allowed to reach confluence.

MDCK constitutively expressing the different basolateral amino acid transporters and the apical amino acid transporter B°AT1 together with accessory protein TMEM27 were obtained by consecutive transduction steps as shown in Figure 2.1. To achieve homogenous expression of the transduced construct, MDCK cells were selected at every transduction step with different antibiotics: for pLHCX-LAT2-4F2hc, Hygromycin B (H3274, Sigma-Aldrich) was used at a concentration of 50 µg/ml; for pLenti6-LAT4 and pLenti6-TAT1, Blasticidin S (R210-01, Life Technologies) was used at a concentration of 6 µg/ml; for pLPCX-B°AT1-TMEM27, Puromycin dihydrochloride (P8833, Sigma) was used at a concentration of 2 µg/ml.

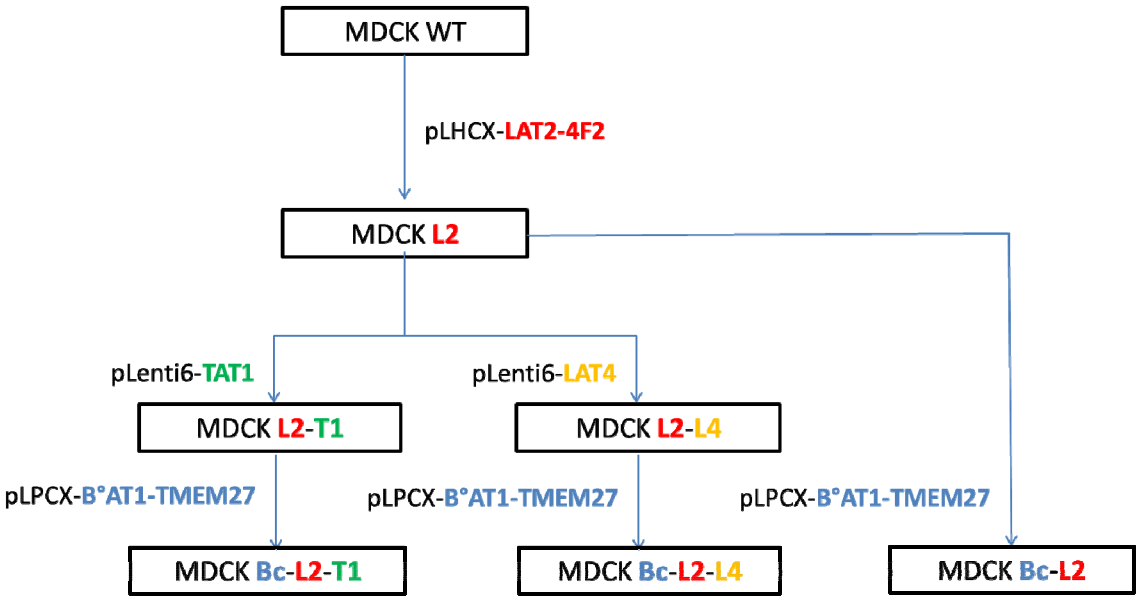

Figure 4.1. Sequential transduction scheme for establishment of MDCK cell lines. Firstly, the basolateral amino acid transport set was reconstituted by transducing the MDCK cell wildtypes with the pLHCX-LAT2-4F2hc fusion construct and subsequently with either human TAT1 or LAT4 in pLenti6 vector. The apical transporter B°AT1 and accessory protein TMEM27 were finally transduced via pLPCX vector with an IRES between the two ORFs.

4.3 Immunofluorescence staining on MDCK cells

MDCK cells were grown on poly-D-lysine (Sigma) coated coverslips or differentiated on polycarbonate filters according to the cell culture protocol. For LAT4 and TAT1 detection, cells were washed once with ice-cold PBS and fixed with absolute methanol for 5 min at -20°C. For LAT2-4F2hc fusion protein detection, cells were washed once with PBS at room-temperature (RT) and fixed with 3% paraformaldehyde (PFA) dissolved in 1x PBS pH 7.4 for 20 min at room-temperature (RT). Cells were washed repetitively with ice-cold PBS and incubated with PBS-Triton X-100/BSA (2%) for 30 min at RT. The same blocking solution was used to incubate primary and secondary antibodies. Incubation with primary antibody was performed in a humidified chamber overnight at 4°C. For TAT1 detection, a previously described antibody was used at 1:500 dilution (Ramadan *et al.*, 2007). For human LAT4 detection, an antibody targeted to the N-terminal peptide (N-APTLATAHRRRWWMAC-C) was generated in rabbit and used in a 1:500 dilution. To detect LAT2-4F2hc, a previously described antibody was used at 1:1000 dilution

(Mastroberardino *et al.*, 1998). After washing, cells were incubated for 1 h at RT with the respective following secondary antibodies at 1:2000 dilution: Alexa Fluor 594 anti-rabbit (Cat. No. A21207, Invitrogen), Alexa Fluor 488 anti-mouse (Cat. No. A21202, Invitrogen) and Alexa Fluor 488 anti-rabbit (Cat. No. A11008, Invitrogen). 4',6-Diamidino-2-Phenylindole Dihydrochloride (DAPI, Invitrogen) was added to the secondary antibody mixture (1:5000 dilution) in order to counterstain the nuclei. Coverslips or filter pieces were mounted in DAKO-Glycergel and analyzed at the fluorescent light microscope (Nikon) or confocal laser scan microscope (Leica).

4.4 Western blotting

MDCK cells grown on plastic supports (6-well plates or 10 cm dishes) or polycarbonate filters (24-mm filters) were washed three times for 5 min with ice-cold PBS, scraped from their support in 500-1000 µL of ice-cold PBS and centrifuged at 1000 g for 5 min at 4°C. For total membrane preparation, cell pellet was then homogenized in 200 µl resuspension buffer (200 mM D-Mannitol, 80 mM HEPES, 41 mM KOH, pH 7.5) supplemented with Protease Inhibitor Cocktail (Sigma) by sonication 2 times at 10% intensity (Bender&Hobein, Zurich, Switzerland). Cell debris was then centrifuge at 2500 g for 10 min at 4°C and the supernatant was further ultracentrifuged at 41000 rpm (rotor RP45A) for 1 h at 4°C. Supernatant was then collected as cytosolic fraction, whereas the pellet was resuspended in 50 µl resuspension buffer.

Protein sample concentration was determined by DC-Protein Assay, following the manufacturer's guidelines (Bio-Rad) and using the BioTek Microplate Spectrophotometer µQuant. 20 µg of protein lysate were diluted in 4x Laemmli buffer supplemented with 10% β-Mercaptoethanol, incubated at 37°C for 30 min and loaded on 10 or 12% polyacrylamide gel. After separation by electrophoresis, proteins were transferred to PVDF membrane (Immobilion-P, Millipore). Blots were blocked (1 h at RT) with 5% milk powder in Tris-buffered saline supplemented with 0.1% Tween-20 (TBS-T) and incubated (overnight at 4°C) with the primary antibody diluted in 5% milk in TBS-T. The following primary antibodies were used: in house rabbit anti-human B°AT1 at 1:1000 dilution, mouse anti-human TMEM27 (Cat. No. H00057393-B01P, Abnova) at 1:1000 dilution, rabbit

polyclonal anti-FLAG epitope (Cat. No. F7425, Sigma) at 1:1000 dilution and rabbit anti-human LAT4 (see the previous section) at 1:500 dilution. After washing the blot with TBS-T, the following secondary antibodies were respectively applied at 1:5000 dilution in 5% milk in TBS-T for 1 h at RT: anti-rabbit horseradish peroxidase (HRP)-conjugated (Cat. No. W401B, Promega), anti-mouse HRP-conjugated (Cat. No. W402B, Promega), anti-rabbit alkaline phosphatase (AP)-conjugated (Cat. No. S373B, Promega) and anti-mouse AP-conjugated (Cat. No. S372B, Promega). The antibody binding was detected with Immobilion Western Chemiluminescent HRP substrate (Millipore) or CDP-Star (Roche) and visualized with FujiFilm Las-4000 camera (Fujifilm AG, Switzerland) according to the manufacturer's instructions. Image-J software was used for densitometric analysis of the Western blots.

4.5 Amino acid uptake in MDCK cells

MDCK cells were grown on filters according to the standard cell culture protocol. The trans-epithelial electrical resistance across intact monolayers of MDCK cells was measured using EVOHM device (World Precision Instruments, Berlin, Germany). Cells were washed three times and then incubated for 30 min at 37°C with uptake buffer (150 mM NaCl, 10 mM HEPES pH 7.4, 1 mM $CaCl_2$, 5 mM KCl, 1 mM $MgCl_2$, 10 mM glucose). Fresh uptake buffer was then applied on the basolateral side whereas the apical compartment received the uptake buffer supplemented with the corresponding amino acid at the indicated concentration and the corresponding ^{3}H-labeled or ^{14}C-labeled amino acid as tracer. In the indicated experiments, ^{14}C-labeled mannitol was used as a control for the integrity of the cell monolayer. After the indicated time of incubation at 37°C, the uptake was stopped by replacing the apical and basolateral solutions with ice-cold uptake buffer. The cells were washed three times and the filters were excised and placed into scintillation fluid and shaken overnight at RT. Radioactivity was measured by liquid scintillation analyzer (Packard Tri-Carb 2900TR, PerkinElmer).

4.6 Measurement of intracellular amino acid concentration

MDCK cells were grown on filters and let differentiate according to usual protocol. Apical and basolateral medium was collected separately after the indicated time and the cells were washed two times in ice-cold PBS, scraped from their support in 500 µL of ice-cold PBS and centrifuged at 2000 g for 2 min at 4°C. Cell pellets were then weighted and homogenized by vigorous pipetting in 100 µL of 10% sulfosalicylic acid. Cell debris were pelleted with centrifugation at 12000 g for 5 min and supernatant was stored at -20°C before amino acid measurement.

The amino acid analysis was performed by Dr. Markus Heck at the University Children Hospital, Zurich. Briefly, deproteinized samples were derivatized using EZ:faast^{TM} kit (Phenomenex) and further analyzed by LC-MS/MS using API Sciex 2000 instrument (Ab Sciex).

4.7 *Xenopus laevis* preparation and cRNA injection

Oocytes at stage IV as described in (Dumont, 1972) were treated with collagenase A for 2-3 h at room temperature in Ca^{2+}-free buffer (82.5 mM NaCl, 2 mM MgCl2 and 10 mM HEPES pH 7.4) and kept at 16°C in Modified Barth's solution (88 mM NaCl, 1 mM KCl, 0.82 mM $MgSO_4$, 0.41 mM $CaCl_2$, 0.33 mM $Ca(NO_3)_2$, 2.4 mM $NaHCO_3$, 10 mM HEPES, 5 mg/l Gentamicin, 5 mg/l Doxycycline). Remaining follicular layers were manually removed. 25 ng of LAT4 cRNA was injected and oocytes were incubated for 3 days at 16°C in ND96 solution (96 mM NaCl, 2 mM KCl, 1 mM $MgCl_2$, 1.8 mM $CaCl_2$, 5 mM HEPES-Tris pH 7.4, supplemented with 50 mg/l tetracycline).

4.8 Uptake experiments in *Xenopus laevis* oocytes

Oocytes were washed six times with 2 ml Na^+-buffer (100 mM NaCl, 2 mM KCl, 1 mM CaCl2, 1 mM MgCl2, 10 mM HEPES pH 7.4) and then pre-warmed for 2 minutes at 25°C in a water bath. Subsequently, the pre-warming solution was aspirated and 100 µl of Na^+-buffer containing unlabeled L-Phe at the indicated concentrations together with [H3]-L-Phe (10 µCi/ml) as tracer (Hartmann Analytic, Braunschweig, Germany) were added. Oocytes

were then incubated for 10 minutes at 25°C. Thereafter, uptake solution was removed, oocytes were washed six times with 2 ml ice-cold Na^+-buffer and separately dissolved in 250 µl 2% SDS under agitation for at least 30 min. Upon addition of 3 ml scintillation fluid (Emulsifier-Safe™), radioactivity was counted on a liquid scintillation counter (TRI-CARB 2900TR, Packard Instrument, Meriden, CT). For analysis, the amount of amino acid uptake of not injected oocytes was subtracted from oocytes expressing the transporter. Uptakes values were corrected by subtracting the values obtained from non-injected oocytes. Curves corresponding to the Michaelis-Menten equation were fitted to the data sets using GraphPad Prism 5.0, GraphPad Software, San Diego, CA).

4.9 Efflux experiments in *Xenopus laevis* oocytes

Oocytes were injected with 50 nl of different L-Phe solutions (10 mM, 25 mM, 50 mM, 100 mM and 200 mM) together with [H3]-L-Phe (0.2 µCi/µl) as tracer. Assuming an oocyte volume of about 400 µl (Taylor & Smith, 1987), the resulting oocyte internal L-Phe concentration upon injection corresponded respectively to 1.11 mM, 2.78 mM, 5.56 mM, 11.11 mM and 22.22 mM. Oocytes were subsequently washed four times in ND96 solution and 200 µl ND96 were given to each oocyte. Efflux was allowed to take place for 10 minutes at 25°C before recovering the ND96 solution and washing the oocyte four times with ND96. For the oocytes lysis and data analysis, see "Uptake of amino acids in *Xenopus laevis* oocytes".

4.10 Immunofluorescence staining on *Xenopus laevis* oocytes

Xenopus laevis oocytes were washed once in ice-cold PBS and fixed for 4 h with 3% paraformaldehyde at 4°C. Oocytes were then washed three times in ice-cold ND96 solution and frozen in liquid propane. 7 µm and 10 µm sections were prepared on Superfrost®Plus Menzel slides (Gerhard Menzel, GmbH, Braunschweig, Germany). Sections were blocked at room temperature for 30 min with a blocking buffer containing 2% bovine serum albumin, 0.04% Triton X-100 in PBS pH 7.4. Primary antibodies were incubated in the same blocking buffer at 4°C overnight. For LAT1 and 4F2hc detection, previously described antibodies were used at a dilution of 1:1000 (Mastroberardino *et al.*, 1998). For

HA-tagged LAPTM4B detection, a commercial antibody was used (ab9110, Abcam). Sections were then washed three times at room temperature with PBS and incubated with the following secondary antibodies diluted 1:1000 in blocking buffer: Alexa Fluor 594 anti-mouse (Cat. No. A21203, Invitrogen) and Alexa Fluor 488 anti-rabbit (Cat. No. A11008, Invitrogen). Sections were then again washed three times at room temperature with PBS, mounted in DAKO-Glycergel and analyzed at the fluorescent light microscope (Nikon).

4.11 Generation of *Lat4 -/-* KO mouse via gene trapping

The *Lat4*$^{-/-}$ KO mouse was produced by the Phenogenomic Center of Toronto (www.phenogenomics.ca). Embrionic stem (ES) cell lines were mutated by insertional mutagenesis using a UPA gene trap vector (Shigeoka *et al.*, 2005) in the 6th intron of the *Lat4* gene. Cells were prepared for aggregation with diploid embryos to produced chimeric mice. R1 cells were in a 129 mouse background, whereas the germline was tested by crossing the chimera to CD-1 mice and assessing coat color. Mice were subsequently breeded into C57BL/6 background. All animals were housed in standard conditions and fed a standard diet prior experiment. All handling procedures were performed according to the Swiss Animal Welfare laws and were approved by the Kantonales Veterinäramt Zürich.

4.12 Immunofluorescence staining on mouse sections

Organs were isolated and immediately frozen in liquid propane. 7 µm sections were prepared on Superfrost®Plus Menzel slides (Gerhard Menzel GmbH, Braunschweig, Germany). For Lat4 and NKCC2 colocalization, 4 µm consecutive sections were prepared. Sections were then fixed with methanol at -20 °C for 90 seconds, rehydrated for 15 min at room-temperature (RT), washed three times for 5 min with phosphate- buffered solution (PBS) at RT. For Lat4 detection, epitope retrieval was performed by incubating slides in 10 mM sodium citrate pH 6.0 for 10 min at 98 °C with a microwave (Histos 3, Milestone, USA). For NKCC2 detection, no epitope retrieval was performed. Sections were then washed again three times for 5 min with PBS at RT and incubated with blocking solution (2% bovine serum albumin, 0.04% Triton X-100 in PBS pH 7.4) for 1 hour at RT. Primary antibodies were diluted in blocking solution and incubated overnight at 4°C with the

respective dilutions: 1:500 for Lat4, 1:1000 for Tmem27, 1:2000 for NKCC2, 1:500 for NCC. Lat4 antibody targeted to the C-terminal part of the Lat4 protein (N-CQLQQKREDSKLFL-C) was generated in rabbit (Pineda, Berlin, Germany). Tmem27 antibodies targeted to the C-terminal peptide (N- CDPLDMKGGHINDGFLT-C) were raised in guinea-pig (Pineda, Berlin, Germany). Anti-mouse NCC (Loffing *et al.*, 2004), anti-mouse NKCC2 (Kaplan *et al.*, 1996), anti-mouse Mdr1 (Fickert *et al.*, 2001) were previously characterized. For Glut4 detection, commercially antibodies were used (Abcam, ab65267, Cambridge, UK). Sections were then washed three times for 5 min in PBS at RT. The secondary antibodies were applied with 1:500 dilutions for 1 hour at RT and were described in the previous section. Staining of nuclei was performed with 4',6-diamidino-2-phenylindole (DAPI) at 1:500 dilution.

4.13 Morphological analysis of organs

Organs isolation, 7 µm sections preparation and section fixation were performed as described before. Classical Hematoxylin & Eosin staining was performed as described elsewhere (Mariotta *et al.*, 2012).

4.14 Metabolic cages experiments with *Lat4 +/-* mice

Seven-week old *Lat4 +/-* and *Lat4 +/+* littermates were fed a normal protein diet (20% casein) in metabolic cages. Experimental setup and determination of amino acids in urine and plasma were performed as described elsewhere (Mariotta *et al.*, 2012).

4.15 RNA extraction and real-time PCR

Mice at the indicated day after birth were sacrificed by decapitation and organs were immediately rinsed several times with ice-cold PBS prior to being rapidly frozen in liquid propane until further use. Total RNA was extracted and reverse transcription was performed as described elsewhere (Ramadan *et al.*, 2006). For real-time PCR, 10 ng of cDNA template were used and the reaction was set according to Applied Biosystems recommendations (TaqMan® Universal PCR master mix, Applied Biosystems). The

abundance of target mRNAs was standardized relative to 18S ribosomal RNA. Primers and probes for Lat2 (Slc7a8), Lat4 (Slc43a2), 4F2hc (Slc3a2), y^+Lat1 (Slc7a7), y^+Lat2 (Slc7a6), Asct2 (Slc1a5), Tat1 (Slc16a10) and B°AT1 (Slc6a19) were previously described (Moret *et al.*, 2007; Mariotta *et al.*, 2012).

4.16 Plasma amino acid and acylcarnitines measurements

Amino acids and acylcarnitines were measured after extraction with methanol without derivatisation (Neobase Kit, Perkin Elmer, Switzerland) on an Acquity-TQD tandem mass spectrometer (Waters). Briefly, 3 µL of plasma were spotted onto prepunched plain filter paper (Ahlstom 226) in 96-well plain uncoated microtiter plates. Amino acids and acylcarnitines were extracted with 100 µL methanolic extraction solution containing stable isotope labeled internal standards by shaking for 45 min at 45°C. 30 µL of extract were then injected with a flow rate of 10 µL/min directly into the tandem mass spectrometer and measured after in MRM-mode (multiple reaction monitoring).

4.17 RNA sequencing analysis of liver

Organs were isolated and RNA was extracted as described before. The quality of the isolated RNA was determined with a Qubit® (1.0) Fluorometer (Life Technologies, California, USA) and a Bioanalyzer 2100 (Agilent, Waldbronn, Germany). Only those samples with a 260 nm/280 nm ratio between 1.8–2.1 and a 28S/18S ratio within 1.5–2 were further processed. The TruSeq RNA Sample Prep Kit v2 (Illumina, Inc, California, USA) was used in the succeeding steps. Briefly, total RNA samples (100-1000 ng) were polyA enriched and then reverse-transcribed into double-stranded cDNA. The cDNA samples was fragmented, end-repaired and polyadenylated before ligation of TruSeq adapters containing the index for multiplexing Fragments containing TruSeq adapters on both ends were selectively enriched with PCR. The quality and quantity of the enriched libraries were validated using Qubit® (1.0) Fluorometer and the Caliper GX LabChip® GX (Caliper Life Sciences, Inc., USA). The product is a smear with an average fragment size of approximately 260 bp. The libraries were normalized to 10 nM in Tris-Cl 10 mM, pH 8.5 with 0.1% Tween 20. The TruSeq PE Cluster Kit v3-cBot-HS or TruSeq SR Cluster Kit v3-

cBot-HS (Illumina, Inc, California, USA) was used for cluster generation using 10 pM of pooled normalized libraries on the cBOT. Sequencing was performed on the Illumina HiSeq 2000 paired end at 2 X 101 bp or single end 100 bp using the TruSeq SBS Kit v3-HS (Illumina, Inc, California, USA). RNA-seq reads were quality-checked with fastqc which computes various quality metrics for the raw reads. Reads were aligned to the genome and transcriptome with Tophat v1.3.3. Before mapping, the low quality ends of the reads were clipped (3 bases from the read start and 10 bases from the read end). Tophat v1.3.3 was run with default options. The fragment length parameter was set to 100 bases with a standard deviation of 100 bases. Based on these alignments the distribution of the reads across genomic features was assessed. Isoform expression was quantified with the RSEM algorithm (www.biomedcentral.com/1471-2105/12/323) with the option for estimation of the read start position distribution turned on.

4.18 Determination of radiolabeled leucine distribution after oral administration

Mice at day 1 after birth were starved for 30 min in a humidified chamber on a warming plate set at 37°C. Thereafter, 5 µl of radiolabeled amino acid solution (1 mM leucine, [H3]-labeled leucine 0.2 µCi/µl, 1 mM lysine, [C14]-labeled lysine 0.04 µCi/µl) was administered and the mouse was placed again in the aforementioned chamber for 30 min. Thereafter, mice were sacrificed by decapitation and plasma was collected as described before. Organs were isolated, rinsed several times with ice-cold PBS and weighted. Subsequently, organs were lysed in Solvable (Perkin Elmer, Switzerland) overnight at 50 °C and bleached with 200 µl of 30% H_2O_2. Radioactivity was determined upon addition of 12 ml of Ultima Gold scintillation liquid (Perkin Elmer, Switzerland) as described before. AA accumulation within each organ was normalized to organ weight.

4.19 Blood glucose measurement

Mice at day 1 were sacrificed by decapitation and blood glucose was measured with reactive test stripes Accu-Check ® (Roche Diagnostics, Mannheim, Germany).

4.20 Statistics

Analysis of the experimental data was performed by Graph Pad Prism 5.0. Differences between mean values of groups were tested with Student's *t*-test, one-way or two-way analysis-of-variance (ANOVA) followed by Dunnett, linear trend or Bonferroni posttests. Level of significance are given as * $p < 0.05$, ** $p < 0.01$, *** $p < 0.001$. Data are expressed as mean ± SEM.

5. Results

5.1 Original research article: "Amino acid transporter Lat4 (*Slc43a2*) is essential for mice postnatal development"

This section contains an original research article, which was submitted to the Journal of Physiology on December 2nd 2013. In revision since January 6th 2014.

All the experiments described in the manuscript were performed by Adriano Guetg with the help of Luca Mariotta, Lukas Bock, Brigitte Herzog, Ralph Fingerhut and Simone Camargo. The writing and revision of the manuscript was performed by Adriano Guetg with the help of François Verrey.

Title: Amino acid transporter Lat4 (*Slc43a2*) is essential for mice postnatal development

Authors: Adriano Guetg[1], Luca Mariotta[1], Lukas Bock[1], Brigitte Herzog[1], Ralph Fingerhut[2], Simone M.R. Camargo[1] and François Verrey[1].

Affiliation: [1]Institute of Physiology and Zurich Center of Integrative Human Physiology, University of Zurich, Switzerland. [2]University Children's Hospital, Children`s Research Center, Zurich, Switzerland

Additional information:

A) Running title: Amino acid homeostasis and postnatal development

B) Keywords: Lat4, branched-chain amino acids, postnatal development

C) Total words in the paper excluding figure legends and references: 6610

D) Corresponding Author: François Verrey

Institute of Physiology, University of Zürich

Winterthurerstr. 190, CH-8057 Zürich, Switzerland

Phone +41 44 635 50 44/46 Fax +41 635 68 14

verrey@access.uzh.ch

Key points summary:

- Amino acid transporter Lat4 (*Slc43a2*) is expressed at the basolateral membrane of epithelial cells in small intestine and kidney proximal tubule, thick ascending limb and distal convoluted tubule.
- Lat4 is a symmetric uniporter that mediates the equilibration of intra- and extracellular branched-chain amino acids, phenylalanine and methionine.
- Lack of Lat4 leads to postnatal malnutrition and early death.

Word count: 57

Abstract (max. 250 words)

Amino acid uniporter Lat4 (*Slc43a2*) mediates facilitated diffusion of branched-chain amino acids, methionine and phenylalanine, but its physiological role and subcellular localization has not been addressed yet. We report here that *Slc43a2* knock-out mice were born without phenotype at expected Mendelian frequency. Their postnatal growth was however strongly reduced and they died within 9 days such that further investigations were made within few days after birth. Lat4 immunofluorescence labeling showed a strong basolateral signal in small intestine, kidney proximal tubule and thick ascending limb epithelial cells of wild type but not *Slc43a2* null littermates and no signal in liver and skeletal muscle was observed. Experiments performed in *Xenopus laevis* oocytes demonstrated that Lat4 is a symmetrical low affinity uniporter with a $K_{0.5}$ of approximately 5 mM for both in- and efflux. Plasma amino acid concentration was decreased in *Slc43a2* null pups, in particular non-essential alanine, serine, histidine and proline. Together with an increased level of plasma long chain acylcarnitines and a strong alteration of liver gene expression, this amino acid profile indicates malnutrition. Attempts to rescue pups by decreasing the litter size or by intraperitoneal nutrients injection didn't succeed. Radioactively labeled leucine but not lysine given *per os* accumulated in small intestine of *Slc43a2* null pups suggesting defective transcellular transport of Lat4 substrates. Taken together, Lat4 is shown to be a symmetrical uniporter for neutral essential amino acids localizing at the basolateral side of (re)absorbing epithelia and to be necessary for early postnatal nutrition and development.

Abbreviations: AA, amino acid; DA, dicarboxylacylcarnitine; DCT, distal convoluted tubule; LPI, lysinuric protein intolerance; NCC, sodium-chloride cotransporter; NKCC2, sodium-potassium-chloride cotransporter 2; PT, proximal tubule; TAL, thick ascending limb.

Introduction

Dietary protein intake is an essential and tightly regulated process, which needs to meet the physiological body requirements especially during highly anabolic periods (Poncet & Taylor, 2013). The enzyme-mediated hydrolysis of the dietary proteins in the gastrointestinal lumen produces oligopeptides and individual amino acids (AAs) that are absorbed by moving sequentially across apical and basolateral cell membranes of small intestine enterocytes (Nassl *et al.*, 2011). The zwitterionic nature of AAs prevents the direct crossing of the epithelial lipid bilayer by simple diffusion and imposes the presence of membrane-spanning transporter proteins (Braun *et al.*, 2011). Severe malabsorption and aminoaciduria syndromes have been linked to defects of specific AA transporters substantiating the essential role, which transepithelial transport plays for body AA homeostasis (Verrey *et al.*, 2009; Broer & Palacin, 2011).

The luminal step of neutral AA absorption and reabsorption at the level of the small intestine and kidney, respectively, is to a large extent mediated by the apical transporter B°AT1 (*SLC6A19*). This luminal symporter uses the driving force exerted by the Na^+ gradient and the membrane potential on the co-transported Na^+ ion for the concentrative import of its neutral amino acid substrates (secondary active transport) (Rudnick et al., 2014). Interestingly, it requires a tissue-specific accessory protein for proper surface expression, specifically Ace2 in small intestine and collectrin (*TMEM27*) in the kidney proximal tubule (Danilczyk *et al.*, 2006; Camargo et al., 2009). Once inside the enterocytes or kidney proximal tubule cells, neutral AAs can be effluxed across the basolateral membrane by cooperating AA exchangers and uniporters. Indeed, all neutral AAs can be effluxed by the major basolateral neutral AA antiporter (obligatory exchanger), the

heterodimeric LAT2-4F2hc (*SLC7A8-SLC3A2*). It is however important to realize that for each exported AA this antiporter imports another AA. Thus, this antiporter does not perform a net transmembrane AA efflux (Meier *et al.*, 2002). Surprisingly, no genetic diseases involving defects of LAT2-4F2hc have been described yet, whereas mutations in the other basolateral antiporter y^+LAT1-4F2hc (*SLC7A7-SLC3A2*), which exchanges preferentially intracellular cationic AAs against neutral AAs and $Na^{+,}$ cause the autosomal recessive disease lysinuric protein intolerance (LPI) (Borsani *et al.*, 1999). The respective physiological roles of both exchangers were also investigated using knock-out (KO) mice. While the lack of LAT2 resulted in a mild phenotype with a minor aminoaciduria (Braun *et al.*, 2011), the lack of y^+LAT1 caused intrauterine growth restriction and resulted in premature death for about 90% of the newborn *Slc7a7*$^{-/-}$ homozygous mice (Sperandeo *et al.*, 2007).

To achieve a net efflux of all different AAs from small intestine enterocytes and proximal kidney tubule epithelial cells, transporters are required that mediate the net efflux of some AAs that can then recycle into the cells via the above mentioned antiporters and thereby drive their efflux activity (Verrey *et al.*, 2009). The T-type aromatic AA uniporter TAT1 (*Slc16a10)* represents the best characterized such transporter expressed at the basolateral membrane (Ramadan *et al.*, 2006; Ramadan *et al.*, 2007). Using the *Xenopus laevis* oocytes expression system it has indeed been shown to mediate the facilitated diffusion of the essential aromatic AAs phenylalanine, tryptophan and tyrosine with symmetric apparent affinities (i.e. $K_m \approx 30$ mM for) and thereby drive the efflux of other LAT2-4F2hc substrates such as the non-essential AA glutamine (Ramadan *et al.*, 2006; Ramadan *et al.*, 2007). Recently, we characterized the physiological role of TAT1 using *Slc16a10* deficient

mice. Interestingly, these mice presented a mild phenotype with increased plasma, kidney and muscle aromatic AAs, independently of dietary protein quantity, combined with a major aromatic aminoaciduria under high protein diet (Mariotta *et al.*, 2012). The lack of neurological symptoms and important metabolic dysfunctions despite the defective intestinal absorption of aromatic AAs like phenylalanine, which is the metabolic precursors of the hormone thyroxine and the neurotransmitter dopamine, suggested a possible compensatory mechanism by another basolateral uniporter. We suggested that the uniporter LAT4 (*SLC43A2*) could play this role.

LAT4 belongs to the SLC43 family which includes two additional members: LAT3 (*SLC43A1*), which is a uniporter for large essential neutral AAs and has been shown to be upregulated in liver and skeletal muscle upon starvation and displays only a low mRNA expression level in small intestine and kidney (Babu *et al.*, 2003; Fukuhara *et al.*, 2007), and the orphan transporter EEG1 (*SLC43A3*). The latter gene product has been recently shown by Bodoy *et al.* to be prominently expressed in human liver and heart and, based on immunohistochemistry, to be expressed at the basolateral membrane of human kidney proximal convoluted tubule (Bodoy *et al.*, 2005). LAT4 shows only about 30% identity with EEG1 and has been shown by Northern blot analysis of human RNA to be highly expressed in placenta, peripheral blood leucocytes and kidney and additionally, by Northern blot analysis of mouse RNA, to be expressed in small intestine and brain (Bodoy *et al.*, 2005). Microarray data available on internet (BioGPS.org) confirm these localizations and additionally show substantial expression in macrophages, microglia and osteoclasts. Based on *in situ* hybridization, Lat4 was suggested to be expressed in kidney distal tubule and collecting duct and the images suggested also that it is expressed in

proximal tubule. In small intestine, the signal appeared to localize more to crypt cells (Bodoy *et al.*, 2005). Lat4 mRNA was also detected in cell lines isolated from mouse kidney proximal tubule, which is consistent with the mRNA expression in isolated proximal tubules reported by Cheval *et al.* (Cheval *et al.*, 2011). Furthermore, kinetic analysis of phenylalanine uptake in these cells suggested Lat4 involvement supporting the possibility that this uniporter might play a role in proximal tubule AA reabsorption.
The preferential substrates of LAT4 are only essential AAs, specifically the branched-chain ones (leucine, isoleucine, valine) and additionally phenylalanine and methionine (Bodoy *et al.*, 2005; Wu, 2009). To test the physiological role of Lat4 in whole-body AA homeostasis and epithelial transport, we generated a global *Slc43a2*$^{-/-}$ KO mouse and provide in the following report the analysis of its phenotype.

Materials and Methods

Ethical approval. All procedures for mice handling and experimental interventions were according to the Swiss Animal Welfare laws and approved by the Kantonales Veterinäramt Zürich.

Generation of *Slc43a2*/*Lat4*$^{-/-}$ *KO* mice by gene trapping. The *Slc43a2*$^{-/-}$ KO mouse was produced by the Phenogenomic Center of Toronto (www.phenogenomics.ca). Embryonic stem (ES) cell lines were mutated by insertional mutagenesis using a UPA gene trap vector (Shigeoka *et al.*, 2005) in the 6th intron of the *Slc43a2* gene. Cells were prepared for aggregation with diploid embryos to produce chimeric mice. R1 cells were in a 129 mouse background, whereas the germline was tested by crossing the chimera to CD-1 mice and

assessing coat color. The interruption of the gene leads to the production of a truncated transcript presumably subject to nonsense mediated decay and thus of low abundance. Mice were bred into C57BL/6 background. All animals were housed in standard conditions and fed a standard diet prior experiment.

Antibodies. Anti-mouse Lat4 antibodies targeted to the C-terminal peptide (N-CQLQQKREDSKLFL-C) and anti-mouse Tmem27 antibodies targeted to the C-terminal peptide (N-CDPLDMKGGHINDGFLT-C) were raised in rabbit and guinea-pig, respectively (Pineda, Berlin, Germany). Anti-mouse NCC (Loffing *et al.*, 2004), anti-mouse NKCC2 (Kaplan *et al.*, 1996), anti-mouse Mdr1 (Fickert *et al.*, 2001) were previously characterized.

Immunofluorescence. Organs were isolated and immediately frozen in liquid propane. 7 µm sections were prepared on Superfrost®Plus Menzel slides (Gerhard Menzel GmbH, Braunschweig, Germany). For Lat4 and NKCC2 colocalization, 4 µm consecutive sections were prepared. Sections were then fixed with methanol at -20 °C for 90 seconds, rehydrated for 15 min at room-temperature (RT), washed three times for 5 min with phosphate-buffered solution (PBS) at RT. For Lat4 detection, epitope retrieval was performed by incubating slides in 10 mM sodium citrate pH 6.0 for 10 min at 98 °C with a microwave (Histos 3, Milestone, USA). For NKCC2 detection, no epitope retrieval was performed. Sections were then washed again three times for 5 min with PBS at RT and incubated with blocking solution (2% bovine serum albumin, 0.04% Triton X-100 in PBS pH 7.4) for 1 hour at RT. Primary antibodies were diluted in blocking solution and incubated overnight at 4°C with the respective dilutions: 1:500 for Lat4, 1:1000 for Tmem27, 1:2000 for NKCC2, 1:500 for NCC. Sections were then washed three times for 5 min in PBS at RT. The

following secondary antibodies were applied with 1:500 dilutions for 1 hour at RT: Alexa Fluor® 488 anti-rabbit, Alexa Fluor® 594 anti-rabbit and Alexa Fluor® 568 anti-guinea-pig. Staining of nuclei was performed with 4',6-diamidino-2-phenylindole (DAPI) at 1:500 dilution.

Morphological analysis of organs. Organs isolation, 7 µm sections preparation and section fixation were performed as described before. Classical Hematoxylin & Eosin staining was performed as described elsewhere (Mariotta *et al.*, 2012).

Cloning of hLAT4 cDNA and cRNA synthesis. Human LAT4 cDNA in pTLN vector was kindly provided by Manuel Palacin (Bodoy *et al.*, 2005). The construct was linearized using the *BglII* restriction site and cRNA was synthesized using the MEGAscript high-yield *in vitro* transcription kit (Ambion, Austin, TX) according to manufacturer's instructions.

***Xenopus laevis* oocytes preparation and cRNA injection.** Oocytes at stage IV as described in (Dumont, 1972) were treated with collagenase A for 2-3 h at room temperature in Ca^{2+}-free buffer (82.5 mM NaCl, 2 mM MgCl2 and 10 mM HEPES pH 7.4) and kept at 16°C in Modified Barth's solution (88 mM NaCl, 1 mM KCl, 0.82 mM $MgSO_4$, 0.41 mM $CaCl_2$, 0.33 mM $Ca(NO_3)_2$, 2.4 mM $NaHCO_3$, 10 mM HEPES, 5 mg/l Gentamicin, 5 mg/l Doxycycline). Remaining follicular layers were manually removed. 25 ng of LAT4 cRNA was injected and oocytes were incubated for 3 days at 16°C in ND96 solution (96 mM NaCl, 2 mM KCl, 1 mM $MgCl_2$, 1.8 mM $CaCl_2$, 5 mM HEPES-Tris pH 7.4, supplemented with 50 mg/l tetracycline).

Uptake of amino acids in *Xenopus laevis* oocytes. Oocytes were washed six times with 2 ml Na^+-buffer (100 mM NaCl, 2 mM KCl, 1 mM CaCl2, 1 mM MgCl2, 10 mM HEPES pH 7.4) and then pre-warmed for 2 minutes at 25°C in a water bath. Subsequently, the pre-

warming solution was aspirated and 100 µl of Na^+-buffer containing unlabeled phenylalanine at the indicated concentrations together with [^{3}H]-L-phenylalanine (10 µCi/ml) as tracer (Hartmann Analytic, Braunschweig, Germany) were added. Oocytes were then incubated for 10 minutes at 25°C. Thereafter, uptake solution was removed, oocytes were washed six times with 2 ml ice-cold Na^+-buffer and separately dissolved in 250 µl 2% SDS under agitation for at least 30 min. Upon addition of 3 ml scintillation fluid (Emulsifier-Safe™), radioactivity was counted on a liquid scintillation counter (TRI-CARB 2900TR, Packard Instrument, Meriden, CT). Uptake values were corrected by subtracting the values obtained from non-injected oocytes. Curves corresponding to the Michaelis-Menten equation were fitted to the data sets using GraphPad Prism 5.0 (GraphPad Software, San Diego, CA).

Efflux of amino acids in *Xenopus laevis* oocytes. Oocytes were injected with 50 nl of different phenylalanine solutions (10 mM, 25 mM, 50 mM, 100 mM and 200 mM) together with [^{3}H]-L-phenylalanine (0.2 µCi/µl) as tracer. Assuming an oocyte volume of about 400 µl (Taylor & Smith, 1987), the resulting oocyte internal phenylalanine concentration upon injection corresponded respectively to 1.11 mM, 2.78 mM, 5.56 mM, 11.11 mM and 22.22 mM. Oocytes were subsequently washed four times in ND96 solution and 200 µl ND96 were given to each oocyte. Efflux was allowed to take place for 10 minutes at 25°C before recovering the ND96 solution and washing the oocyte four times with ND96. For the oocytes lysis and data analysis, see "Uptake of amino acids in *Xenopus laevis* oocytes".

Metabolic cage experiments with *Slc43a2*$^{+/-}$ mice. Seven-week old *Slc43a2*$^{+/-}$ and *Slc43a2*$^{+/+}$ littermates were fed a normal protein diet (20% casein) in metabolic cages.

Experimental setup and determination of amino acids in urine and plasma were performed as described elsewhere (Mariotta *et al.*, 2012).

RNA extraction and real-time PCR. Mice at the indicated day after birth were sacrificed by decapitation and organs were immediately rinsed several times with ice-cold PBS prior to being rapidly frozen in liquid propane until further use. Total RNA was extracted and reverse transcription was performed as described elsewhere (Ramadan *et al.*, 2006). For real-time PCR, 10 ng of cDNA template were used and the reaction was set according to Applied Biosystems recommendations (TaqMan® Universal PCR master mix, Applied Biosystems). The abundance of target mRNAs was standardized relative to 18S ribosomal RNA. Primers and probes for Lat2 (*Slc7a8*), 4F2hc (*Slc3a2*), y^+Lat1 (*Slc7a7*), y^+Lat2 (*Slc7a6*), Asct2 (*Slc1a5*), Tat1 (*Slc16a10*) and B°AT1 (*Slc6a19*) were previously described (Moret *et al.*, 2007; Mariotta *et al.*, 2012). For Lat4 detection, the following primers and probe were used: 5'GCTGATTGCATATGGAGCAAGTAAC 3' (for), 5'CGAAGTGAACGTCATGCACAT 3' (rev) and 5'CTCTCTGTGCTCATCTTTATCGCCTTGGC3' (probe).

Plasma amino acid and acylcarnitine measurements. Amino acids and acylcarnitines were measured after extraction with methanol without derivatisation (Neobase Kit, Perkin Elmer, Turku, Finnland) on an Acquity-TQD tandem mass spectrometer (Waters, Milford, USA). Briefly, 3 µL of plasma were spotted onto prepunched plain filter paper (Ahlstom 226) in 96-well plain uncoated microtiter plates. Amino acids and acylcarnitines were extracted with 100 µL methanolic extraction solution containing stable isotope labelled internal standards by shaking for 45 min at 45°C. 30 µL of extract were then injected with a

flow rate of 10 µL/min directly into the tandem mass spectrometer and measured afterwards in MRM-mode (multiple reaction monitoring).

RNA-Sequencing analysis of liver. Organs were isolated and RNA was extracted as described before. The quality of the isolated RNA was determined with a Qubit® (1.0) Fluorometer (Life Technologies, California, USA) and a Bioanalyzer 2100 (Agilent, Waldbronn, Germany). Only those samples with a 260 nm/280 nm ratio between 1.8–2.1 and a 28S/18S ratio within 1.5–2 were further processed. The TruSeq RNA Sample Prep Kit v2 (Illumina, Inc, California, USA) was used in the succeeding steps. Briefly, total RNA samples (100-1000 ng) were polyA enriched and then reverse-transcribed into double-stranded cDNA. The cDNA samples were fragmented, end-repaired and polyadenylated before ligation of TruSeq adapters containing the index for multiplexing. Fragments containing TruSeq adapters on both ends were selectively enriched with PCR. The quality and quantity of the enriched libraries were validated using Qubit® (1.0) Fluorometer and the Caliper GX LabChip® GX (Caliper Life Sciences, Inc., USA). The product is a smear with an average fragment size of approximately 260 bp. The libraries were normalized to 10 nM in Tris-Cl 10 mM, pH 8.5 with 0.1% Tween 20. The TruSeq PE Cluster Kit v3-cBot-HS or TruSeq SR Cluster Kit v3-cBot-HS (Illumina, Inc, California, USA) was used for cluster generation using 10 pM of pooled normalized libraries on the cBOT. Sequencing were performed on the Illumina HiSeq 2000 paired end at 2 X101 bp or single end 100 bp using the TruSeq SBS Kit v3-HS (Illumina, Inc, California, USA). RNA-seq reads were quality-checked with fastqc which computes various quality metrics for the raw reads. Reads were aligned to the genome and transcriptome with Tophat v1.3.3. Before mapping, the low quality ends of the reads were clipped (3 bases from the read start and 10

bases from the read end). Tophat v1.3.3 was run with default options. The fragment length parameter was set to 100 bases with a standard deviation of 100 bases. Based on these alignments the distribution of the reads across genomic features was assessed. Isoform expression was quantified with the RSEM algorithm (www.biomedcentral.com/1471-2105/12/323) with the option for estimation of the read start position distribution turned on. Raw data are available on the NCBI BioProject platform (http://www.ncbi.nlm.nih.gov/bioproject/) under the BioProject ID: PRJNA226691.

Determination of radiolabeled leucine and lysine distribution after oral administration. Mice at day 2 after birth were starved for 30 min in a humidified chamber on a warming plate set at 37°C. Thereafter, 5 µl of radiolabeled amino acid solution (1 mM leucine, [^{3}H]-L-leucine 0.2 µCi/µl, 1 mM lysine, [^{14}C]-L-lysine 0.04 µCi/µl) was administered and the mouse was placed again in the aforementioned chamber for 30 min. Thereafter, mice were sacrificed by decapitation and plasma was collected as described before. Organs were isolated, rinsed several times with ice-cold PBS and weighted. Subsequently, organs were lysed in Solvable (Perkin Elmer, Switzerland) overnight at 50 °C and bleached with 200 µl of 30% H_2O_2. Radioactivity was determined upon addition of 12 ml of Ultima Gold scintillation liquid (Perkin Elmer, Switzerland) as described before. AA accumulation within each organ was normalized to organ weight.

Blood glucose measurement. Mice at day 2 were sacrificed by decapitation and blood glucose was measured with reactive test stripes Accu-Check ® (Roche Diagnostics, Mannheim, Germany).

Results

Lat4 protein absence in *Slc43a2*$^{-/-}$ mice and localization in wild type mice epithelia

Immunofluorescence images of the small intestine and kidney proximal tubule of 3 days old pups using anti-Lat4 antibody confirmed the absence of Lat4 protein in *Slc43a2* null pups in comparison with wild type littermates (Fig. 1A-D). The integrity of the KO tissues showing no Lat4 signal was demonstrated by co-labeling with specific markers, for instance Tmem27 for kidney and Mdr1 for liver. The lack of Lat4 signal in *Slc43a2* null mice additionally demonstrated the specificity of the immunofluorescence signals obtained using our antibody. Indeed, Fig. 1 shows Lat4 expression on the basolateral membrane of kidney tubule (panel A) and small intestine (panel C) epithelial cells, whereas there is no equivalent signal in *Slc43a2* null mice (panels B and D). As expected based on previous mRNA data (Bodoy *et al.*, 2005), Lat4 expression was not detected in skeletal muscle and liver wild type and KO pups (Fig. 1E-H) (Bodoy *et al.*, 2005).

Whereas a strong Lat4-specific labeling was detected on small intestine villi at the basolateral membrane of enterocytes, we detected no clear specific Lat4 signal within the crypts (Fig. 2A). To investigate in more details the localization of Lat4 along the mouse kidney nephron, we performed co-stainings with tubule-specific markers. The strong expression of Lat4 in the proximal tubule (PT) was confirmed by co-labeling of the SLC6-transporter accessory protein Tmem27 (Danilczyk 2006) (Fig. 2B) and the colocalization with the aromatic AA uniporter Tat1 (Fig. 2C and D) (Ramadan *et al.*, 2006). A weaker expression of Lat4 was detected in the distal convoluted tubule (DCT) co-labeled with the apical sodium-chloride cotransporter (NCC) (Fig 2E), whereas a strong expression of Lat4 was revealed in the thick-ascending limb of Henle's loop (TAL) by labeling the sodium-

potassium-chloride cotransporter 2 (NKCC2) in consecutive sections (Fig. 2F and G) (Wagner *et al.*, 2008). Taken together, our immunofluorescence data show that Lat4 protein is expressed at the basolateral membrane of small intestine enterocytes and kidney proximal tubule, thick ascending limb and, to a minor extent, distal convoluted tubule.

Kinetic properties of LAT4 expressed in *Xenopus laevis* oocytes

In the original report by Bodoy *et al.,* Lat4 was suggested to function as a uniporter based on the observation that it facilitated the efflux of phenylalanine from *Xenopus laevis* oocytes independent of extracellular AAs (Bodoy *et al.*, 2005). To determine the kinetic properties of Lat4, we performed a series of uptake and efflux rate measurements with different concentrations of phenylalanine using the *Xenopus laevis* oocytes expression system (Fig. 3). Fitting Michaelis-Menten kinetics curves to the experimental phenylalanine uptake results, we derived a K_m constant of 5.2 ± 0.5 mM (R^2 = 0.89). This value corresponds to a low-affinity transport comparable to that previously reported by Bodoy *et al.* (Bodoy *et al.*, 2005), but no additional high-affinity/low capacity component was noticed (Fig. 3A). To determine the efflux kinetic properties, oocytes were injected with increasing concentrations of phenylalanine and the resulting intracellular concentration of phenylalanine were estimated assuming an oocyte volume of 400 nl as previously described by Meier *et. al.* (Meier *et al.*, 2002). Fitting the Michaelis-Menten kinetics to the efflux values measured after 10 min yielded a low-affinity K_m of 6.0 ± 1.4 mM (R^2 = 0.66), which is comparable with the apparent affinity value obtained for the uptake (Fig. 3B). Based on these results, we conclude that Lat4 shows symmetric intracellular and extracellular apparent affinities for phenylalanine.

Growth defect, metabolic alterations and early postnatal lethality of *Slc43a2*$^{-/-}$ mice

Slc43a2$^{-/-}$ mice generated from *Slc43a2*$^{+/-}$ intercrosses were born without significant deviation from the expected Mendelian ratio ($p = 0.48$, χ^2-test with $n > 100$ pups), with a normal weight and no detectable pathological signs at birth. They indeed presented a normal skin color and the presence of a white area at the left side of the abdomen, i.e. the so-called "milk spot", confirming normal milk delivery by the mother. However, monitoring of the postnatal weight revealed that *Slc43a2*$^{-/-}$ pups gained only very little weight compared to littermates (Fig. 4A and 4B). Furthermore, they all died within few days after birth, as shown in the Kaplan-Meier survival analysis (Fig. 4C). Indeed, more than 50% of the observed *Slc43a2*$^{-/-}$ pups died until postnatal day 7 and the mortality reached 100% at day 10.

In order to obtain more information about the possible pathophysiological mechanisms underlying the early lethality we measured the concentration of AAs in the plasma of 3 days old *Slc43a2*$^{-/-}$ pups and compared it to age-matched littermates (Fig. 5A). We observed a major decrease of certain AAs of *Slc43a2*$^{-/-}$ mice in comparison with *Slc43a2*$^{+/+}$: The highest relative difference was observed for non-essential amino acids that are not substrates of Lat4, for instance proline with about 75% reduction followed by histidine, serine and alanine. Most other Lat4 substrates were also reduced in *Slc43a2*$^{-/-}$ mice, methionine and tyrosine strongly (>50%) and branched-chain AAs less, but their decrease was not statistically significantly. The only Lat4 substrate that didn't appear to be decreased was phenylalanine. Thus, this blood AA pattern does not reflect a specific lack of Lat4 substrates, but results probably from the interplay of transport and metabolic pathways that are altered in the *Slc43a2*$^{-/-}$ mice. Additionally to the decrease in plasma amino acids, an

increase of plasma acylcarnitine-conjugated fatty acids, in particular of dicarboxylic acids and long chain unsaturated fatty acids was detected that also suggests malnutrition (Fig. 5B and C). As regards glucose homeostasis, *Slc43a2*$^{-/-}$ mice sacrificed at day 2 showed a high blood concentration variability compared to *Slc43a2*$^{+/+}$ and *Slc43a2*$^{+/-}$ mice (Fig. 5D). Hypothesizing that this variability was due to different feeding status of single animals and that *Slc43a2*$^{-/-}$ pups might display a defect in glucose disposal (impaired insulin release) and gluconeogenesis, pups were starved 30 min before sacrifice and blood collection (Fig. 5E). Indeed, in these conditions all *Slc43a2*$^{-/-}$ mice displayed a reduction in blood glucose concentration of about 50% compared to their wild type littermates. Heterozygous *Slc43a2*$^{+/-}$ mice showed in this and also in all other tested parameters no difference with their *Slc43a2*$^{+/+}$ littermates.

Because *Slc43a2*$^{-/-}$ pups displayed a failure to grow and signs of malnutrition, we made attempts to rescue them. Considering that an early defect in weight gain might represent a competitive disadvantage for obtaining breastfeeding within a large litter, we decreased this potential disadvantage by removing all *Slc43a2*$^{+/-}$ littermates on day 3, leaving only an equal number of *Slc43a2*$^{+/+}$ and *Slc43a2*$^{-/-}$ pups (Supplementary Figure 1). However, also in the context of reduced litters, *Slc43a2*$^{-/-}$ mice did not grow and/or survive better. Another attempt to compensate malnutrition by subcutaneous administration of an AA-containing solution (Aminoven 10%, Fresenius KABI, 80 µl injection twice a day) did also not increase the weight gain and/or the lifespan of *Slc43a2*$^{-/-}$ mice.

Liver morphology and gene expression of *Slc43a2* null pups

Since the liver plays a central role in nutrients metabolism, we investigated the possible impact of *Slc43a2* defect on its morphology and gene expression pattern. Histological staining showed indeed sites of leucocyte infiltration in its periportal regions (Fig. 6B). Liver RNA-sequencing identified 16'078 transcripts as 'present' (Tophat software) with 1433 displaying a statistically significant ($p < 0.01$) differential expression (Fig. 6A). From these transcripts, the expression of 144 was changed more than three-fold, 77 up- and 67 downwards (Supplementary Table 1). Among the upregulated genes, many are known to be involved in liver regeneration (*Dmbt1* (Bisgaard *et al.*, 2002)), cell proliferation (*Htr2b* (Soll *et al.*, 2010)), tissue remodeling (*Mep1a* and *Mep1b* (Sterchi *et al.*, 2008)) and detoxification (*Gpx6 and Ggt6* (Gridley *et al.*, 2011) (Heisterkamp *et al.*, 2008)). Interestingly, the transcripts encoding acetyl-CoA carboxylase β (*Acab*), involved in lipogenesis (Postic & Girard, 2008) and glucokinase (*Gck*), involved in liver gluconeogenesis (Massa *et al.*), were also upregulated. In contrast, genes involved in fatty acids biosynthesis like *Fas, Srbp1* and *Scd1* were not significantly changed. As expected based on the leucocyte infiltration, *Cyp2a5* and *Ceacam3* expression was increased (Sipowicz *et al.*, 1997). The downregulation of the transcripts *Car3, Dio3* and *Inmt* as well as of genes involved in hepatobiliary cholesterol excretion (*Abcg5* and *Abcg8* (Back *et al.*, 2013)) and circadian clock (*Dbp* (Ando *et al.*, 2011)) similarly suggest major metabolic changes, inflammation, toxicity and regeneration at the level of the liver (Hsieh *et al.*, 2009; Dudek *et al.*, 2013) that might explain in part the increase in plasma fatty acids and the selective decrease of plasma AAs.

At the level of the kidney that also plays an important role for the systemic metabolism of amino acids (Makrides *et al*., 2014 Comp Physiol), we tested the expression of AA transporters, but did not identify any major alterations in *Slc43a2*$^{-/-}$ mice (Fig. 6C).

Accumulation of leucine in the proximal part of the small intestine

The major metabolic changes described above suggested that the early death of *Slc43a2*$^{-/-}$ mice might be due to a status of malnutrition. Since we showed that Lat4 is expressed at the basolateral membrane of enterocytes (Fig. 2), we hypothesized that this malnutrition might result from a defective intestinal AA absorption. To test this hypothesis, we starved pups for 30 min and then fed them with 5 µl of an AA solution containing 1 mM of each leucine and lysine with corresponding ^{3}H and ^{14}C tracers. Leucine was chosen as Lat4 substrate because it is not transported by the other basolateral uniporter Tat1, whereas lysine was chosen because it is not transported by Lat4. Upon administration of this AA mixture, we monitored the appearance of the labeled AAs in plasma and their accumulation in different organs after 30 min (Fig. 7). Compared to wild type littermates, pups lacking Lat4 displayed a marked 2-fold increased retention of leucine, but not of lysine, in the first part of the small intestine (Fig. 7A and C). This selective retention of the Lat4 substrate leucine in the small intestine of *Slc43a2* pups suggests its intracellular retention in the absence of basolateral Lat4. This selective retention was not associated with a visible morphological difference as observed on hematoxylin and eosin stained small intestine sections. It also didn't lead to differences in terms of AA appearance in plasma or levels in other organs after 30 min (Fig. 7B and 7D).

Discussion

Lat4 is considered a 'system L' transporter because it transports large neutral AAs independent of Na^+. This functional denomination however does not include other important transport characteristics like transport type and affinity that clearly differentiate Lat4 from the classical system L transporters Lat1 and Lat2 (Lat1-4F2hc/*Slc7a5-Slc3a2* and Lat2-4F2hc/*Slc7a8-Slc3a2*). Indeed, as originally suggested by Bodoy *et al.* (Bodoy *et al.*, 2005), Lat4 functions as a uniporter (facilitated diffusion pathway) and we show here that it does this with a low, symmetrical apparent affinity (Fig. 3). These functional characteristics contrast with those of the classical system L transporters Lat1 and Lat2 that function as asymmetric antiporters with high apparent affinity for the uptake of their substrates (Meier et al., 2002). Additionally, the selectivity of Lat4 is more limited and includes only essential AAs, specifically the branched-chain ones plus phenylalanine and methionine. Since the *in vivo* role of this AA transporter has yet not been investigated, we here further analyzed its localization and tested its physiological function using a newly generated general KO mouse model.

The main observation reported here is the fact that mice defective in Lat4 are born at a normal Mendelian frequency with no recognizable phenotype but do nearly not grow after birth and die within a few days, despite the fact that breast feeding is indicated by a normal 'milk spot'. The question is thus what functional defect the lack of Lat4 provokes, which leads to this postnatal problem. The phenotype does not appear to depend on the genetic background since it was not modified by backcrossing for 6 generations with C57BL/6 or S129 mice. Despite the fact that attempts to rescue the pups by litter size reduction

(decreased competition) or parenteral nutritional supplementation didn't succeed, we consider it likely that this postnatal phenotype is largely due to defective intestinal absorption of AAs and possibly of consecutive enterocyte malfunction.

Lat4 is a basolateral uniporter for essential neutral AAs in small intestine and kidney tubule

A first crucial aspect towards understanding the function of Lat4 is its tissue and subcellular localization. In the original study of Bodoy *et al.*, which reported its identification and mRNA expression in human and mouse tissues, Lat4 mRNA was shown to be present at high levels in placenta, kidney and small intestine as well as at lower levels in several other tissues and in a proximal tubule cell line (Bodoy et al., 2005). Additionally, expression data from microarray analysis available on internet (Biogps.com) indicate a strong expression also in macrophages, microglia and osteoclasts. As previously hypothesized by us, we show here using a newly generated antibody that Lat4 localizes to the basolateral membrane of AA transporting cells of small intestine and kidney proximal tubule and confirm the selectivity of the staining at these locations using the KO mouse model. These images show that Lat4 is expressed in the small intestine at a much higher level in the villi than in the crypts, similar to other AA transporters involved in transepithelial transport (Fig. 2A) (Dave *et al.*, 2004). These data strongly support the hypothesis that Lat4 plays an important role for the (re)absorption of AAs. Interestingly, in kidney, a strong basolateral signal is present next to proximal tubule also in thick ascending limb and a weaker one in distal convoluted tubule (Fig. 2E-G). The low level or absence of Lat4 protein expression in liver

and skeletal muscle suggested by previous mRNA data is also confirmed by our immunofluorescence results (Fig. 1E-H).

As demonstrated in this study with expression experiments in *Xenopus laevis* oocytes, Lat4 is a symmetrical uniporter with low affinity for its substrates (Fig. 3). Thus, at physiological substrate concentrations, its directional transport activity is proportional to the transmembrane substrate concentration difference. This allows Lat4, if expressed at a sufficiently high level, to mediate the equilibration of its AA substrates (branched chain AAs, phenylalanine and methionine) between the extracellular space and the cytosol. It can thus thereby mediate a directional transport of its substrates across the plasma membrane, for instance their basolateral efflux following luminal uptake from the intestinal lumen or primary urine. We postulate that this directional basolateral efflux transport represents also a recycling pathway for AAs that are taken up across the same basolateral membrane with high affinity by the parallel localized heterodimeric antiporters *Slc7a8-Slc3a2*/Lat2-4F2hc and *Slc7a7-Slc3a2*/y^+Lat1-4F2hc. Such a high affinity uptake of essential AAs by these antiporters allows them to efflux in exchange non-essential AAs present mostly at much higher concentration than essential amino acids in these epithelial cells. Thus Lat4 may exert a quantitative control of the Lat2 and y^+Lat1 antiporter efflux activity by recycling to the outside the essential AAs they take up in exchange. Correspondingly, the expectation is that the lack of Lat4 could affect the transepithelial transport of other, in particular non-essential AAs. Such a functional relationship/cooperation with antiporters for the efflux of non-essential AAs has previously been demonstrated in the *Xenopus laevis* oocytes expression system and *in vivo* for the aromatic AA transporter Tat1, another essential AA uniporter expressed at the basolateral membrane of transporting epithelial cells (Ramadan

et al., 2007; Mariotta et al., 2012). However, in the present case functional experiments aiming at testing the impact of Lat4 defect on the transport of AAs were strongly limited by the fact that Lat4 mice did not develop normally and died a few days after birth.

As regards Lat4 localization, an intriguing observation is that Lat4 is expressed at a high level also in kidney thick ascending limb, as previously shown at the mRNA level (Cheval *et al.*, 2011). We postulate that the basolateral expression of Lat4 in these cells plays a role rather for energy metabolism than AA transepithelial transport and that these cells might actually import branched-chain AAs via Lat4 to use them as catabolic substrates for the production of ATP or to drive the influx of non-essential AAs, such as glutamine, that then function as metabolic fuel (opposite net transport directions compared to transepithelial transport).

Postnatal failure to grow, malnutrition and death of Lat4 knockout mice

The fact that newborn Lat4 null pups were born without recognizable phenotype and at normal Mendelian frequency and nearly didn't grow after birth despite a normal 'milk spot', suggested that there is a main problem linked to the enteral absorption of nutrition or metabolism. Indeed, based on the expression of Lat4 in small intestine enterocytes (Fig. 2A), it is tempting to speculate that a defect in AA absorption could be at the origin of the growth defect.

Indeed, the metabolic status of the *Slc43a2*$^{-/-}$ pups already 3 days after birth shows many analogies with starvation, despite the presence of a milk spot. At first glance surprisingly, methionine is the only Lat4 substrate to be highly decreased in their plasma, whereas branched-chain AAs and phenylalanine show only a minor reduction. In contrast, many of

the non-essential amino acids are markedly decreased, mostly alanine and proline. However, based on the suggested function of Lat4 as a 'gate keeper' for the epithelial basolateral efflux of non-essential AAs via antiporters (see above), it is not surprising that a *Slc43a2*$^{-/-}$ KO-induced defect in AA absorption may lead to a catabolic state in which the decrease in non-essential AAs is more marked than that of essential ones.

Interestingly, non-essential AAs are also specifically decreased in fasted children (Wolfsdorf *et al.*, 1982) and upon prolonged endurance exercise, in particular alanine and proline that are central for AA metabolism and gluconeogenesis (Ji *et al.*, 1987; Huq *et al.*, 1993). Also the decrease in tyrosine, histidine and serine can be explained by their catabolic usage to provide substrates for the Krebs cycle. The increase in plasma acylcarnitine-conjugated dicarboxylic and long-chain unsaturated fatty acids in *Slc43a2*$^{-/-}$ mice is an additional metabolic fingerprint indicating that the *Slc43a2*$^{-/-}$ pups are in a state of starvation (Costa *et al.*, 1999; Hunt & Alexson, 2002). Additionally, the histological examination and the gene expression analysis of the liver, by indicating processes of inflammation, regeneration and alteration of glucose and fatty acids metabolism, further indicated that *Slc43a2* null pups suffered from malnutrition. Indeed, an alteration in glucose metabolism, which is a hallmark of nutritional defects in children (Bandsma *et al.*, 2010; Spoelstra *et al.*, 2012) was also present in *Slc43a2*$^{-/-}$ mice as shown by the marked decrease in blood glucose concentration measured upon 30 min starvation.

The hypothesis that Lat4 impacts on AA absorption was further supported by our observation that leucine administered orally was retained in the proximal part of the small intestine of *Slc43a2*$^{-/-}$ mice unlike lysine which is not a Lat4 substrate. This suggests that leucine, taken up luminally, accumulated in small intestine enterocytes from which it could

not be efficiently released basolaterally. However, we didn't observe in these mice a concomitant alteration in plasma appearance or organ accumulation of leucine such that this experiment did not verify a possible major defect in AA absorption. It is however possible that the non-physiological administration of two AAs at a high concentration (1 mM each) bypassed a defect preventing sufficient absorption from mother's milk.

An interesting observation is that out of five mouse KO models of small intestine and kidney proximal tubule AA transporters the KO of Lat4 is only the second that leads to a lethal phenotype. Neither the lack of luminal B^0AT1 transporter, nor the lack of the basolateral L-type antiporter Lat2 (*Slc7a8*) and the aromatic amino acid uniporter Tat1 (*Slc16a10*) prevent normal life and reproduction in laboratory conditions. In contrast to these three models and to the Lat4 pups, animals lacking the cationic amino acid antiporter y^+Lat1 displayed already marked intrauterine growth retardation and metabolic alterations and did mostly not survive more than 24h, if born alive. Thus, the KO of Lat4 is the first AA defect leading to severe postnatal malnutrition followed by early death. Many observations presented here suggest that the primary cause for the malnutrition of *Slc43a2*$^{-/-}$ pups may be a defect in AA absorption from the gut. However, it cannot be ruled out that the observed malnutrition syndrome could be due to an insufficient suckling drive or another alteration preventing the appropriate use of mother's milk as nutrition source.

In conclusion, we provided here the first characterization of a total *Slc43a2* KO mouse model. According to the reported early lethal phenotype, we conclude that Lat4 is an essential AA transporter required for the proper postnatal nutrient absorption and development.

References

Ando H, Kumazaki M, Motosugi Y, Ushijima K, Maekawa T, Ishikawa E & Fujimura A (2011). Impairment of peripheral circadian clocks precedes metabolic abnormalities in ob/ob mice. *Endocrinology* **152,** 1347-1354.

Babu E, Kanai Y, Chairoungdua A, Kim DK, Iribe Y, Tangtrongsup S, Jutabha P, Li Y, Ahmed N, Sakamoto S, Anzai N, Nagamori S & Endou H (2003). Identification of a novel system L amino acid transporter structurally distinct from heterodimeric amino acid transporters. *J Biol Chem* **278,** 43838-43845.

Back SS, Kim J, Choi D, Lee ES, Choi SY & Han K (2013). Cooperative transcriptional activation of ATP-binding cassette sterol transporters ABCG5 and ABCG8 genes by nuclear receptors including Liver-X-Receptor. *BMB Rep* **46,** 322-327.

Bandsma RH, Mendel M, Spoelstra MN, Reijngoud DJ, Boer T, Stellaard F, Brabin B, Schellekens R, Senga E & Heikens GT (2010). Mechanisms behind decreased endogenous glucose production in malnourished children. *Pediatr Res* **68,** 423-428.

Bisgaard HC, Holmskov U, Santoni-Rugiu E, Nagy P, Nielsen O, Ott P, Hage E, Dalhoff K, Rasmussen LJ & Tygstrup N (2002). Heterogeneity of ductular reactions in adult rat and human liver revealed by novel expression of deleted in malignant brain tumor 1. *Am J Pathol* **161,** 1187-1198.

Bodoy S, Martin L, Zorzano A, Palacin M, Estevez R & Bertran J (2005). Identification of LAT4, a novel amino acid transporter with system L activity. *J Biol Chem* **280,** 12002-12011.

Borsani G, Bassi MT, Sperandeo MP, De Grandi A, Buoninconti A, Riboni M, Manzoni M, Incerti B, Pepe A, Andria G, Ballabio A & Sebastio G (1999). SLC7A7, encoding a

putative permease-related protein, is mutated in patients with lysinuric protein intolerance. *Nat Genet* **21,** 297-301.

Braun D, Wirth EK, Wohlgemuth F, Reix N, Klein MO, Gruters A, Kohrle J & Schweizer U (2011). Aminoaciduria, but normal thyroid hormone levels and signaling, in mice lacking the amino acid and thyroid hormone transporter Slc7a8. *Biochem J* **439,** 249-255.

Broer S & Palacin M (2011). The role of amino acid transporters in inherited and acquired diseases. *Biochem J* **436,** 193-211.

Camargo SM, Singer D, Makrides V, Huggel K, Pos KM, Wagner CA, Kuba K, Danilczyk U, Skovby F, Kleta R, Penninger JM & Verrey F. (2009). Tissue-specific amino acid transporter partners ACE2 and collectrin differentially interact with hartnup mutations. *Gastroenterology* **136,** 872-882.

Cheval L, Pierrat F, Dossat C, Genete M, Imbert-Teboul M, Duong Van Huyen JP, Poulain J, Wincker P, Weissenbach J, Piquemal D & Doucet A (2011). Atlas of gene expression in the mouse kidney: new features of glomerular parietal cells. *Physiol Genomics* **43,** 161-173.

Costa CC, de Almeida IT, Jakobs C, Poll-The BT & Duran M (1999). Dynamic changes of plasma acylcarnitine levels induced by fasting and sunflower oil challenge test in children. *Pediatr Res* **46,** 440-444.

Danilczyk U, Sarao R, Remy C, Benabbas C, Stange G, Richter A, Arya S, Pospisilik JA, Singer D, Camargo SM, Makrides V, Ramadan T, Verrey F, Wagner CA & Penninger JM (2006). Essential role for collectrin in renal amino acid transport. *Nature* **444,** 1088-1091.

Dave MH, Schulz N, Zecevic M, Wagner CA & Verrey F (2004). Expression of heteromeric amino acid transporters along the murine intestine. *J Physiol* **558,** 597-610.

Dudek KM, Suter L, Darras VM, Marczylo EL & Gant TW (2013). Decreased translation of Dio3 mRNA is associated with drug-induced hepatotoxicity. *Biochem J* **453,** 71-82.

Dumont JN (1972). Oogenesis in Xenopus laevis (Daudin). I. Stages of oocyte development in laboratory maintained animals. *J Morphol* **136,** 153-179.

Fickert P, Zollner G, Fuchsbichler A, Stumptner C, Pojer C, Zenz R, Lammert F, Stieger B, Meier PJ, Zatloukal K, Denk H & Trauner M (2001). Effects of ursodeoxycholic and cholic acid feeding on hepatocellular transporter expression in mouse liver. *Gastroenterology* **121,** 170-183.

Fukuhara D, Kanai Y, Chairoungdua A, Babu E, Bessho F, Kawano T, Akimoto Y, Endou H & Yan K (2007). Protein characterization of NA+-independent system L amino acid transporter 3 in mice: a potential role in supply of branched-chain amino acids under nutrient starvation. *Am J Pathol* **170,** 888-898.

Gridley DS, Freeman TL, Makinde AY, Wroe AJ, Luo-Owen X, Tian J, Mao XW, Rightnar S, Kennedy AR, Slater JM & Pecaut MJ (2011). Comparison of proton and electron radiation effects on biological responses in liver, spleen and blood. *Int J Radiat Biol* **87,** 1173-1181.

Heisterkamp N, Groffen J, Warburton D & Sneddon TP (2008). The human gamma-glutamyltransferase gene family. *Hum Genet* **123,** 321-332.

Hsieh HC, Chen YT, Li JM, Chou TY, Chang MF, Huang SC, Tseng TL, Liu CC & Chen SF (2009). Protein profilings in mouse liver regeneration after partial hepatectomy using iTRAQ technology. *J Proteome Res* **8,** 1004-1013.

Hunt MC & Alexson SE (2002). The role Acyl-CoA thioesterases play in mediating intracellular lipid metabolism. *Prog Lipid Res* **41,** 99-130.

Huq F, Thompson M & Ruell P (1993). Changes in serum amino acid concentrations during prolonged endurance running. *Jpn J Physiol* **43,** 797-807.

Ji LL, Miller RH, Nagle FJ, Lardy HA & Stratman FW (1987). Amino acid metabolism during exercise in trained rats: the potential role of carnitine in the metabolic fate of branched-chain amino acids. *Metabolism* **36,** 748-752.

Kaplan MR, Plotkin MD, Lee WS, Xu ZC, Lytton J & Hebert SC (1996). Apical localization of the Na-K-Cl cotransporter, rBSC1, on rat thick ascending limbs. *Kidney Int* **49,** 40-47.

Loffing J, Vallon V, Loffing-Cueni D, Aregger F, Richter K, Pietri L, Bloch-Faure M, Hoenderop JG, Shull GE, Meneton P & Kaissling B (2004). Altered renal distal tubule structure and renal Na(+) and Ca(2+) handling in a mouse model for Gitelman's syndrome. *J Am Soc Nephrol* **15,** 2276-2288.

Makrides V, Camargo SMR, and Verrey F. Transport of amino acids in the kidney. *Comprehensive physiology*, in press.

Mariotta L, Ramadan T, Singer D, Guetg A, Herzog B, Stoeger C, Palacin M, Lahoutte T, Camargo SM & Verrey F (2012). T-type amino acid transporter TAT1 (Slc16a10) is essential for extracellular aromatic amino acid homeostasis control. *J Physiol* **590,** 6413-6424.

Massa ML, Gagliardino JJ & Francini F (2011). Liver glucokinase: An overview on the regulatory mechanisms of its activity. *IUBMB Life* **63,** 1-6.

Meier C, Ristic Z, Klauser S, Verrey F (2002). Activation of system L heterodimeric amino acid exchangers by intracellular substrates. *EMBO J* **21,** 580-589.

Moret C, Dave MH, Schulz N, Jiang JX, Verrey F & Wagner CA (2007). Regulation of renal amino acid transporters during metabolic acidosis. *Am J Physiol Renal Physiol* **292,** F555-566.

Nassl AM, Rubio-Aliaga I, Sailer M & Daniel H (2011). The intestinal peptide transporter PEPT1 is involved in food intake regulation in mice fed a high-protein diet. *PLoS One* **6,** e26407.

Poncet N & Taylor PM (2013). The role of amino acid transporters in nutrition. *Curr Opin Clin Nutr Metab Care* **16,** 57-65.

Postic C & Girard J (2008). Contribution of de novo fatty acid synthesis to hepatic steatosis and insulin resistance: lessons from genetically engineered mice. *J Clin Invest* **118,** 829-838.

Ramadan T, Camargo SM, Herzog B, Bordin M, Pos KM & Verrey F (2007). Recycling of aromatic amino acids via TAT1 allows efflux of neutral amino acids via LAT2-4F2hc exchanger. *Pflugers Arch* **454,** 507-516.

Ramadan T, Camargo SM, Summa V, Hunziker P, Chesnov S, Pos KM & Verrey F (2006). Basolateral aromatic amino acid transporter TAT1 (Slc16a10) functions as an efflux pathway. *J Cell Physiol* **206,** 771-779.

Rudnick G, Krämer R, Blakely RD, Murphy DL & Verrey F (2014). The SLC6 Transporters: perspective on structure, functions, regulation and models for transporter dysfunction. *Pflugers Arch,* in press.

Shigeoka T, Kawaichi M & Ishida Y (2005). Suppression of nonsense-mediated mRNA decay permits unbiased gene trapping in mouse embryonic stem cells. *Nucleic Acids Res* 33, e20.

Sipowicz MA, Chomarat P, Diwan BA, Anver MA, Awasthi YC, Ward JM, Rice JM, Kasprzak KS, Wild CP & Anderson LM (1997). Increased oxidative DNA damage and hepatocyte overexpression of specific cytochrome P450 isoforms in hepatitis of mice infected with Helicobacter hepaticus. *Am J Pathol* **151,** 933-941.

Soll C, Jang JH, Riener MO, Moritz W, Wild PJ, Graf R & Clavien PA (2010). Serotonin promotes tumor growth in human hepatocellular cancer. *Hepatology* **51,** 1244-1254.

Sperandeo MP, Annunziata P, Bozzato A, Piccolo P, Maiuri L, D'Armiento M, Ballabio A, Corso G, Andria G, Borsani G & Sebastio G (2007). Slc7a7 disruption causes fetal growth retardation by downregulating Igf1 in the mouse model of lysinuric protein intolerance. *Am J Physiol Cell Physiol* **293,** C191-198.

Spoelstra MN, Mari A, Mendel M, Senga E, van Rheenen P, van Dijk TH, Reijngoud DJ, Zegers RG, Heikens GT & Bandsma RH (2012). Kwashiorkor and marasmus are both associated with impaired glucose clearance related to pancreatic beta-cell dysfunction. *Metabolism* **61,** 1224-1230.

Sterchi EE, Stocker W & Bond JS (2008). Meprins, membrane-bound and secreted astacin metalloproteinases. *Mol Aspects Med* **29,** 309-328.

Taylor MA & Smith LD (1987). Accumulation of free amino acids in growing Xenopus laevis oocytes. *Dev Biol* **124,** 287-290.

Verrey F, Singer D, Ramadan T, Vuille-dit-Bille RN, Mariotta L & Camargo SM (2009). Kidney amino acid transport. *Pflugers Arch* **458,** 53-60.

Wagner CA, Loffing-Cueni D, Yan Q, Schulz N, Fakitsas P, Carrel M, Wang T, Verrey F, Geibel JP, Giebisch G, Hebert SC & Loffing J (2008). Mouse model of type II Bartter's syndrome. II. Altered expression of renal sodium- and water-transporting proteins. *Am J Physiol Renal Physiol* **294,** F1373-1380.

Wolfsdorf JI, Sadeghi-Nejad A & Senior B (1982). Hypoalaninemia and ketotic hypoglycemia: cause or consequence? *Eur J Pediatr* **138,** 28-31.

Wu G (2009). Amino acids: metabolism, functions, and nutrition. *Amino Acids* **37,** 1-17.

Competing interests: All authors declare no competing financial, personal, or professional interests that could be construed to have influenced this paper.

Author contributions: Conception and design of the experiment: A.G., L.M. and F.V. Collection, analysis and interpretation of data: A.G., L.M., L.B., B.H., R.F., S.M.R.C. and F.V. Drafting and revising the article: A.G. and F.V. All authors approved the final version.

Funding: The laboratory of FV is supported by Swiss NSF grant 31-130471/1 and the National Centre of Competence in Research (NCCR) Kidney.CH.

Acknowledgments: The authors thank Giancarlo Russo for his help with the analysis of the RNA sequencing data and Achim Weber for his help with the liver histological analysis.

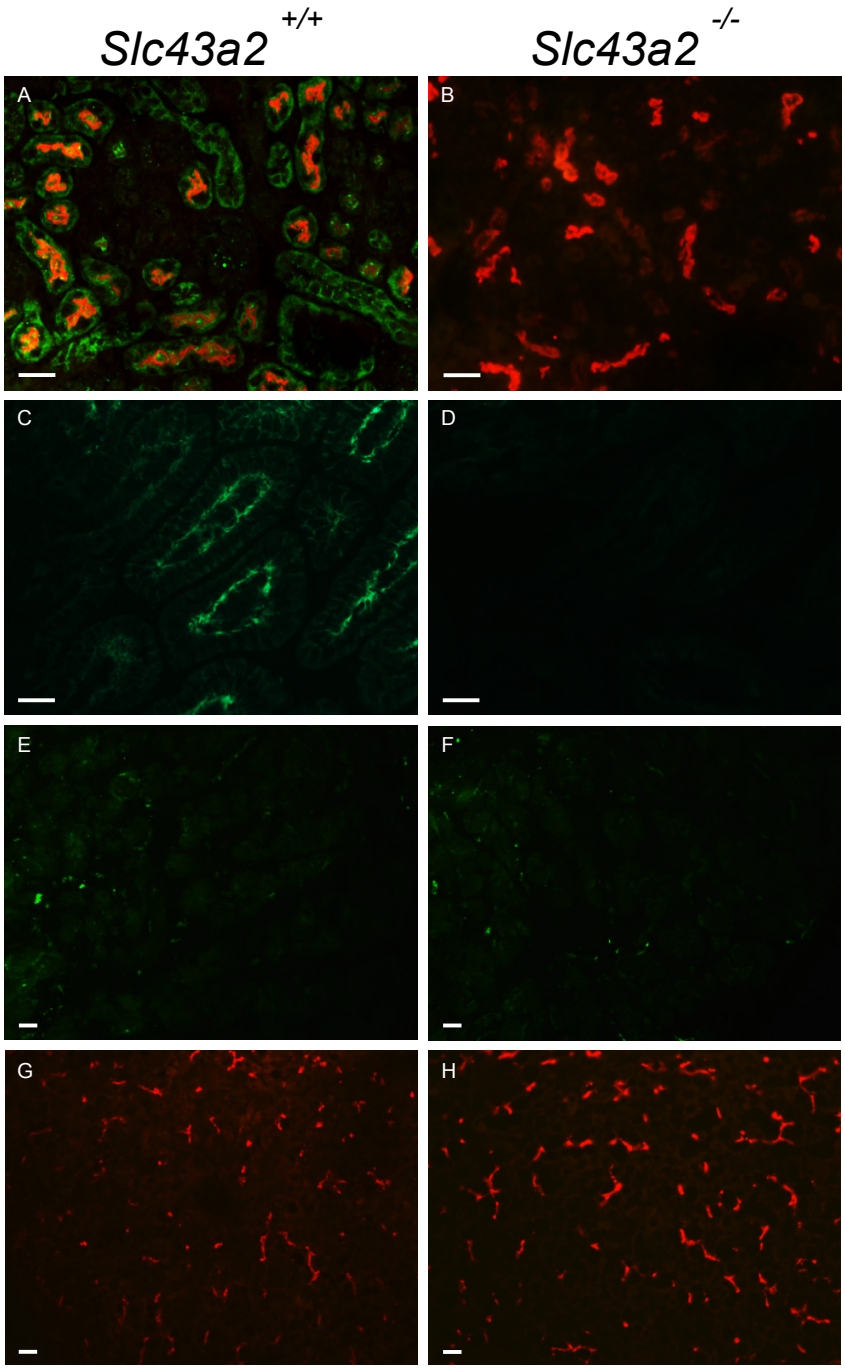

Figure 1. Confirmation of Lat4 deletion and validation of Lat4 antibody by immunofluorescence. A basolateral signal is seen with Lat4 antibody (*green*) in kidney (**A**) and small intestine (**C**) of 3 days old wildtype pups; whereas no such signal is visible in knock-out mice (**B** and **D**). No signal is observed in skeletal muscle (**E**) and liver (**G**) of wildtype pups besides the background also visible in the knock-outs (**F** and **H**). As luminal marker for kidney proximal tubule, TMEM27 (*red*) was used (**A** and **B)**; whereas MDR1 (*red*) was used as canalicular membrane marker for liver (**G** and **H)**. Scale bar: 20 µm.

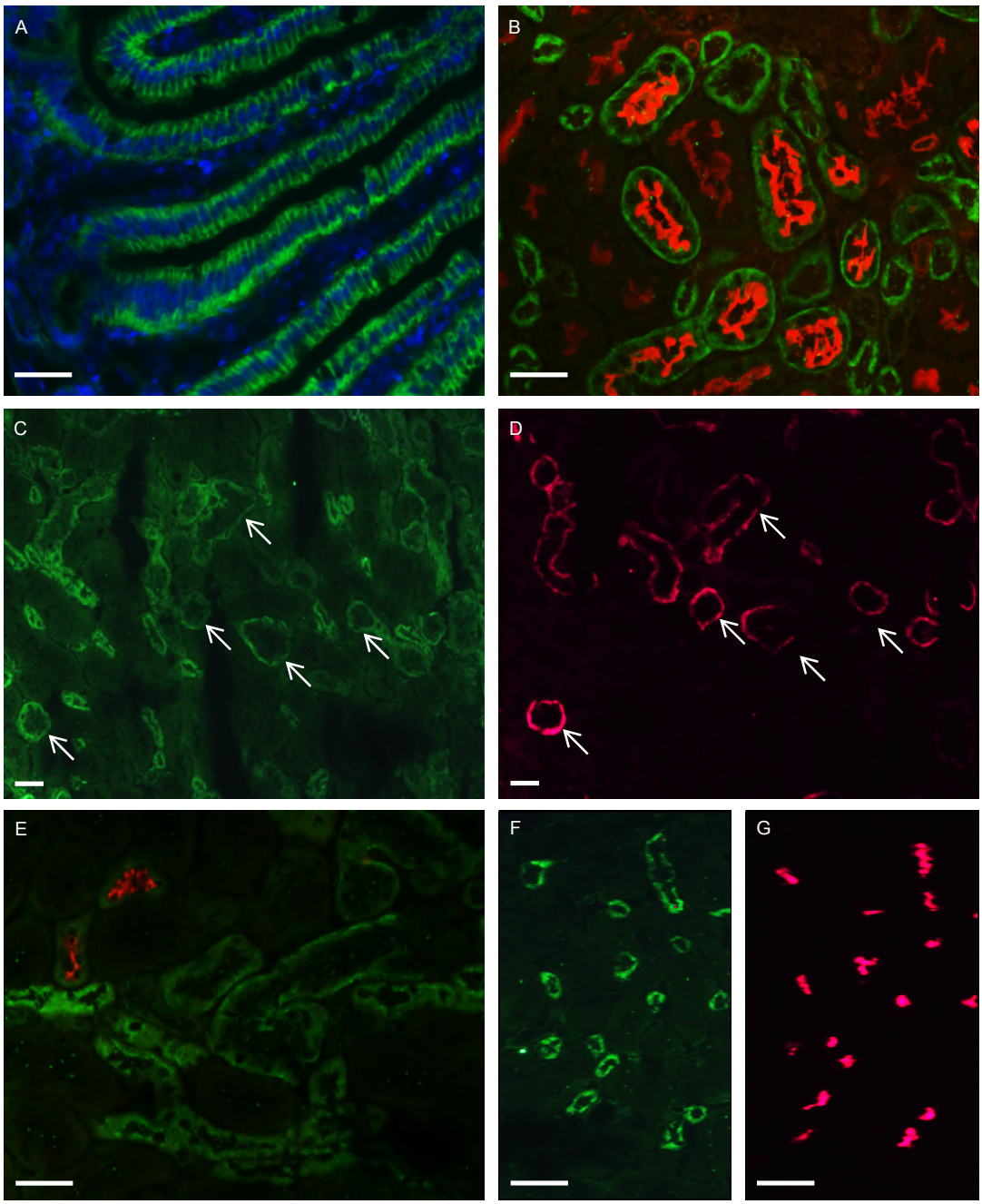

Figure 2. Localization of Lat4 on small intestine and kidney sections by immunofluorescence. (**A**) On this duodenum section a strong Lat4 signal (*green*) is visible at the basolateral membrane of enterocytes along the villi but not in the crypts. DAPI (*blue*) was used to label the nuclei. (**B**) Lat4 (*green*) is expressed at the basolateral side of kidney proximal tubule (PT) as shown by the colocalization with the luminal protein TMEM27 (*red*) and, on consecutive sections (**C** and **D**), with the aromatic AA uniporter Tat1 (*pink*). (**E**) Colabeling with NCC (*red*) shows a weaker expression of Lat4 in the distal convoluted tubule (DCT) and consecutive sections with NKCC2 (*pink*) (**F** and **G**) a strong signal for Lat4 in the thick ascending limb (TAL). Scale bar: 20 µm.

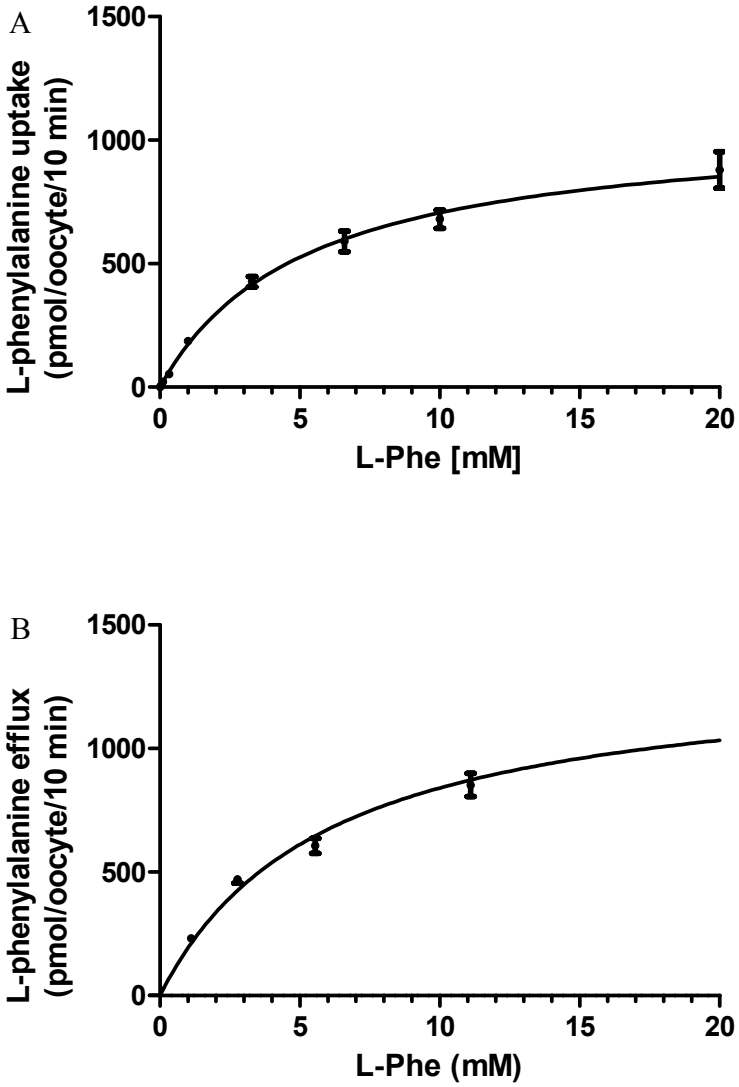

Figure 3. Concentration-dependence of L-phenylalanine uptake and efflux in *X. laevis oocytes* expressing human LAT4. Oocytes were injected with 25 ng of hSLC43A2 cRNA and incubated for 3 days. (**A**) Concentration-dependent uptakes were performed for 10 min with 9 different concentrations of phenylalanine; n = 8-24 oocytes pooled from three independent experiments. (**B**) For the efflux experiments, oocytes were injected with 50 nl of phenylalanine at 5 different concentrations; n = 12-14 oocytes pooled from three independent experiments. Represented are means and SEM. Curves corresponding to the Michaelis-Menten equation were fitted to the experimental data using a non-linear regression routine (Graph Prism 5.0).

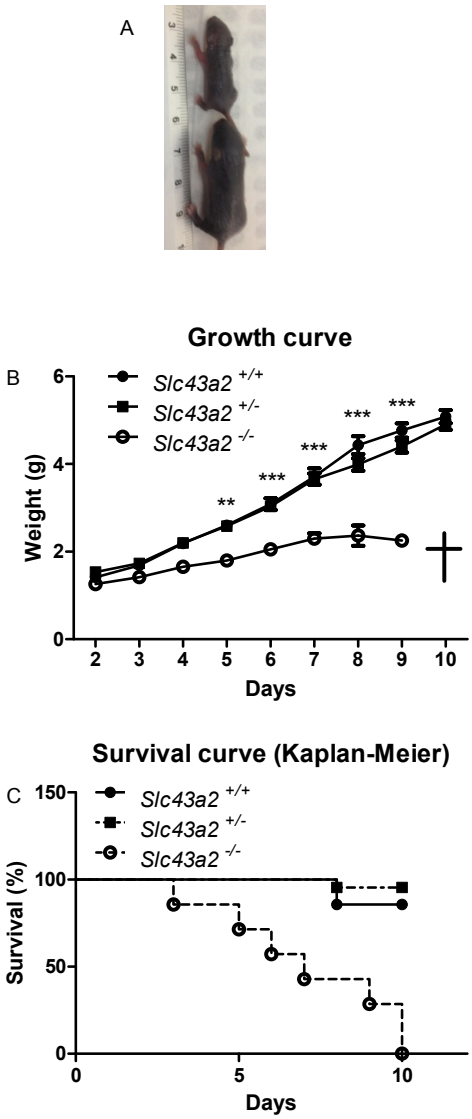

Figure 4. Postnatal growth retardation and premature death *of Slc43a2*$^{-/-}$ mice. (**A**) Representative picture of a *Slc43a2*$^{-/-}$ mouse (top) versus a *Slc43a2*$^{+/+}$mouse (bottom) at day 7 after birth. (**B**) Growth curves for *Slc43a2*$^{+/+}$, *Slc43a2*$^{+/-}$ and *Slc43a2*$^{-/-}$ mice; represented are means and SEM, n = 7 for *Slc43a2*$^{+/+}$, n = 22 for *Slc43a2*$^{+/-}$, n = 7 for *Slc43a2*$^{-/-}$; comparison of *Slc43a2*$^{+/+}$ and *Slc43a2*$^{-/-}$ by two-way ANOVA and Bonferroni posttest: ** $p < 0.01$, *** $p < 0.001$; cross represents death of all *Slc43a2*$^{-/-}$ mice. (**C**) Survival curves for the same mice as (**B**).

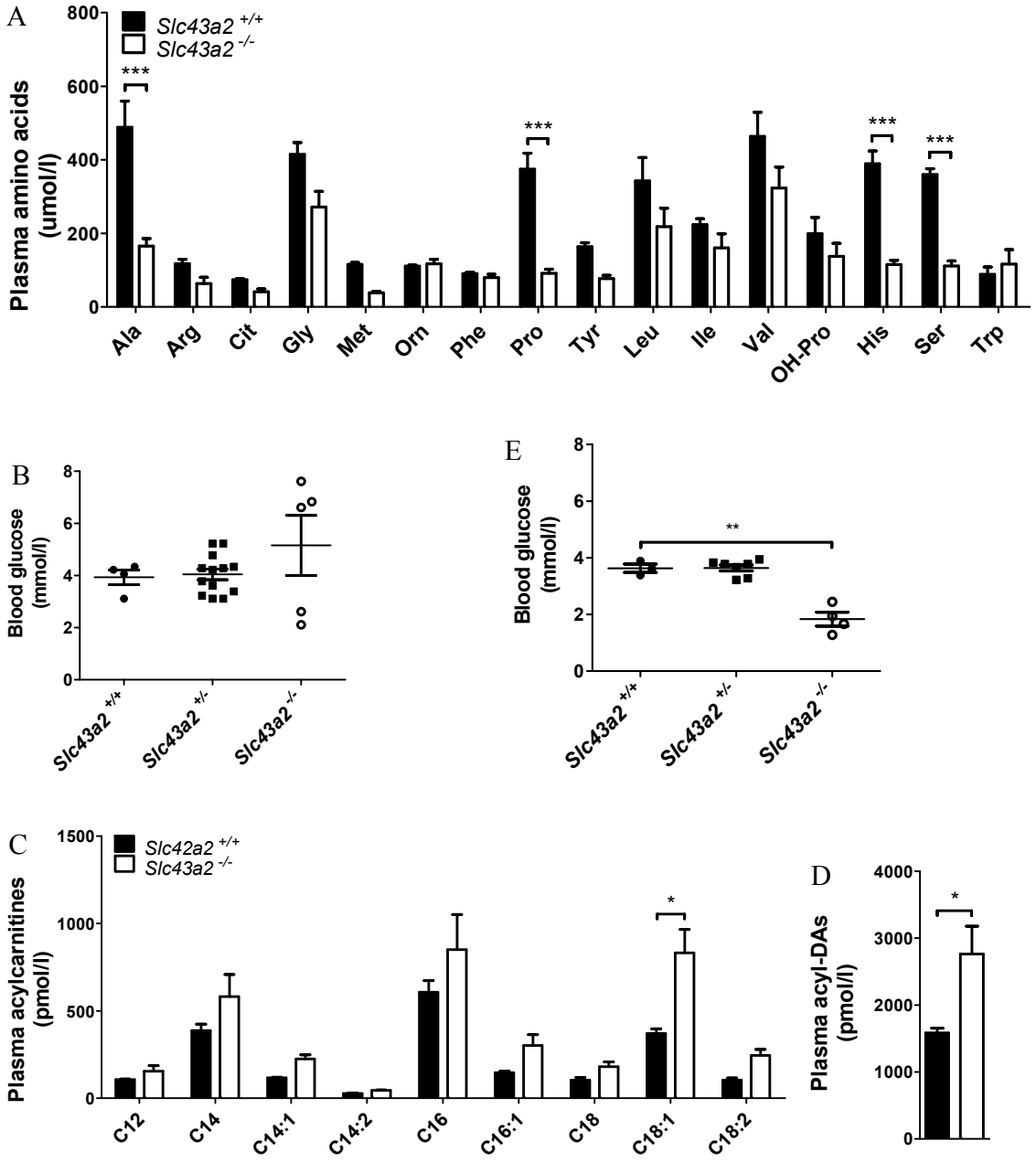

Figure 5. Impact of *Slc43a2* deletion on plasma amino acids, acylcarnitines and glucose. (**A**) Plasma amino acids, (**C**) long-chain unsaturated acylcarnitines and (**D**) dicarboxylacylcarnitines (DAs). Represented are means and SEM, n = 3 for *Slc43a2*$^{+/+}$ (black bars), n = 6 for *Slc43a2*$^{-/-}$ (white bars), two-way ANOVA, Bonferroni posttest, * $p < 0.05$, ** $p < 0.001$. (**B** and **E**) Blood glucose measurement from mice at day 2 without (**B**) and with 30 min starvation (**E**) prior to sample collection. Represented are means and SEM, Student's *t*-test, ** $p < 0.01$.

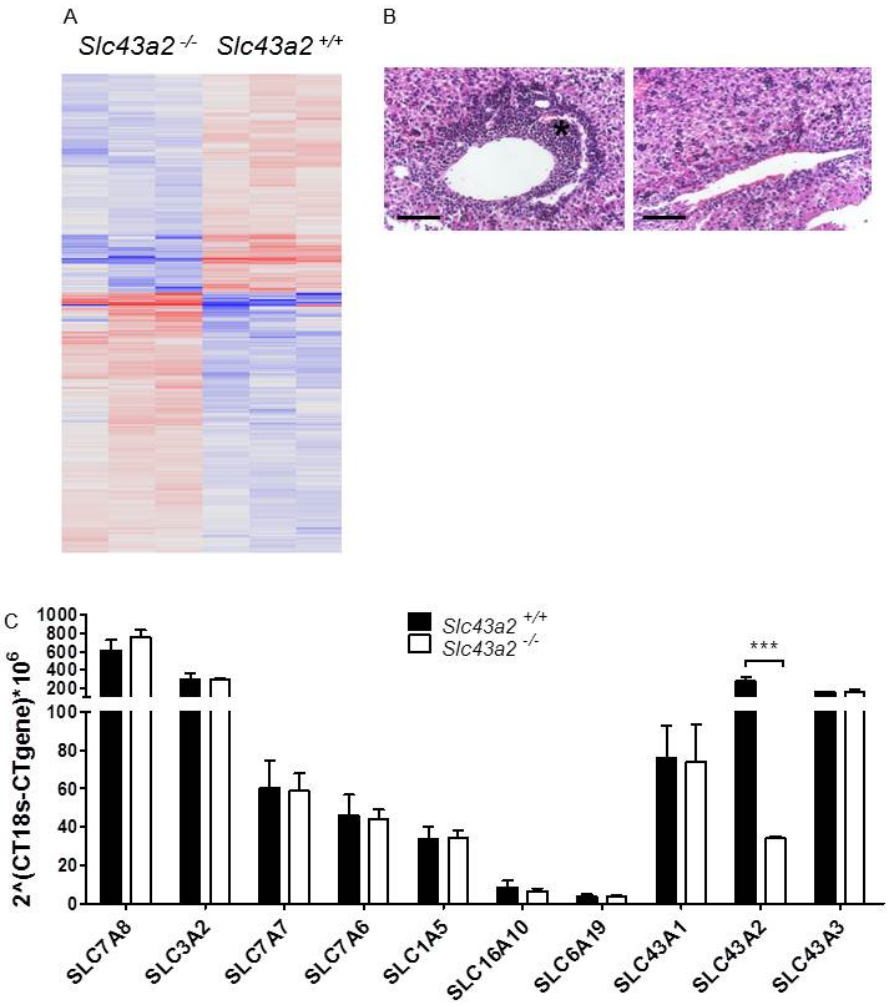

Figure 6. Effect of *Slc43a2* deletion on kidney and liver. (**A**) Heatmap summary of differential gene expression pattern in *Slc43a2*$^{-/-}$ liver. RNA was isolated from mice at day 2 and each column represents a different mice. Upregulated genes are labeled red, downregulated blue. (**B**) Hematoxylin and eosin staining of liver. Left panel: liver section of *Slc43a2*$^{-/-}$ KO mice. Right panel: liver section of *Slc43a2*$^{+/+}$ mice. (*) shows leucocyte infiltration in the periportal region of *Slc43a2*$^{-/-}$ mice liver. Scale bar: 50 µm. (**C**) Gene expression of selected amino acid transporters in the kidney of *Slc43a2*$^{+/+}$ (black bars) and *Slc43a2*$^{-/-}$ (white bars). Represented are means and SEM, n = 3, two-way ANOVA, Bonferroni posttest, ** $p < 0.01$.

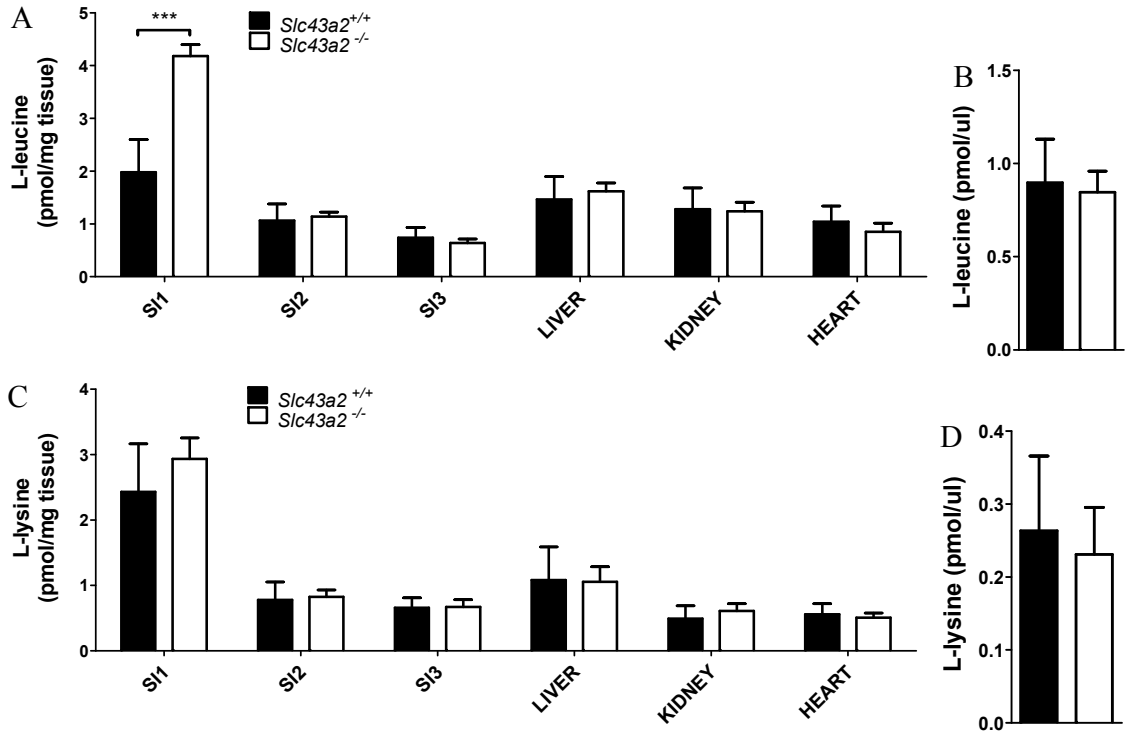

Figure 7. Distribution of radiolabeled L-leucine and L-lysine in different organs after oral administration. Mice were starved 30 min prior to oral administration of radiolabeled AA solution. (**A**) leucine and (**C**) lysine accumulation in different organs normalized by weight. (**B**) leucine and (**D**) lysine concentration in plasma 30 min after oral administration (*Slc43a2*$^{+/+}$: black bars, *Slc43a2*$^{-/-}$: white bars). The whole intestine of the small pups was divided in three equals parts named from proximal to distal: SI1, SI2 and SI3. Represented are means and SEM pooled from three independent experiments, n = 6 for *Slc43a2*$^{+/+}$ mice, n = 8 for *Slc43a2*$^{-/-}$ mice, two-way ANOVA, Bonferroni posttest, *** $p < 0.001$.

Supplementary material

Amino acid transporter Lat4 (*Slc43a2*) is essential for mice postnatal development

Adriano Guetg, Luca Mariotta, Lukas Bock, Brigitte Herzog, Simone M.R. Camargo and François Verrey.

Supplementary Tables

Supplementary Table 1a. Upregulated genes (≥ 3-fold increase) in liver of *Slc43a2*$^{-/-}$ mice compared to wildtype mice.

Gene symbol	RefSeq accession number	log2 Ratio	pValue	Slc43a2-/- (log2 of mean)	Slc43a2+/+ (log2 of mean)
Sult1e1	NM_023135	5.49	4.16E-10	4.16	-0.85
Sypl2	NM_008596	5.34	7.40E-04	1.62	-1.10
Hapln1	NM_013500	4.66	1.16E-34	7.03	2.11
2210415F13Rik	NM_001083884; NM_027339	4.57	2.43E-06	3.25	-0.75
Dmbt1	NM_007769	4.45	8.19E-07	4.37	1.28
1700012B07Rik	NM_027038; NM_001162428	3.99	5.22E-07	3.96	-0.24
Trnp1	NM_001081156	3.89	5.36E-07	3.91	0.04
Asb11	NM_026853	3.52	4.80E-07	4.36	0.48
Syt17	NM_138649	3.52	8.20E-04	2.25	-0.79
Ttll8	NM_172818	3.47	1.37E-04	2.94	-0.40
Zan	NM_011741	3.45	6.62E-48	8.83	5.32
Olfr78	NM_001168503; NM_130866	3.44	4.31E-04	2.65	0.91
AA465934	NR_028363	3.25	5.85E-45	8.79	5.56
Ceacam3	NM_054059	3.12	6.80E-03	1.73	-0.82
Lce6a	NM_001166172	3.12	6.67E-03	1.73	-0.72
Glod5	NM_027227	3.12	1.16E-10	5.53	2.43
Mep1a	NM_008585	3.08	4.74E-09	5.13	1.65
Myo16	NM_001081397	3.04	2.75E-04	3.43	0.23
Slc38a11	NM_177074	2.81	7.08E-09	5.30	2.51
Htr2b	NM_008311	2.75	3.03E-03	2.28	-0.21
Tectb	NM_009348	2.74	2.44E-04	3.22	0.38
Gpx6	NM_145451	2.62	2.10E-04	3.89	1.09

Psg16	NM_007676	2.59	3.47E-06	4.51	1.65
Esrrg	NM_011935; NM_001243792	2.58	2.79E-16	7.11	4.60
Gm13003	NR_040443	2.55	4.56E-03	2.50	0.22
Fgfbp1	NM_008009	2.45	4.65E-07	5.74	3.57
Ms4a8a	NM_022430	2.42	4.08E-04	3.74	1.24
Insl6	NM_013754	2.40	4.09E-04	3.64	0.64
Tmem100	NM_026433	2.36	6.91E-06	5.20	2.95
Elfn1	NM_175522	2.30	1.29E-05	4.81	2.58
O3far1	NM_181748	2.27	1.75E-10	7.09	4.99
Hapln4	NM_177900	2.27	2.71E-04	3.74	1.24
Gck	NM_010292	2.24	7.54E-07	5.57	3.46
E030010A14Rik	NM_183160	2.22	1.34E-06	5.57	3.43
Scn8a	NM_011323; NM_001077499	2.19	2.13E-06	5.58	3.51
Xirp1	NM_011724	2.18	1.19E-03	3.55	1.16
Arhgap36	NM_001081123	2.17	4.45E-07	5.37	3.21
Rgs1	NM_015811	2.15	1.65E-05	6.50	4.97
Npas2	NM_008719	2.11	3.52E-07	6.24	4.24
Lrrc3b	NM_146052	2.06	4.93E-03	2.86	0.72
Vwa3a	NM_177697	2.05	1.43E-03	3.70	1.77
Fam57b	NM_029978; NM_026884; NM_001146347	2.04	4.93E-03	3.21	1.38
D030018L15Rik	NR_003627	2.02	3.70E-03	3.06	0.91
Tmeff2	NM_019790	2.01	4.58E-08	6.07	4.00
Extl1	NM_019578	2.00	9.79E-05	4.61	2.51
Mep1b	NM_008586	2.00	1.06E-04	4.62	2.57
Fbxw15	NM_199036	1.98	6.85E-03	2.78	0.58
Gjc3	NM_080450	1.94	3.96E-08	6.22	4.24
Obscn	NM_199152; NM_001171512	1.93	4.41E-07	7.28	5.55
Cox7a1	NM_009944	1.90	3.35E-08	6.20	4.28
Scn2a1	NM_001099298	1.89	6.13E-04	4.34	1.99
Tmem212	NM_001164437	1.89	3.45E-03	3.69	1.60
Gstt3	NM_133994	1.87	2.23E-29	10.37	8.54
Cyp17a1	NM_007809	1.80	1.79E-13	7.79	6.01
Itgae	NM_008399; NM_172944	1.79	1.20E-10	7.21	5.46
Nudt11	NM_021431	1.79	8.70E-03	3.14	1.24
Cyp2a5	NM_007812	1.79	3.04E-22	10.64	8.85
Tmem200b	NM_001201367	1.77	5.82E-14	7.94	6.15
Acacb	NM_133904	1.72	5.11E-12	9.06	7.38
Cyp2a4	NM_009997	1.71	1.37E-15	10.36	8.67
Gdpd2	NM_023608	1.68	5.60E-03	3.70	2.11
Fam83e	NM_001033170	1.67	9.92E-03	3.12	1.44

Spock2	NM_052994	1.63	2.07E-03	5.25	3.46
Cdkn1a	NM_007669; NM_001111099	1.63	5.02E-10	10.15	8.59
Tmc7	NM_172476	1.63	1.64E-05	5.82	4.25
Glp2r	NM_175681	1.61	1.76E-06	6.33	4.71
Cpt1b	NM_009948	1.60	9.89E-16	10.28	8.67
Arg1	NM_007482	1.60	1.18E-15	14.30	12.76
Wnt9b	NM_011719	1.57	3.73E-05	5.66	4.10
AI450353	NR_028364	1.56	1.52E-08	7.00	5.42
Ggt6	NM_027819	1.56	9.62E-05	5.66	4.05
2410137F16Rik	NR_015595	1.56	1.50E-04	5.36	3.82
Pafah2	NM_133880	1.54	6.17E-22	10.74	9.25
Per1	NM_001159367; NM_011065	1.51	7.03E-16	10.52	9.08
Baiap2l2	NM_177580	1.51	9.03E-12	8.32	6.86
Ccl6	NM_009139	1.51	2.97E-10	9.64	8.27
Slc22a30	NM_177002	1.50	1.16E-04	5.78	4.43

Supplementary Table 1b. Downregulated genes (≥ 3-fold decrease) in liver of *Slc43a2*$^{-/-}$ mice compared to wildtype mice.

Gene symbol	RefSeq accession number	log2 Ratio	pValue	Slc43a2-/- (log2 of mean)	Slc43a2+/+ (log2 of mean)
Abcg5	NM_031884	-1.51	6.76E-17	7.98	9.48
Mbl2	NM_010776	-1.51	3.76E-10	10.56	12.22
Adra1d	NM_013460	-1.52	7.41E-03	2.41	3.97
Cyp2c37	NM_010001	-1.53	9.46E-12	9.68	11.36
1110032F04Rik	NM_001167996	-1.55	1.33E-03	3.26	5.17
Apol7c	NM_175391	-1.55	4.58E-04	3.45	5.07
Cd209f	NM_026956	-1.56	2.46E-06	5.17	6.81
Cyp2c50	NM_001167877; NM_134144; NM_001167875	-1.59	2.76E-10	6.88	8.55
Rgs16	NM_011267	-1.59	1.99E-13	8.89	10.39
Cyp2g1	NM_013809	-1.60	2.81E-03	2.82	4.46
Slc44a5	NM_001081263	-1.61	8.10E-04	2.89	4.53
Ncr1	NM_010746	-1.62	1.40E-03	2.67	4.69
Nlrc5	NM_001033207	-1.63	9.98E-12	6.09	7.73
9030619P08Rik	NM_001039720	-1.65	3.47E-04	3.26	4.92
Gm12250	NM_001135115	-1.69	1.58E-07	4.61	6.31
Dbp	NM_016974	-1.70	8.35E-08	6.35	7.87

B930025P03Rik	NR_040705	-1.71	1.41E-07	5.78	7.65
Htra4	NM_001081187	-1.72	5.18E-03	1.81	3.68
AW112010	NM_001177351	-1.72	1.17E-20	7.08	8.81
Mcpt4	NM_010779	-1.72	1.85E-03	2.01	4.16
Xcr1	NM_011798	-1.74	4.10E-03	1.55	3.62
Olfr56	NM_010999	-1.75	3.78E-11	5.39	7.17
Abcg8	NM_026180	-1.79	3.56E-27	7.63	9.44
Slc1a2	NM_001077515; NM_001077514; NM_011393	-1.83	9.69E-06	3.82	5.64
Cxcl9	NM_008599	-1.88	3.23E-05	3.22	5.25
Tgtp2	NM_001145164	-1.88	5.57E-32	8.39	10.30
Gbp6	NM_194336	-1.88	1.11E-38	8.55	10.46
Fam189a1	NM_183087	-1.89	3.93E-03	1.25	3.41
Gm8221	NR_033577	-1.90	4.77E-03	1.15	3.25
Tgtp1	NM_011579	-1.96	9.84E-35	8.73	10.72
Mug2	NM_008646	-1.96	7.12E-17	5.96	7.97
Cyp2c54	NM_206537	-2.00	6.37E-12	6.27	8.24
Ido2	NM_145949	-2.01	3.07E-06	3.60	5.57
Gbp10	NM_001039646	-2.03	1.02E-33	7.44	9.51
Dclk3	NM_172928	-2.04	7.83E-06	3.37	5.41
Gabbr2	NM_001081141	-2.07	3.94E-07	3.77	6.00
Gm10319	NR_003624	-2.07	2.29E-06	3.30	5.38
Ifi47	NM_008330	-2.08	2.03E-44	8.02	10.11
Mmp13	NM_008607	-2.10	9.05E-03	0.62	2.51
Chrdl1	NM_031258; NM_001114385	-2.10	8.14E-05	2.39	4.57
Gimap7	NM_146167	-2.11	1.58E-03	0.95	3.31
Slc4a5	NM_001166067	-2.13	5.21E-03	1.01	3.02
9330175E14Rik	NR_015514	-2.21	2.44E-04	1.48	3.79
4930432K21Rik	NM_001163752; NM_029045	-2.22	8.10E-05	1.75	4.31
Zbp1	NM_021394; NM_001139519	-2.22	8.18E-14	4.79	7.02
Mug-ps1	NR_027619	-2.25	1.59E-22	6.04	8.30
Dio3	NM_172119	-2.25	1.76E-04	1.39	3.98
Fam155a	NM_173446	-2.28	6.88E-04	1.01	3.47
Ankrd55	NM_029898; NM_001168405; NM_001168404; NM_001168403	-2.39	1.70E-07	3.59	6.01
Prok1	NM_001044382	-2.46	7.58E-16	4.49	6.98
Apol9a	NM_173786; NM_001162883	-2.64	2.85E-07	2.45	5.18
A630076J17Rik	NM_001256174	-2.68	1.43E-21	5.16	8.03
Dio3os	NR_002866	-2.69	8.19E-13	3.67	6.41
Apol9b	NM_173743; NM_001168660	-2.72	3.98E-09	2.94	5.65

Oas1e	NM_145210	-2.77	3.98E-03	-0.66	2.18
Tnfaip8l3	NM_001033535	-2.85	4.16E-06	1.34	4.20
Abcc12	NM_172912	-2.86	2.05E-03	-0.47	2.35
Slc6a11	NM_172890	-2.95	1.58E-04	0.09	3.64
E130309D14Rik	NM_001013784	-2.98	5.80E-43	5.76	8.82
Cyp2b10	NM_009999	-3.01	2.74E-10	2.76	5.70
Car3	NM_007606	-3.07	2.96E-42	7.78	10.87
Ins2	NM_001185083; NM_001185084; NM_008387	-3.07	4.45E-03	2.05	1.79
Ubd	NM_023137	-3.45	1.21E-10	1.87	5.33
Gbp11	NM_001039647	-4.01	1.04E-85	5.70	9.73
Clec2h	NM_053165	-4.47	1.31E-16	1.59	6.03
Inmt	NM_009349	-4.71	1.21E-41	3.55	8.20
Trp63	NM_001127262; NM_001127260; NM_001127265; NM_001127263; NM_001127264; NM_011641; NM_001127261; NM_001127259	-5.98	3.13E-05	-0.94	2.24

Supplementary Figures

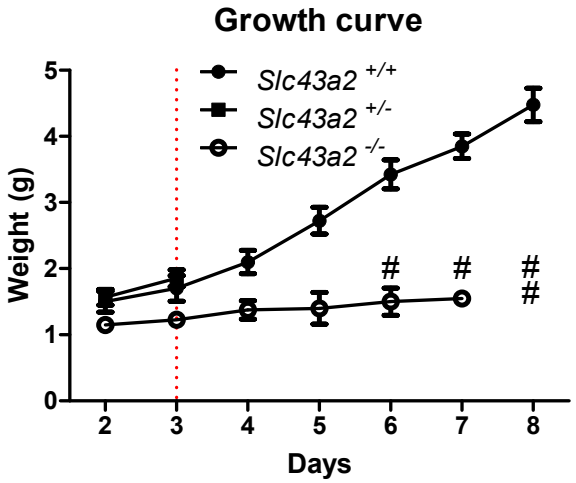

Supplementary Figure 1. Effect of litter size reduction on growth curve of *Slc43a2*$^{-/-}$ mice. Mice were genotyped and weighted according to usual protocol and from the third day on (dashed line) the *Slc43a2*$^{+/-}$littermates were removed. Each (#) represents death of one *Slc43a2*$^{-/-}$ mouse. Represented are means and SEM pooled from two independent litters, n = 4.

5.2 Cooperation of uniporters TAT1 and LAT4 with the exchanger LAT2 in MDCK cells

5.2.1 Establishment of the LAT2-4F2hc fusion construct and functional test

To investigate the transepithelial transport of neutral amino acids we decided to reconstitute in MDCK cells the neutral amino acid transport machinery, which in our cases consisted of the apical transporter B°AT1 together with the accessory protein TMEM27, the basolateral exchanger LAT2 together with the accessory protein 4F2hc and one basolateral uniporter being either TAT1 or LAT4 (see Material and Methods). This setup provides two major advantages: the use of differentiated MDCK cells with clear distinct apical and basolateral membranes represents a better physiological *in vitro* model to investigate the transepithelial amino acid transport compared to the *Xenopus laevis* oocytes expression system. Moreover, the parallel expression of the exchanger LAT2 and either TAT1 or LAT4 in MDCK cell epithelia provides the possibility to investigate the cooperation between LAT2 and TAT1 in the context of an epithelium, whereas this cooperation had as yet been studied in the non-polarized context of oocytes. An additional aim was to test whether this cooperation takes plays also with the uniporter LAT4.

Since the establishment of this cell model involves the consecutive transduction of different heterologous constructs and antibiotic-mediated selection to achieve a homogenous level of expression, we decided to delineate a strategy to reduce the number of transduction steps and to restrain the stress imposed on the cells. The two main strategies applied were the establishment of a fusion construct between LAT2 and 4F2hc and the transduction of B°AT1 and TMEM27 via a bicistronic expression vector (pIRES2). Together with the transduction of the uniporter, the previously outlined technical features enabled the reconstitution of the neutral amino acid transport machinery with three transduction steps.

The functionality of the LAT2-4F2hc fusion protein was tested in the *Xenopus laevis* oocytes expression system and MDCK cells (Fig. 3.1). To determine whether the molecular engineering of the fusion construct might affect the kinetic properties of LAT2, we determined the Michaelis-Menten constant of LAT2-4F2hc using leucine as substrate (Fig

5.1A). We calculated a K_m value of about 40 µM; whereas, the K_m value for the separated proteins LAT2 and 4F2hc was about 80 µM. The obtained values are comparable and characteristic of a high-affinity transport type (i.e. K_m between 10 and 100 µM), which corresponds to what was previously reported for LAT2 (Rossier *et al.*, 1999). This indicates that the fusion of the two proteins did not affect the kinetic properties of LAT2 and that the fusion construct LAT2-4F2hc can therefore be used as a convenient tool to achieve the simultaneous expression of LAT2 and the accessory protein 4F2hc with one transduction step and presumably thereby also avoiding the possible association of either transduced subunit with an endogenous partner instead, as previously shown for the fusion protein made of $b^{0,+}$ and rBAT (Pfeiffer et al., EMBO J, 1999). Furthermore, we tested the functionality of LAT2-4F2hc also in MDCK cells (Fig. 5.1B). LAT2-4F2hc-expressing MDCK cells showed a higher phenylalanine uptake compared to control cells confirming the proper functionality of LAT2-4F2hc.

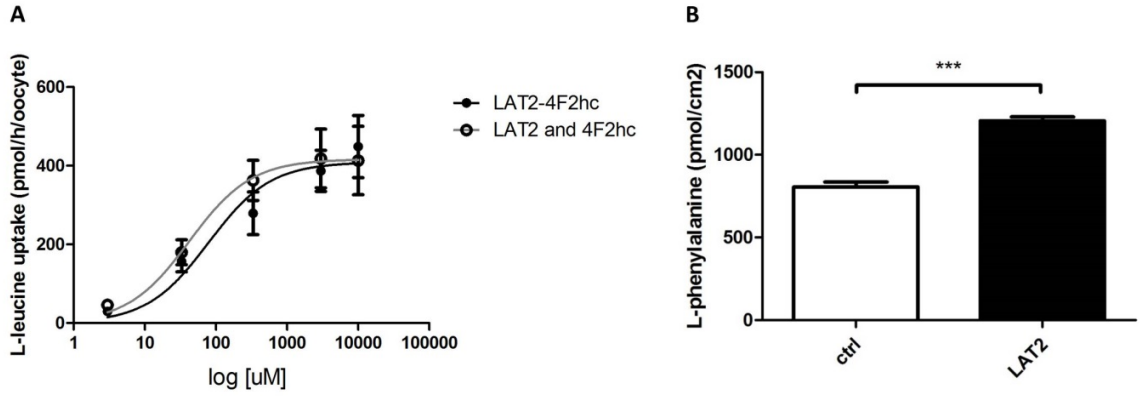

Figure 5.1 Functional test of the cloned fusion construct LAT2-4F2hc. (**A**) Uptake rates of LAT2-4F2hc fusion protein and the separated proteins LAT2 and 4F2hc were determined at increasing leucine concentration in *Xenopus laevis* oocytes. [^{3}H]-labeled leucine (10 µCi/ml) was used as tracer. Represented are means ± SEM; n = 7, Curves corresponding to the Michaelis-Menten kinetics were fitted to the points. (**B**) Uptake of phenylalanine (100 µM, [^{3}H]-labeled phenylalanine 10 µCi/ml as tracer) by LAT2-4F2hc fusion protein-expressing MDCK cells and control transduced cells. Represented are means ± SEM; n = 3, Student *t*-test, *** $p < 0.001$).

5.2.2 Expression of the amino acid transporters in MDCK cells and functional tests

The reconstitution of the amino acid transport machinery in MDCK cells was performed sequentially with three transduction steps as indicated in "Materials and Methods". The expression of the fusion protein LAT2-4F2hc and of TAT1 were confirmed by immunofluorescence (Fig. 5.2A); whereas, the expression of B°AT1, TMEM27 and LAT4 were confirmed by Western blotting (Fig. 5.2B).

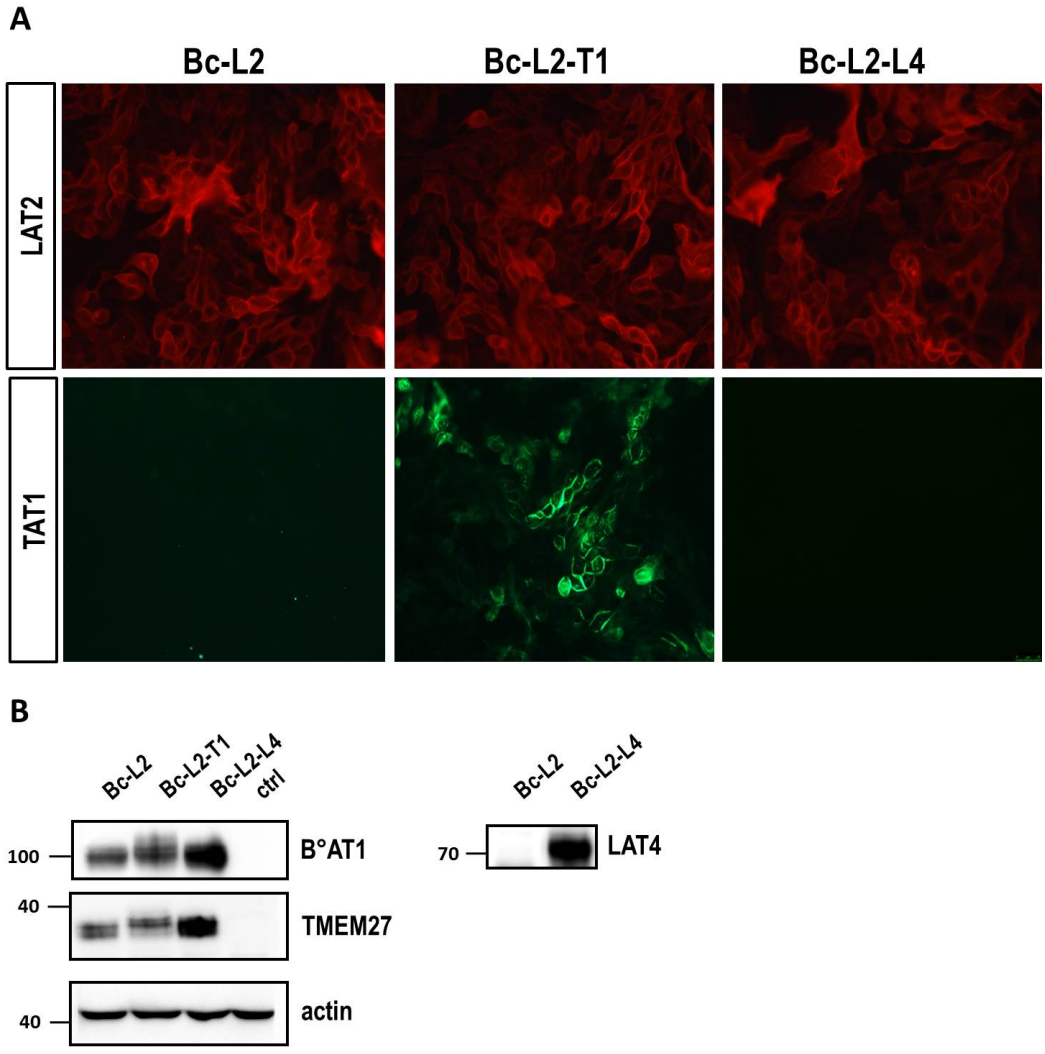

Figure 5.2 Expression of the different amino acid transporters by MDCK cells. (**A**) Expression of the exchanger LAT2 and the uniporter TAT1 were tested by immunofluorescence. (**B**) Expression of B°AT1, TMEM27 and uniporter LAT4 was tested by Western blotting. Bc-L2: MDCK cells expressing B°AT1,

TMEM27 and LAT2. Bc-L2-T1: MDCK cells expressing B°AT1, TMEM27, LAT2 and TAT1. Bc-L2-L4: MDCK cells expressing B°AT1, TMEM27, LAT2 and LAT4.

To investigate whether the cooperation of the uniporters (i.e. either TAT1 or LAT4) with the exchanger LAT2 might impact on the intracellular amino acid concentration, MDCK cells expressing B°AT1, TMEM27, LAT2 (MDCK Bc-L2) and MDCK expressing B°AT1, TMEM27, LAT2 and TAT1 or LAT4 (Bc-L2-T1 or Bc-L2-L4) were differentiated on filters according to usual procedure. After they had reached confluence and established a high electrical resistance (> 3 kΩ) they were cultured two additional days in normal cell culture medium before their intracellular amino acid concentration was determined (Fig 5.3). The additional expression of TAT1 significantly impacted on the intracellular concentration of different amino acids (Fig. 5.3A): i.e. the aromatic amino acids phenylalanine, tyrosine and tryptophan were decreased by respectively 40% (phenylalanine and tyrosine) and 55% (tryptophan), which is most probably due to the TAT1-mediated efflux. Interestingly, additional amino acids were found significantly decreased in Bc-L2-T1 cells compared to Bc-L2 cells: valine (40% decrease), leucine (45%), glutamine (75%), asparagine (71%), threonine (60%) and proline (65%). We hypothesize that this decrease is due to a functional cooperation between TAT1 and LAT2 as already shown in analogous way in *Xenopus laevis* oocytes by Ramadan *et al.* (Ramadan *et al.*, 2007). In this sense, the additional presence of the uniporter TAT1 would enable the efflux of aromatic amino acids in the basolateral compartment providing extracellular substrates for the exchanger LAT2. The exchange of these extracellular amino acids for intracellular ones by LAT2 would finally lead to an increased accumulation of LAT2 intracellular amino acid substrates in the basolateral compartment. It is important to mention that not all LAT2 substrates were decreased in Bc-L2-T1 cells: i.e. serine, alanine, histidine and methionine did not show marked differences compared to Bc-L2 cells. Surprisingly, the decreased intracellular concentrations of specific amino acids did not translate in a change of their concentration in the basolateral compartment (Fig. 5.3B).

The same type of intracellular amino acid analysis was performed comparing Bc-L2 and Bc-L2-L4 cells. In contrast to the observation made in Bc-L2-T1, the additional expression of the uniporter LAT4 did not impact on the intracellular amino acid concentrations (Fig. 5.4A) as well as the basolateral concentrations (Fig. 5.4B), suggesting that LAT2 is was

probably not undergoing a substantial functional cooperation with LAT4. Interestingly, LAT4 substrates are as well not decreased in Bc-L2-L4 raising the question whether LAT4 is functional in these cells. To investigate this issue, we compared the transepithelial efflux of [^{3}H]-labeled phenylalanine in Bc-L2 cells versus Bc-L2-L4 (Fig. 5.5). 1 mM phenylalanine, together with [^{3}H]-labeled phenylalanine (1 μCi/ml), was given apically to the tested cells and 10 min after phenylalanine accumulation was determined in the cellular (C) and basolateral (B) compartments as schematically indicated in Fig. 5.5A. No differences were detected in the measurement of phenylalanine in the apical compartment (Fig. 5.5B); whereas, a statistically significant decrease in intracellular phenylalanine concentration was detected in Bc-L2-L4 cells, which translated in a higher basolateral accumulation compared to Bc-L2 cells (Fig. 5.5C). This result suggests that LAT4 might be functionally expressed in Bc-L2-L4 cells; however, an important point to clarify is the level of LAT2 expression in Bc-L2 versus Bc-L2-L4. Indeed, since LAT2 is an exchanger for neutral amino acids it will inevitably transports as well all LAT4 substrates; therefore, the difference in efflux rate observed in the previous outlined experiment could also be due to a higher LAT2 expression in Bc-L2-L4 cells. Unfortunately, the quantification of LAT2 in Bc-L2 and Bc-L2-L4 cells was not possible due to lack of specific antibodies recognizing the fusion protein (data not shown) and therefore we decided to estimate the expression level by testing LAT2 function in these cells (Fig. 5.6). We therefore compared the basolateral uptake of leucine (1 mM) and alanine (1 mM) between Bc-L2 and Bc-L2-L4 cells. Leucine was used to test the functionality of LAT4; whereas, the alanine uptake is aimed to test LAT2 function, since alanine is not transported by LAT4. To prevent the interference of LAT2 with the leucine uptake by LAT4, the leucine uptake was performed in the presence of an excess of another LAT2 substrate in the basolateral compartment, namely glutamine. A statistically significant intracellular leucine accumulation by Bc-L2-L4 was observed after 2 min uptake (Fig. 5.6A) with a corresponding reduced basolateral leucine concentration (Fig. 5.6B); whereas, the leucine accumulation in the apical compartment did not differ (Fig. 5.6C). Concerning alanine distribution, we could not report any difference in the intracellular accumulation (Fig. 5.6D), but, unexpectedly, Bc-L2-L4 showed a higher apical accumulation (Fig. 5.6E) and a corresponding reduced basolateral alanine concentration (Fig. 5.6F) suggesting the possibility that a major

paracellular transport of alanine took place by these epithelia. However, according to the equal intracellular alanine concentration, we conclude that the LAT2 functionality does not differ markedly between Bc-L2 and Bc-L2-L4 cells.

In summary, based on the previous outlined experiments, we cannot attribute the fact that LAT4 expression unlike TAT1 had no impact on intracellular amino acid concentration to a lack of LAT4 function nor to a different degree of LAT2 functionality. However, a lower functional expression of LAT4 compared to that of TAT1 is not excluded.

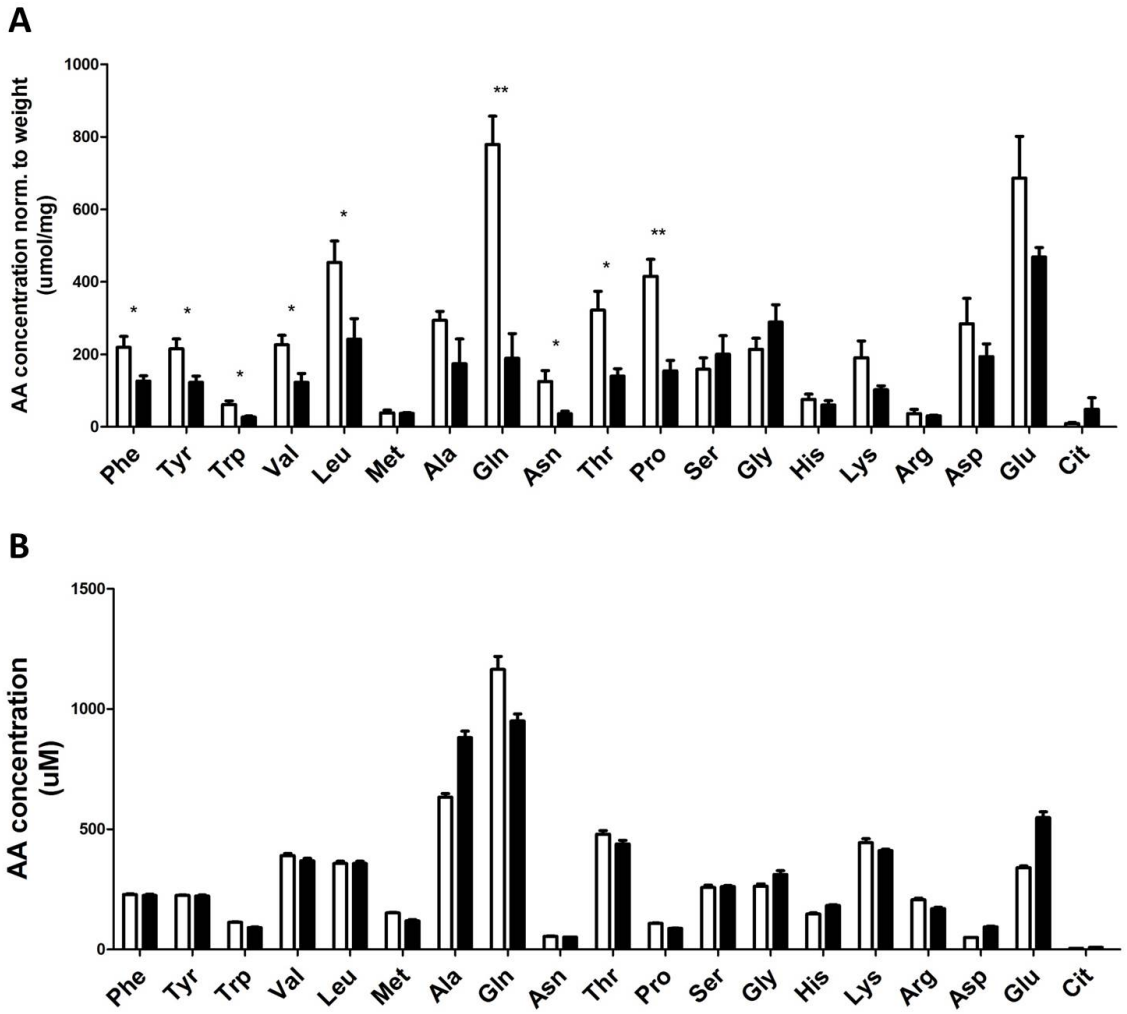

Figure 5.3 Intracellular and basolateral amino acid measurements in Bc-L2 and Bc-L2-T1 cells. (**A**) Bc-L2 (white) and Bc-L2-T1 (black) were lysed 48 h posttdifferentation and the intracellular concentration of the indicated amino acids was determined as described in "Materials and Methods". Concentrations were converted to µmols and normalized per weight of cell pellet. (**B**) The basolateral medium of the same

experiment performed in (**A**) was collected and the concentrations of the indicated amino acids were measured. Represented are means ± SEM; n = 4, Student *t*-test, * $p < 0.05$, ** $p < 0.01$.

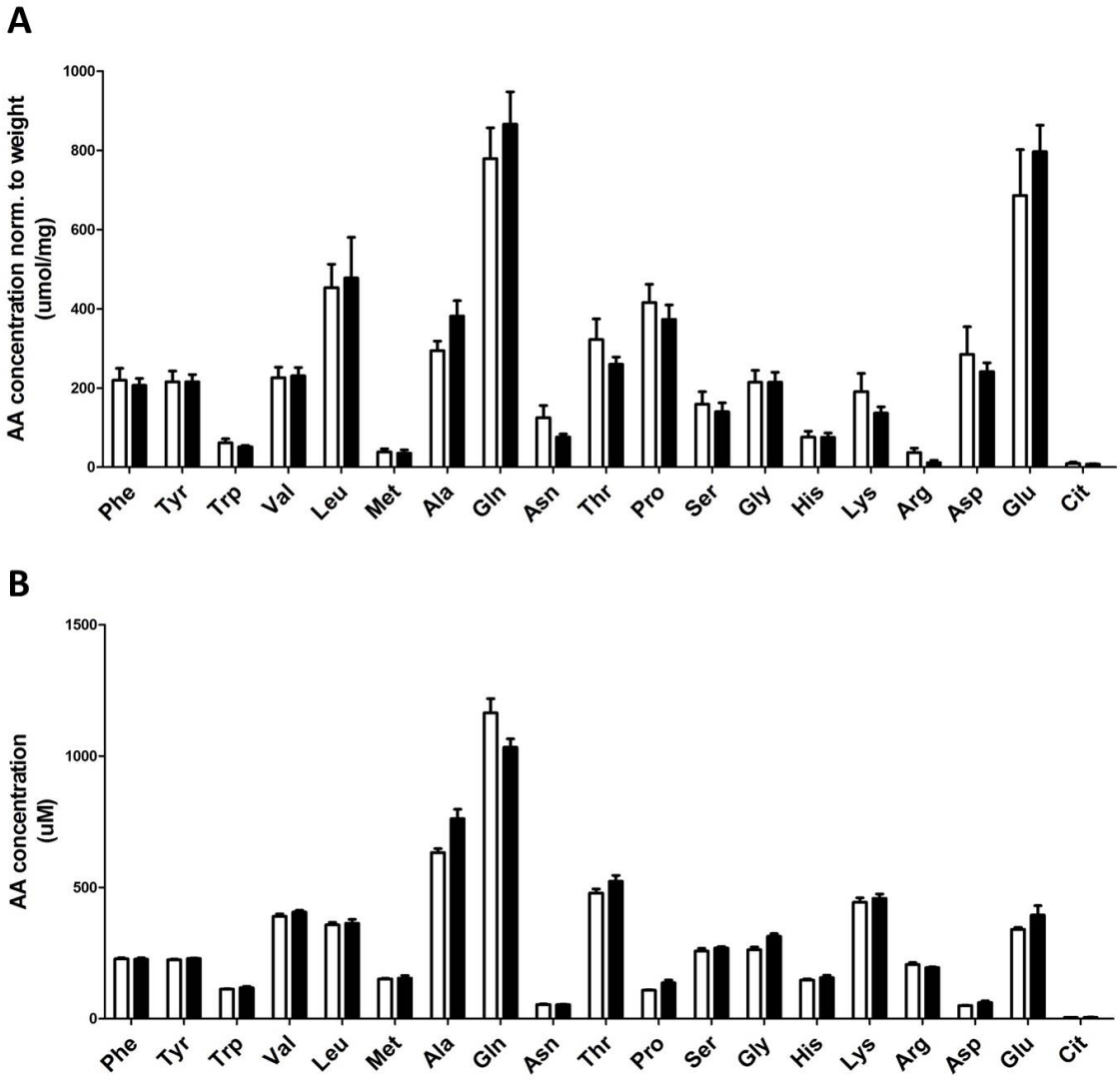

Figure 5.4 Intracellular and basolateral amino acid measurements in Bc-L2 and Bc-L2-L4 cells. (**A**) Bc-L2 (white) and Bc-L2-L4 (black) were lysed 48 h posttdifferentation and the intracellular concentration of the indicated amino acids was determined as described in "Materials and Methods". Concentrations were converted to µmols and normalized per weight of cell pellet. (**B**) The basolateral medium of the same experiment performed in (**A**) was collected and the concentrations of the indicated amino acids were measured. Represented are means ± SEM; n = 4.

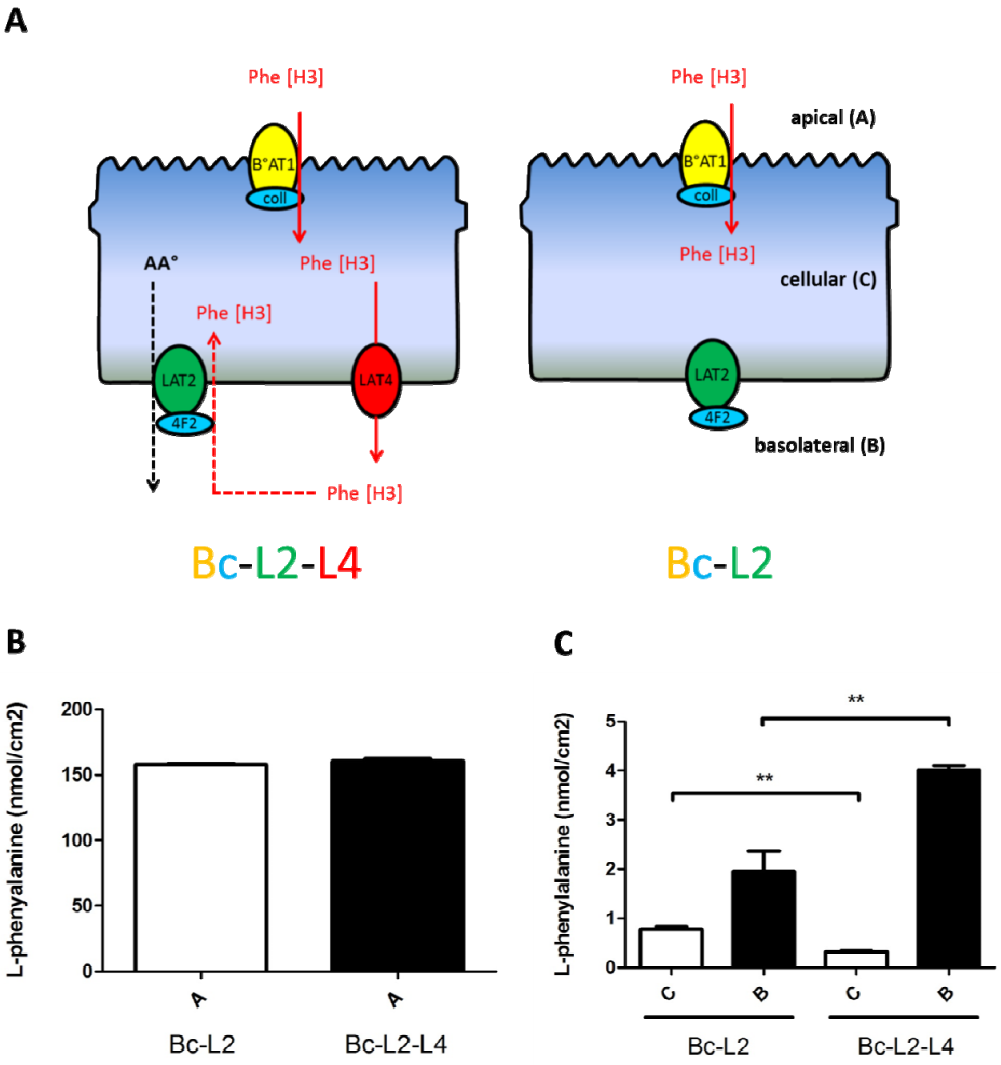

Figure 5.5 Test of LAT4 functionality with radiolabeled phenylalanine. (**A**) Schematic representation of the experimental setup: 1 mM phenylalanine together with [^{3}H]-labeled phenylalanine ([^{3}H]Phe) (1 µCi/ml) was given at the apical compartment and its transepithelial transport was determined after 10 min in the different compartments. Bc-L2-L4: MDCK cells expressing B°AT1, TMEM27, LAT2, 4F2hc and LAT4; Bc-L2: MDCK cells expressing B°AT1, TMEM27, LAT2 and 4F2hc (**B**) Amount of phenylalanine in the apical compartment of Bc-L2 versus Bc-L2-L4 cells. (**C**) Amount of phenylalanine in the intracellular (C) and basolateral compartment (B). Represented are means ± SEM; n = 3, Student *t*-test, ** $p < 0.01$.

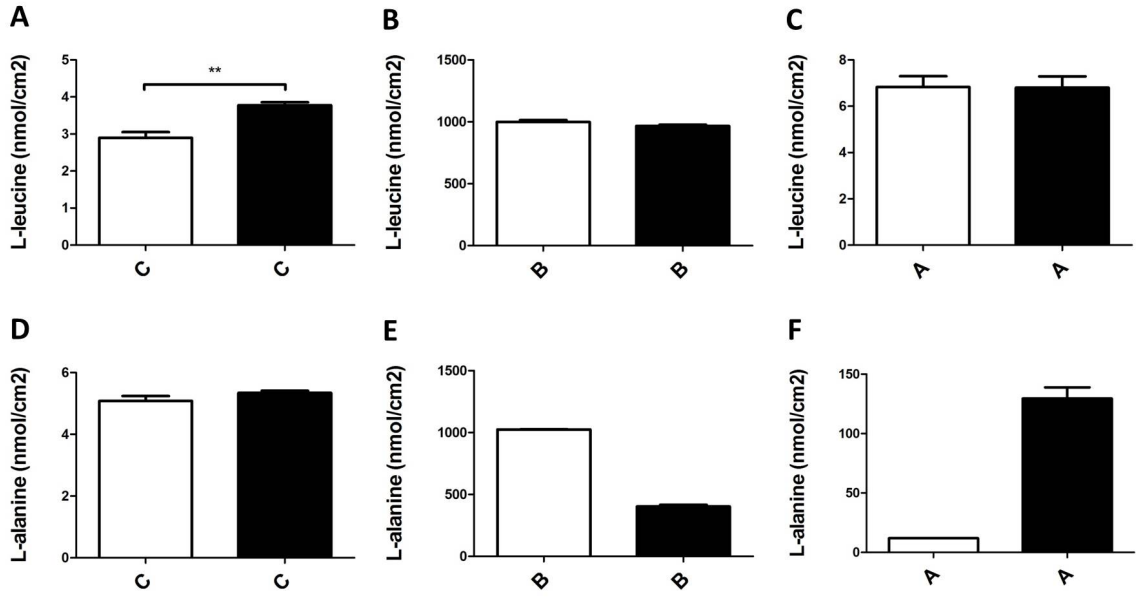

Figure 5.6 Basolateral uptakes of leucine and alanine in Bc-L2 (white) and Bc-L2-L4 cells (black). (**A**, **B** and **C**) 1 mM leucine together with [^{3}H]-labeled leucine (1 µCi/ml) or (**D**, **E** and **F**) 1 mM alanine together with [^{3}H]-labeled alanine (1 µCi/ml) were given to the basolateral compartment and the uptake was allowed to take place for 2 min. For the leucine uptake, 1 mM of glutamine was in addition added to the basolateral compartment. Represented are means ± SEM. n = 3, Student *t*-test, ** $p < 0.01$. C: intracellular compartment. B: basolateral compartment. A: apical compartment.

5.3 Characterization of LAT4 in *Xenopus laevis* oocytes and MDCK cells

5.3.1 LAT4 regulation upon changes in *Xenopus laevis* oocytes volume

Amino acids represent a major portion of the intracellular organic solutes and are known to have important roles in cell volume regulation (Hoffmann & Simonsen, 1989; Lang *et al.*, 1998). Moreover, the concentrative system A transporter SNAT2 has been shown to play important role in the regulatory volume responses upon hypertonic stress *in vitro* and *in vivo* (Bedford & Leader, 1993; Dall'Asta *et al.*, 1994; Dall'Asta *et al.*, 1996). Since LAT4 mediates the facilitated-diffusion of some neutral amino acids, we hypothesize that its function might be sensitive to the cell osmolarity and cell volume in analogy to SNAT2. Therefore, we decided to investigate this issue by expressing LAT4 in *Xenopus laevis*

oocytes and testing the efflux of phenylalanine at different oocyte volumes. 10 nmol of phenylalanine were delivered in LAT4-expressing oocytes with a injection-volume of either 50 nl or 100 nl resulting, respectively, in a final oocyte volume of 450 nl or 500 nl (Fig. 5.7).

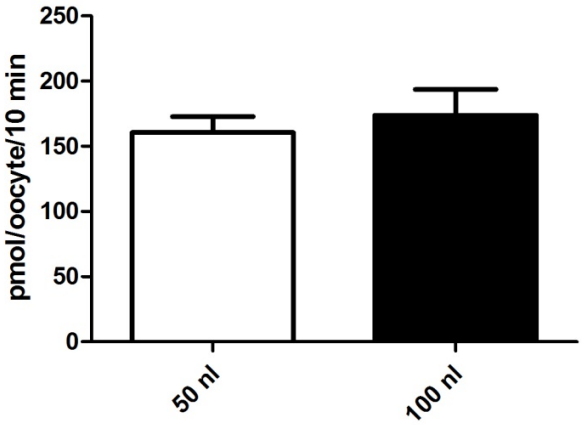

Figure 5.7 Efflux of phenylalanine with different oocyte volume. Oocytes were injected with 10 nmol of phenylalanine in a volume of either 50 nl or 100 nl and efflux was performed for 10 min.The amount of phenylalanine effluxed by control oocytes was substracted. Represented are means ± SEM; n = 8-9.

No difference in phenylalanine efflux was observed between the two volumes indicating that LAT4 function is probably not sensitive to cell volume changes and therefore might not play an important role in the amino acid-dependent osmotic regulation of cells.

5.3.2 Effect of LAT4 phosphorylation on function and localization

Protein phosphorylation at specific amino acid residues has been shown to represent a way of regulating protein function, localization, stability and interaction with other proteins (Deribe *et al.*, ; Mann & Jensen, 2003). for instance, multisite phosphorylation of aquaporin 2 (AQP2) is known to modulate the intracellular trafficking of this transmembrane protein and therefore influences the amount of water reabsorption at the level of kidney collecting duct (Nielsen *et al.*, 1995; Nielsen *et al.*, 2002; Tamma *et al.*, 2008). In 2011, Feric *et al.* identified potential phosphorylation sites on a variety of kidney transmembrane proteins by combining a magnesium precipitation protocol for cortical membrane isolation (Biber *et*

al., 1981; Cutillas *et al.*, 2005) with mass-spectrometric analysis (Feric *et al.*, 2011). Among the different amino acid transporters detected, they could identify the phosphorylation of serine 274 in Lat4. In order to investigate whether this serine phosphorylation site might affect Lat4 function and localization we mutagenized the serine residue into an alanine residue (S274A), which has about the same molecular mass as serine but cannot be phosphorylated, or into a glutamate residue (S274E), whose residual group bears partial negative charges and can therefore chemically mimic a phosphate group. Moreover, all the different constructs were modified at their N-terminal portion with the insertion of a FLAG **(**DYKDDDDK) tag. This tag is aimed to facilitate possible future steps of immunodetection and immunoprecipitation. To assess whether the addition of the FLAG tag might influence the kinetic properties of LAT4, we performed uptake experiments with increasing phenylalanine concentrations and compared the Michaelis-Menten constants between the FLAG-tagged LAT4 protein and the untagged one (Fig. 5.8). Fitting curves corresponding to the Michaelis-Menten kinetics to the experimental data, yielded different V_{max} for both constructs (i.e. V_{max} of about 393 ± 32 pmol for FLAG-tagged LAT4 and V_{max} of about 913 ± 37 pmol for untagged LAT4), which may be due to a difference in protein translation efficiency or to a differential cell surface expression or eventually function. However the K_m values (i.e. K_m of about 3.6 ± 0.97 mM for FLAG-tagged LAT4 and K_m of about 3.6 ± 0.48 mM for untagged LAT4) were apparently unchanged. Since the K_m for both constructs are highly comparable we concluded that the insertion of the FLAG-tag at the N-terminal part of LAT4 did most likely not affect the kinetic properties of the transporter.

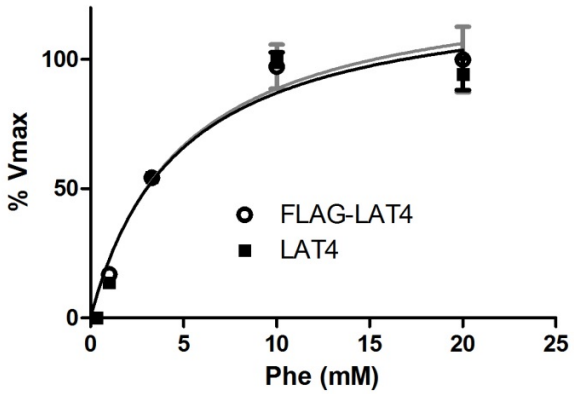

Figure 5.8 Comparison of Michaelis-Menten uptake kinetics between FLAG-tagged and untagged LAT4. Oocytes were injected with 25 ng of respective cRNA and incubated for 3 days. 10 min uptake was performed with different concentration of phenylalanine together with 10 µCi/ml [^{3}H]-labeled phenylalanine as tracer. Represented are means ± SEM; n = 24-27 pooled from three independent experiments.

The different LAT4 constructs were then expressed in oocytes and the functionality was tested by performing a phenylalanine uptake (100 µM) and comparing the uptake rate between different days of protein expression (Fig. 5.9A-D). Regardless of expression time, the S274A constructs showed a higher uptake rate compared to wildtype LAT4, which was about 30% higher after 1, 2 and 3 days of protein expression and slightly lower (i.e. about 10%) after 4 days. On the other hand, the S274E construct showed a statistically significant lower uptake rate upon 2, 3 and 4 days of expression with the highest decrease (i.e. about 30%) after 4 days. Since the S274A construct cannot be phosphorylated in position 274, whereas the S274E construct is thought to mimic a transporter phosphorylated in position S274, the results outlined previously suggest that phosphorylation at serine 274 downregulates LAT4 function; whereas, the removal of the phosphate residue upregulates LAT4 function. These functional results would need of course to be compared with data on surface expression to conclude about possible mechanisms leading to this difference.

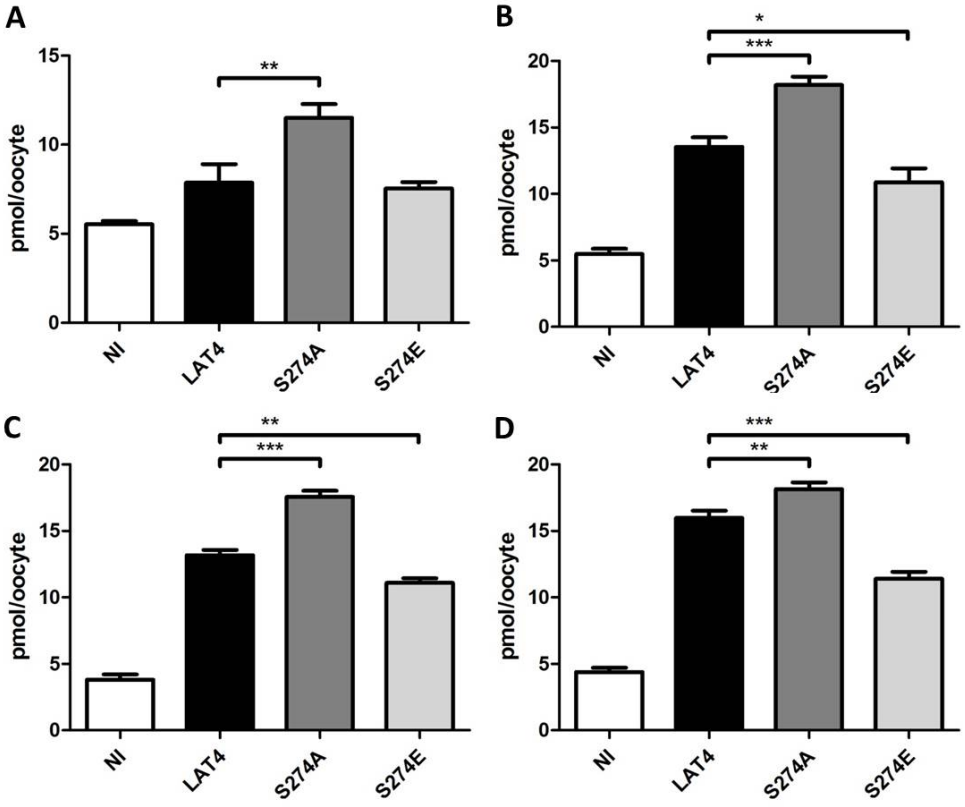

Figure 5.9 Uptake of phenylalanine by the different mutagenized LAT4 constructs upon different days of protein expression. Oocytes were injected with 25 ng of the respective cRNAs and 10 min uptake of phenylalanine (100 µM cold phenylalanine, 10 µCi/ml [^{3}H]-labeled phenylalanine) was performed after 1 (**A**), 2 (**B**), 3 (**C**) and 4 (**D**) day(s) after cRNA injection. Represented are means ± SEM, n = 8-9, one-way ANOVA, Dunnet's posttest, * $p < 0.05$, ** $p < 0.01$, *** $p < 0.001$.

In view of the promising results obtained with the *Xenopus laevis* oocytes expression system, we decided to confirm and further investigate the effect of serine 274 phosphorylation on LAT4 function in MDCK cells. The different LAT4 constructs were transduced in MDCK cells and the proper expression was tested by Western blotting (Fig. 5.10A). Basolateral uptake of phenylalanine confirmed the previously obtained results in oocytes: in comparison with wildtype LAT4, S274A mutant displayed about a 50% higher uptake rate; whereas, S274E showed about a 25% reduction (Fig. 5.10B). Moreover, the different LAT4 mutants showed a different uptake pattern if tested for glutamate, which is not a LAT4 substrate. Indeed, S274 unexpectedly displayed a ~10% higher uptake rate as compared to control cells, which was statistically significant (Fig. 3.10C). Besides that, the

uptake pattern obtained for glutamate confirms the differences in uptake rate observed are LAT4 specific.

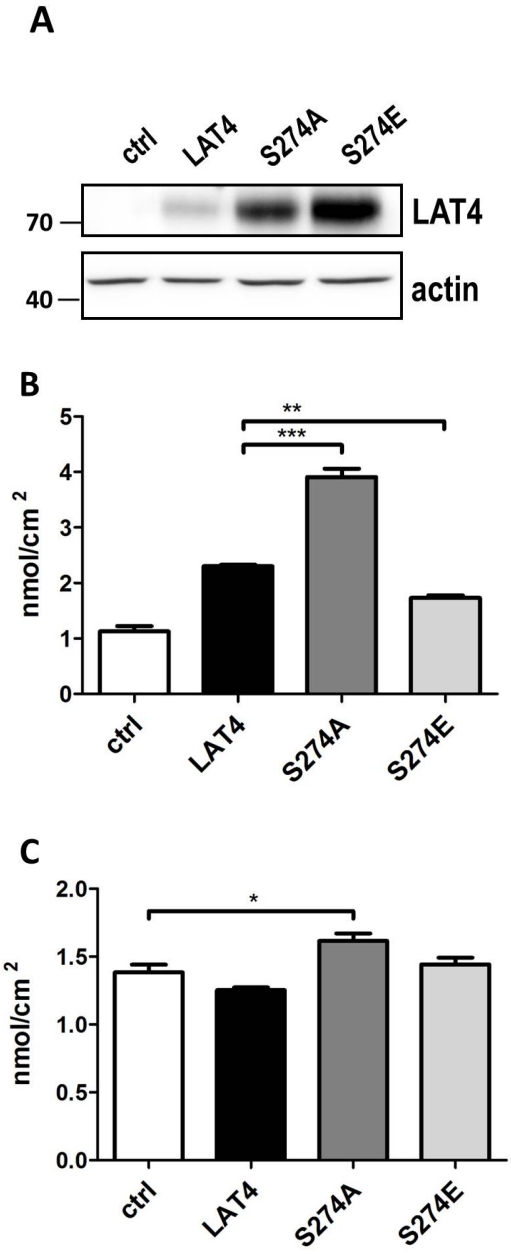

Figure 5.10 Investigation of S274 phosphorylation in MDCK cells. (**A**) Western blotting showing MDCK cells transduced with control vector (ctrl), wildtype LAT4 construct (LAT4), S274A mutagenized construct (S274A) or S274E mutagenized construct (S274E). (**B**) 10 min phenylalanine uptake or (**C**) glutamate (100

µM cold amino acid, 1 µCi/ml [^{3}H]-labeled amino acid, respectively) of MDCK cells seeded on filters and expressing different LAT4 constructs. Represented are means ± SEM, n = 3, one-way ANOVA, Tukey's Multiple Comparison posttest, * $p < 0.05$, ** $p < 0.01$, *** $p < 0.001$.

To investigate whether the functional effect of serine 274 phosphorylation could be explained by a different LAT4 intracellular trafficking in the different mutagenized constructs, we aimed at determine the amount of LAT4 localized at the plasma membrane in the different mutants by performing surface biotinylation.

The labeling of plasma membrane protein with the biotinylation technique notoriously requires optimization steps depending on the cell lysis procedure, the antibody used and the protein of interest. Therefore, before assessing the difference in LAT4 surface expression between the different LAT4 mutants, we first established the surface biotinylation technique with MDCK cells expressing the wildtype LAT4 versus control cells (Fig. 5.11)

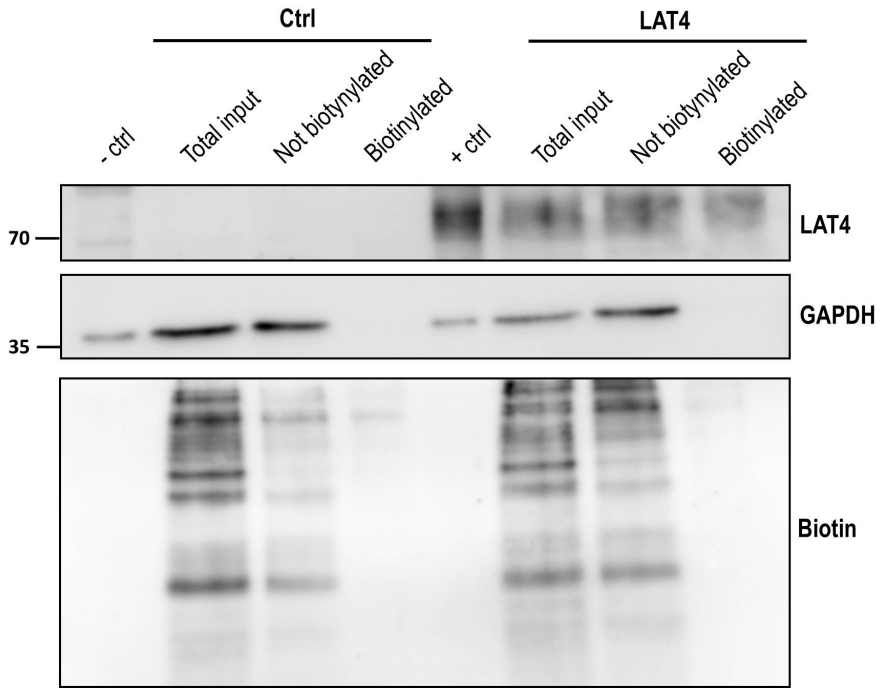

Figure 5.11 Surface biotinylation of LAT4 wildtype-expressing MDCK cells versus control cells. Control MDCK cells (ctrl) and LAT4 wildtype-expressing cells (LAT4) were subjected to surface biotinylation and different proteins were detected by Western blotting. Glyceraldehyde-3-phosphate dehydrogenase (GAPDH) was used as control for intracellular protein contamination. Biotin was used to verify the extent of protein biotinylation. Positive (+ctrl) and negative controls (-ctrl) were used to test LAT4 antibody specificity.

As shown by the biotin control in Fig. 5.11, the streptavidin beads-mediated precipitation step did not enrich the biotinylated fraction compared to the total input. Therefore, the entire procedure was not efficient and still needs to be optimized.
In order to ameliorate the efficiency of biotinylated fraction enrichment, we tested different conditions for cell lysis (Fig. 5.12), but without success.

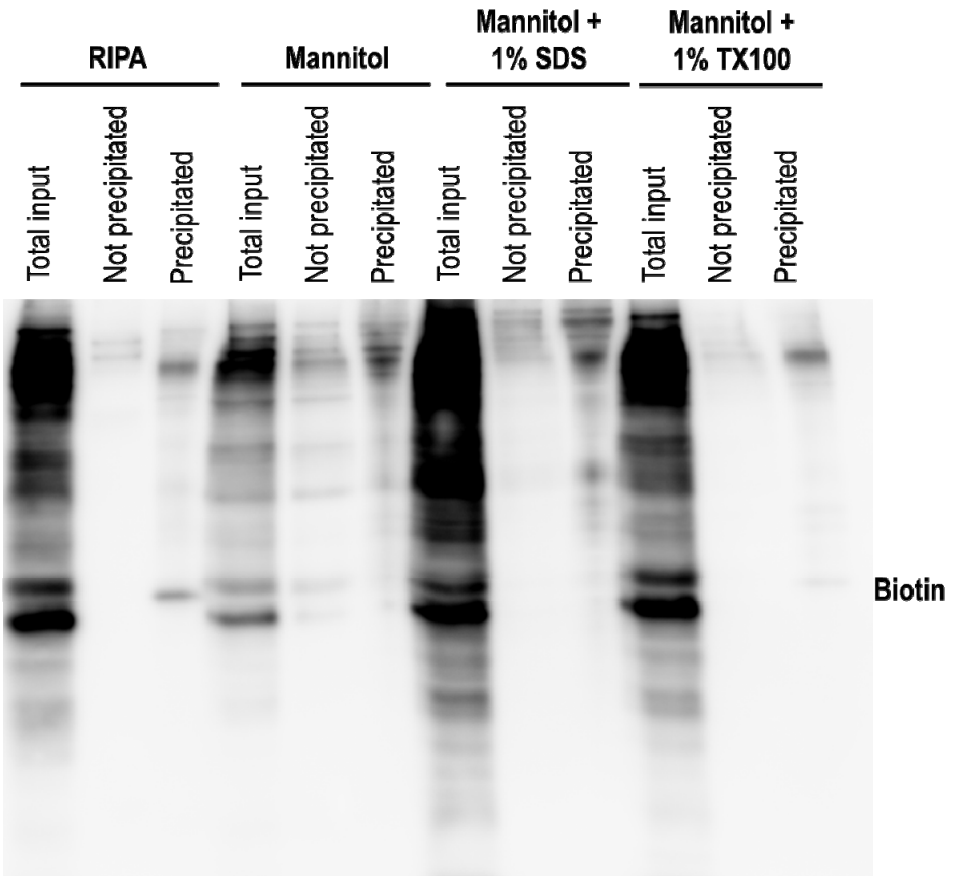

Figure 5.12 Cell surface biotinylation with different detergents for cell lysis. MDCK cells expressing wildtype LAT4 were biotinylated according to usual protocol and different detergents were used to mediate the cell lysis and total membrane isolation. SDS: sodium dodecylsulfate. TX100: Triton X-100.

Due to the technical problems with the surface biotinylation technique, we decided to investigate the surface expression of LAT4 in the different mutants using immunofluorescence and confocal microscopy. The specificity of the anti-FLAG antibody was first validated using conventional immunofluorescence (Fig. 5.13); furthermore, to get

a better resolution of LAT4 membrane localization among the different mutants, confocal microscopy was performed (Fig. 5.14). MDCK cells expressing the wildtype LAT4 shows a clear basolateral expression with almost no detectable intracellular LAT4; whereas, the S274A and S274E mutants reveal a more diffuse protein expression, a significant level of intracellular LAT4 localization being detectable. However, no clear difference in LAT4 intracellular localization between the two mutants, which could explain the differences in LAT4 functionality reported previously, was observed.

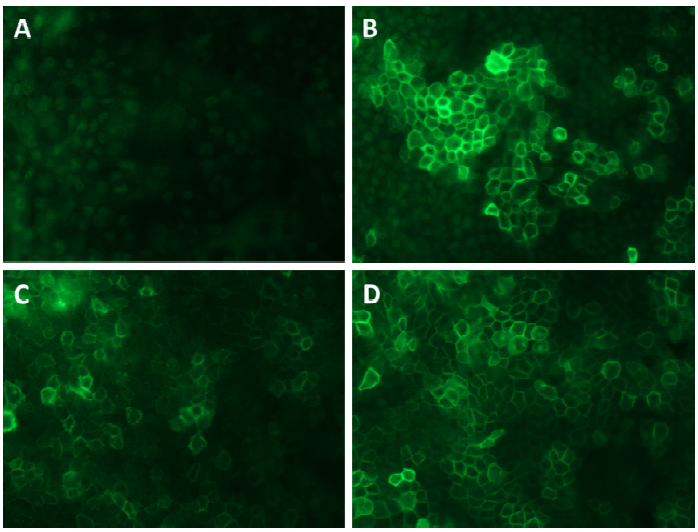

Figure 5.13 Immunofluorescence of MDCK cells expressing different LAT4 mutants. Control MDCK cells (**A**) or MDCK cells expressing wildtype LAT4 (**B**), S274A mutant (**C**) or S274E mutant (**D**) were seed on filters according to usual procedure and the expression of LAT4 protein was verified using an anti-FLAG antibody.

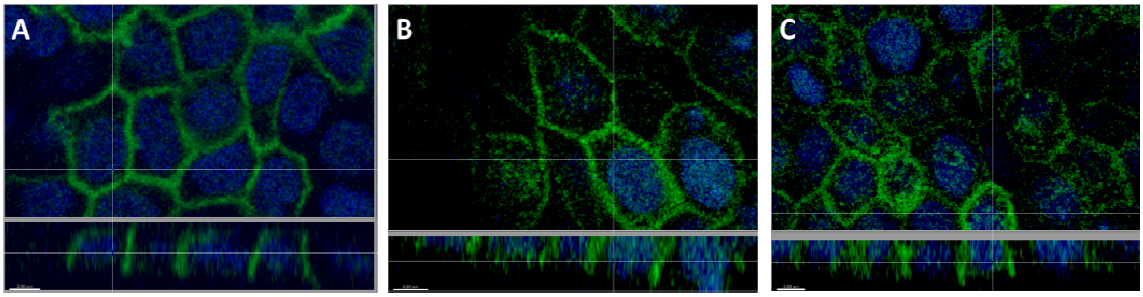

Figure 5.14 Immunofluorescence and laser scanning confocal microscope of MDCK cells expressing different LAT4 mutants. MDCK expressing wildtype LAT4 (**A**), S274A mutant (**B**) or S274E mutant (**C**)

were seeded on filters and LAT4 localization was visualized with laser scanning confocal microscope. Scale bar: 10 μm.

6. Discussion and Outlook

6.1 The use of knock-outs animal models to characterize amino acid transporters *in vivo* and the *Slc43a2* $^{-/-}$ knock-out model

In recent years, the use of genetically modified knock-out mice bearing constitutive or even inducible deletions of target amino acid transporters enabled the achievement of a deeper characterization of the physiological roles and potential regulation of amino acid and oligopeptide transporters. By applying standard physiological techniques, such as urine analysis and amino acid fractional excretion determination, to the characterization of knock-out mouse models, new important findings have been highlighted that contributed to a better understanding of genetic diseases involving amino acid transporters. Currently, 25 knock-out mice models for amino acid and oligopeptides transporters that have been characterized and published (Makrides, 2014). In some cases the mouse model presents pathophysiological hallmarks corresponding to the clinical findings of patients suffering from a defect in the specific amino acid transporter strengthening the mouse as a valuable tool to further investigate the genetic disease. Cystinuria B and A, for example, result from genetic defects in the amino acid transporter $b^{0,+}$ (*Slc7a9*) or its heavy chain accessory protein rBAT (*Slc3a1*), respectively, and the corresponding mouse models present elevated urinary levels of cystine and dibasic amino acids in accordance to the clinical findings in human patients (Feliubadalo *et al.*, 2003; Peters *et al.*, 2003; Font-Llitjos *et al.*, 2007). Another example is represented by genetically defects in the transporter EAAT/EAAC1 (*Slc1a1*) that have been associated to the dicarboxylic aminoaciduria, whose clinical hallmarks are also reproducible in the *Slc1a1*-null mouse (Peghini *et al.*, 1997). Interestingly, in the case of lysinuric protein intolerance disease (LPI), which is caused by dysfunctions in the basolateral heterodimeric amino acid antiporter y^{+}LAT1 (*Slc7a7*) and is characterized by failure to thrive and intellectual impairment, the corresponding knock-out mouse model revealed even a more deleterious phenotype, which resulted for most of the

analyzed mice in intrauterine growth restriction and premature death (Sperandeo *et al.*, 2007).

Furthermore, many additional transporters that are not associated yet with a particular genetic disease have been characterized *in vivo* using knock-out mouse models. For amino acid transporters such as Tat1 (*Slc16a10*) and Lat2 (*Slc7a8*) and the oligopeptides transporter PEPT1 (*Slc15a1*), their specific genetic disruption resulted only in mild phenotypes, despite the widespread tissue expression and the substrate importance (i.e. essential neutral amino acids and oligopeptides) of these transporters (Nassl *et al.*, ; Hu *et al.*, 2008; Mariotta *et al.*, 2012). These findings reveal evolutionary compensatory mechanisms that enable the maintenance of a proper nutritional homeostasis despite the functional defect of a specific component highlighting as well the necessity to investigate double knock-out of selected transporters in order to unravel the physiological consequence of defective amino acid and oligopeptides homeostasis.

In the case of the amino acid transporter LAT4, no aminoaciduria or other amino acid-involving defect have been currently linked to mutations of its gene. However, the *Slc43a2*$^{-/-}$ knock-out (Lat4-null) mouse model characterized in this thesis presented a deleterious phenotype resulting in premature death before weaning. A strong phenotype resulting in premature death has been already characterized in mice defective for the amino acid transporters GLYT1 (*Slc6a9*) (Rubio-Aliaga *et al.*, 2003), GLYT2 (*Slc6a5*) (Gomeza *et al.*, 2003), CAT-1 (*Slc7a2*) (Perkins *et al.*, 1997) and Asc1 (*Slc7a10*) (Xie *et al.*, 2005; Rutter *et al.*, 2007). One important observation is the lack of Lat4 does not have an influence on the prenatal development as we could not report significant differences from the expected Mendelian ratio in the number of *Slc43a2*$^{-/-}$ newborns. Moreover, the lack of any clear pathological signs, such as altered skin color, and the presence of the so-called “milk spot” suggests a proper breastfeeding behavior. Therefore, we hypothesized that the early lethality may be due to a dysfunctional enteric absorption of nutrients.

To provide evidence that Lat4 may have an important role in the absorption of its substrates at the level of the small intestine, we confirmed that Lat4 protein is expressed at the basolateral membrane of enterocytes. Furthermore, we observed a selective leucine accumulation in the first part of the small intestine in *Slc43a2*$^{-/-}$ mice indicating a defective basolateral efflux of Lat4 substrates. Surprisingly, this amino acid retention did not result in

a defective acute accumulation in plasma or other organs tested. However, one should consider that this measurement represents a single time point and does not give indications about the effects of this defective amino acid absorption on the long term amino acid accumulation in the body. Moreover, a fraction of the dietary absorbed leucine is known to be catabolized by the small intestine enterocytes via the branched-chain amino acid transaminase to generate branched-chain α-ketoacids (Stoll *et al.*, 1998; El-Kadi *et al.*, 2006); therefore, the amount of radioactivity determined in plasma and the different organs might not be represented entirely by the orally administered leucine. In addition, if the *Slc43a2*$^{-/-}$ mice would have a different intestinal amino acid metabolism compared to the wildtypes, this would create an important confounding factor, which need to be taken into account by interpreting these results. Finally and probably most importantly, it is likely that the high amount of small solutes like amino acids and glucose that reach the small intestine with the nutrition bolus are absorbed in particular early after birth mainly by a paracellular route that however becomes less leaky within a few days (Wada *et al.*, 2013). This would explain why the absorption of L-leucine after an acute load was not decreased in Lat4-null pups. The low amino acid concentrations found in the plasma of these pups upon sacrifice at 2 days is thus presumably due rather to a continuous paracellular enteral loss of amino acids that normally would be prevented by a continuous transcellular reabsorption, than by a lack of absorption upon acute nutrition. This possibility would also fit our observation that subcutaneous administration of amino acids didn't ameliorate the survival of the knock-out pups.

Concerning further information about Lat4 localization, we could confirm at the protein level the lack of Lat4 expression in liver and skeletal muscle, which was previously reported by Bodoy *et al.* at the mRNA level (Bodoy *et al.*, 2005). In the kidney, we showed a major Lat4 expression in the proximal tubule, as previously reported elsewhere at the mRNA level (Cheval *et al.*, 2011), and in the thick-ascending limb and a minor expression in the distal convoluted tubule. It is known that more than 99% of amino acid reabsorption takes place in the proximal tubule; therefore, the expression of Lat4 in this tubule segments fits with a potential role for this transporter in the context of amino acid reabsorption. The effect of the complete disruption of Lat4 on kidney amino acid reabsorption could not be tested due to the early lethality of *Slc43a2*$^{-/-}$ pups. Metabolic cages experiments were

performed comparing *Slc43a2*$^{+/-}$ mice with wildtype one, but no significant major aminoaciduria was reported confirming the haplosufficiency of the *Slc43a2* gene.

An interesting finding is the expression of Lat4 in the thick ascending limb, which has also been previously reported at the mRNA level by Cheval *et al.* (Cheval *et al.*, 2011) and was shown to be quantitatively only about 6-fold less expressed compared to the thick ascending limb-marker NKCC2 (*Slc12a1*) (i.e. about 20 SAGE mRNA tags for Lat4 versus about 118 tags for NKCC2 considering both cortical and medullary thick ascending limb together). Thus, one can speculate about the possible role of this transporter in this specific nephron segment. As already outlined in the introductory part, the thick ascending limb is responsible for NaCl reabsorption from the tubular fluid; moreover, it plays an important role in Mg^{2+} and Ca^{2+} reabsorption as well as in acid-base homeostasis. Physiological alterations that can chronically affect the NaCl transport in this nephron segment are known to affect the epithelial cell size. High level of water intake in rats and consequent low plasma level of ADH has been shown to result in thick ascending limb hypotrophy (Trinh-Trang-Tan *et al.*, 1987). Since the regulation of cell volume is dependent on mTORC1-depedent signaling, which is itself sensitive to the level of intracellular branched-chain amino acids, Lat4 could possibly have a role in this regulation by equilibrating between its intracellular and extracellular branched-chain amino acids and thereby its defect could influence the cell volume regulatory mechanism outlined before. Moreover, the thick ascending limb is responsible for the production of the Tamm-Horsfall glycoprotein (THP), which is also known as uromodulin and represents the most abundant mammalian protein in the urine under physiological conditions. To synthesize proper amounts of this protein in response to physiological demands, the epithelial cells need to dispose of appropriate concentrations of intracellular amino acids and in this sense Lat4 might contribute to maintain a proper intracellular concentration of its substrates that all together represent about 24% of the total amino acids present in the murine THP (NP_033496.1).

Increased levels of plasma amino acid and acylcarnitines in Lat4-null pups revealed metabolic analogies with a status of starvation and malnutrition (Wolfsdorf *et al.*, 1982; Ji *et al.*, 1987; Huq *et al.*, 1993; Costa *et al.*, 1999), which is most probably leading to the premature death of pups. We hypothesize that this metabolic disruption might be due to a primary defect in amino acid absorption. This would then translate in secondary metabolic

changes especially at the level of the liver, whose gene expression pattern was clearly altered in *Slc43a2*$^{-/-}$ mice. Moreover, we could also highlight a major defect in blood glucose homeostasis upon Lat4 disruption. To further enlarge the metabolic profile of *Slc432a2*$^{-/-}$ mice, it would be interesting to determine additional plasma markers for protein intake, i.e. albumin and prealbumin. Furthermore, 3-methyl-histidine (3MH) measurement would give insights of possible muscle catabolism and proteolysis to compensate the defective dietary amino acid intake; although, the plasma levels of hydroxyproline (OH-Pro) did not differ between *Slc43a2*$^{-/-}$ mice and wildtypes indicating that no massive connective tissue breakdown is taking place.

In addition to the expression in the kidney and small intestine, data available online (BioGPS.org) indicate a considerable Lat4 expression in macrophages, osteoclasts and microglia. The interesting point is whether the lack of Lat4 protein in the aforementioned tissue might result in deleterious effects that might have contributed to the early lethality. The influence of Lat4 on macrophages development and immunocompetence would be an interesting point to deepen with a tissue-specific knock-out animal; however, in the case of our total knock-out mouse model, we hypothesize that a potentially defective macrophages would contribute probably to a minor extent to the lethal phenotype, since mice were housed in high hygienic conditions and with very low probability to get infected by common pathogens. Moreover, mice lacking the colony-stimulating factor 1 (CSF-1), that show a severe combined deficiency of macrophages, osteoclasts and microglia show, in comparison with the *Slc43a2*$^{-/-}$ knock-out mouse, a milder phenotype, which is characterized by reduced body weight, lack of teeth and musculo-skeletal abnormalities (Naito, 2008).

In conclusion, the constitutive disruption of the *Slc43a2* gene revealed its pivotal *in vivo* role in postnatal development. With the obtained findings about Lat4 localization and kinetics, we postulate that Lat4 might play an important role in absorption of amino acid at the small intestine by mediating the basolateral efflux of its amino acid substrates and also by cooperating with basolateral heterodimeric exchangers Lat2-4F2hc and y^+Lat1-4F2hc. To further unravel the physiological role of Lat4 in different organs, such as the kidney thick-ascending limb, more targeted approaches should be considered, such as the use of a

conditional or tissue-specific *Slc42a3*$^{-/-}$ knock-out mouse model or the siRNA-mediated knock-down of Lat4 in isolated primary cell lines.

6.2 The use of *in vitro* models and reconstituted systems to investigate amino acid transporters functionality and cooperation

As outlined in the previous section, the global deletion of an amino acid transporter gene gives interesting insights into the physiological importance of amino acid absorption and reabsorption; however, to better unravel the intricate mechanisms of amino acid transporter regulations and cooperations, a more focused and specific approach is required. In this sense a cell culture model mimicking the physiological conditions of a kidney proximal tubule cell would represent a valuable tool enabling a deeper understanding of how amino acid transporters could react in response to different physiological and pathophysiological changes.

A convenient *in vitro* model, which has been widely used in the field of transporters characterization, is the *Xenopus laevis* oocytes expression system. In the case of Lat4, this *in vitro* model enabled us to investigate the Michaelis-Menten kinetics for uptake and efflux as well as the functionality of mutated Lat4 constructs. Moreover, standard molecular cell biology techniques, such as surface biotinylation, immunofluorescence and Western blotting, can be easily performed with oocytes making them not only a convenient tool to gather information about transporter functionality, but also about intracellular protein localization. Obvious limitation of oocytes as a tool to investigate regulation of heterologous proteins, is its own specific biological function and also the phylogenic distance of *Xenopus laevis* with mammals. In order for the system of expression to be able to biologically interact with the expressed protein and undergo specific modifications (e.g. ubiquitin-dependent internalization of a membrane protein, lysosomal-dependent protein degradation), conserved signaling pathways must be present. As an amphibian, *Xenopus laevis* diverged from the last amniote lineage (i.e. the last common ancestor between

amphibians and mammals) about 360 million years ago; therefore, receptors and other protein mediators involved in complex hormonal and vegetative regulatory pathways present in humans are mostly not conserved. Despite this distant phylogenic relationship, the genome of the Western Clawed Frog (*Xenopus tropicalis*) shows surprisingly a remarkable degree of genetic similarities especially considering genes involved in human diseases (Hellsten *et al.*, 2010). Moreover, signaling pathways and protein interactions have been studies and characterized in *Xenopus laevis* oocytes (Parys *et al.*, 1992; DeLisle *et al.*, 1996; DeLisle *et al.*, 1997; Bhavsar *et al.*, 2011; Bogatikov *et al.*, 2012). However, in the context of an *in vitro* model aimed at mimicking the physiological conditions of a mammalian epithelial cell, the *Xenopus laevis* oocytes expression system faces more restrictive limitations: the lack of an apico-basolateral polarization. This biological constraint does not represent a problem, when focusing on the multiple expression of amino acid transporters expressed "in parallel", such as the uniporter Tat1 and Lat4 that have been shown by Ramadan *et al.* to cooperate with the exchanger Lat2-4F2hc in the oocytes (Ramadan *et al.*, 2007). However, if the aim is to investigate the mechanism of transcellular amino acid transport, which implies two clearly spatial defined steps (i.e. an apical uptake followed by a basolateral efflux), more *in vitro* models with a clear cellular polarization should be taken into account.

The establishment of a proper cell culture model of kidney proximal tubule cells to investigate transport processes, cytotoxic and ischemic effects has been addressed in the past using different methodologies (Bello-Reuss & Weber, 1986; Elliget & Trump, 1991; Sheridan *et al.*, 1993) that were based on cell culture using solid supports. This restricts the cell accessibility to the apical side and therefore presents analogous limitations to the previously described oocyte system. In more recent years, Terryn *et al.* established a new methodology to harvest and culture kidney proximal tubule cells without using aggressive manipulations and with the aim to prevent the dedifferentiation process (Terryn *et al.*, 2007). Moreover, the use of collagen-coated permeable filter supports provides the possibility to culture these primary cells in a polarized state with access to both the apical and the basolateral sides, which is very useful tool in the context of transcellular transport research. Indeed, Terryn *et al.* show that these isolated cells display several morphological and biochemical features typical of kidney proximal tubules cells, such as high expression

of alkaline phosphatases, megalin and γ-glutamyl-transferase. In addition, they tested the functionality of glucose transporters and could show that the apical α-MG (a stable glucose analog) uptake was saturable in a time-dependent manner and was inhibited by the competitive SGLT inhibitor phloridzin. Unfortunately, no functional analysis on amino acid transport was performed; moreover, the measured low resistance (i.e. about 60 $\Omega \cdot cm^2$) might represent a limiting factor for the investigation of transepithelial transport due to the interference with the paracellular leakiness. For the establishment and use of this primary cell line in the field of amino acid transport, it would be interesting to analyze the level of expression of different amino acid transporters upon the differentiation process on permeable filters. Upon establishment of appropriate expression levels, the future steps consist in testing and validate the transepithelial transport in these cells and determine the degree of interference of the paracellular transport. If these cells would represent valuable *in vitro* models to investigate the functional aspects of amino acid transporters, they could indeed be used to complement and further understand how the disruption of single uniporters or antiporters impacts on the kidney amino acid homestasis.

An alternative approach consists in the reconstitution of already established cell lines of kidney origin by the heterologous expression of amino acid transporters. Indeed, interesting and valuable studies about amino acid transport have been published using HEK or OK cells (Fernandez *et al.*, 2003; Ristic *et al.*, 2006); however, these models do not form a tight epithelial monolayer when grown on filters and therefore are not suitable to investigate transepithelial transport. Therefore, in order to achieve a good balance between renal cell origin and the possibility to perform transepithelial function studies, we opted for the use MDCK cell lines and reconstitute them with the necessary transport machinery for neutral amino acids. An analogous approach has been used in 2003 by Bauch *et al.* (Bauch *et al.*, 2003), where they successfully coexpressed the apical amino acid transporter and accessory protein $b^{0,+}$AT-rBAT with basolateral heterodimeric exchangers (i.e. LAT2-4F2hc and y^+LAT1-4F2hc) and could show their functional cooperation in the reabsorption of cationic amino acids.

Using an analogous approach, our aim was to reconstitute in MDCK epithelial the apical transporter B°AT1 together with accessory protein TMEM27 and on the basolateral side the exchanger LAT2 with the accessory protein 4F2hc together with either the uniporter

TAT1 or LAT4. In order to establish this setup, several transduction steps are required that might have deleterious consequences for the proper cellular physiology and homeostasis; therefore, we first planned a strategy aimed at reducing as much as possible the transduction steps imposed. This consisted mainly in the expression of the apical B°AT1 and TMEM27 by using a bicistronic expression vector and the establishment of a fusion construct between LAT2 and 4F2hc. The fusion construct was validated in *X. laevis* oocytes by showing that the fusion protein possessed similar apparent affinities to the separated expressed proteins LAT2 and 4F2hc (Fig. 5.1). After performing the sequential transductions, we showed a proper amino acid transporter expression by the reconstituted MDCK epithelia using immunofluorescence and Western blotting (Fig. 5.2). Interestingly, antipodal results were obtained by testing these cells for the cooperation of LAT2-4F2hc and either TAT1 or LAT4. In the case of MDCK cells expressing B°AT1-TMEM27, LAT2-4F2hc and TAT1 (Bc-L2-T1), measurements of intracellular amino acid concentrations 48hrs postdifferentiation showed a significant reduction in all the aromatic amino acids and numerous neutral amino acids (Fig. 5.3A). This result provides indication that TAT1 is functional in our MDCK model and undergoes a specific cooperation with LAT2-4F2hc as was already shown elsewhere in oocytes (Ramadan *et al.*, 2007) and in *Slc16a10*$^{-/-}$ knock-out mice (Mariotta *et al.*, 2012). It is important to mention that, although we had a major decrease in intracellular amino acid concentration we could not report a corresponding increase in the basolateral medium (Fig. 5.3B). This finding might be explained by the different volumes of the intracellular (50 µl) and the basolateral compartments (500 µl); therefore, the corresponding efflux of intracellular amino acids would not have a major influence on the total amino acid concentration in the cell medium. Alternatively, one could also speculate that the TAT1 expression is also having an additional effect on cell metabolism and the intracellular amino acid pattern in Figure 5.3A is not only the result of amino acid transport but also of amino acid catabolism. This could also explain why some amino acids that are neither TAT1 nor LAT2-4F2hc substrates are decreased in Bc-L2-T1 cells (i.e. proline and lysine). In order to further disentangle this issue, the functionality of TAT1 and LAT2-4F2hc should be assessed by testing the transepithelial transport of specific radiolabeled amino acids.

In contrast to these results obtained with Bc-L2-T1 cells, MDCK epithelial expressing LAT4 instead of TAT1 (i.e. Bc-L2-L4), did not show any statistical significant difference in intracellular and basolateral amino acid concentration compared to control cells Bc-L2 (Fig. 5.4). The only minor differences consists in a small increase of intracellular and basolateral alanine concentration. Since these findings are in apparent contrast with the observations made by Ramadan *et al.* (Ramadan *et al.*, 2007) in *X. laevis* oocytes, we decided to test whether LAT4 is actually functionally active in Bc-L2-L4 by using radiolabeled amino acids. As shown in Figure 5.5B and C, Bc-L2-L4 cells display a higher efflux of [^{3}H]-phenylalanine and corresponding reduced intracellular concentration compared with Bc-L2 cells. We conclude that this basolateral accumulation is due to functional LAT4 expressed at the cell surface. On the other hand, cells expressing only LAT2-4F2hc are unable to transport phenylalanine out of the cells due to the lack of an exchanging amino acid substrate in the basolateral compartment. Since these findings provided good insights for a functional LAT4 in Bc-L2-L4 cells, we also tested the possible cooperation of these transporters using radiolabeled amino acids. As shown in Figure 5.6, the Bc-L2-L4 cells displayed a higher basolateral uptake of leucine compared to Bc-L2 cells; whereas there was no difference regarding alanine transport between the two cell types. These findings further confirmed that LAT4 is functional and suggests that the expression level of LAT2-4F2, which was functionally assessed using alanine, did not differ between Bc-L2 and Bc-L2-L4 cells. Given these functional findings, a still unsolved point is why Bc-L2-L4 did not show a major difference in intracellular amino acid concentrations compared to Bc-L2 (Fig. 5.4). One possible explanation is that LAT4 expression is also having a major effect on cell metabolism and therefore masking the effect of LAT4 and LAT2-4F2hc cooperation. Alternatively, one should also take into account that the established transport machinery in MDCK cell differs from the experimental settings used by Ramadan *et al.* (Ramadan *et al.*, 2007) and that the cooperation of LAT2-4F2hc and LAT4 might be hampered under particular conditions in MDCK epithelia. Finally it is also possible that the particular conditions used for the acute experiments using radiolabeled tracers were permissive for the function of LAT4 whereas the cell culture conditions in very high amino acid conditions inhibit LAT4 function. Such a hypothesis implies however that the function of LAT4 can be regulated acutely.

In conclusion, we reconstituted in MDCK epithelia the amino acid transport machinery for neutral amino acid transport and confirmed the functionality of the expressed transporters. We believe that this *in vitro* model might be used to gain new insight on amino acid transport in a more physiological way compared to the previously used *X. laevis* oocyte expression system. More specifically, these models might represent important tools to explain and mechanistically investigate particular urinary amino acid patterns observed in knock-out mouse models (e.g. *Slc16a10*$^{-/-}$ or *Slc7a8*$^{-/-}$). In addition to this, the establishment and optimization of primary kidney proximal tubule cells combined with the targeted knock-down of selected amino acid transporters should also be considered as an alternative valuable tool to gather new insights into the mechanism and regulation of amino acid transport in the kidney.

6.3 Regulation of amino acid transporters

Amino acids play important roles in a plethora of different physiological process; therefore, their concentration need to be constantly regulated depending on the nutritional availability. This regulation is known to involve different metabolic pathways and physiological responses, where amino acid transporters play a central role. System A for example, is known to be influenced by hormones such as glucocorticoids, glucagon and insulin (Fehlmann *et al.*, 1979; Varoqui & Erickson, 2002) via PKA and CREB pathways (Tovar *et al.*, 2000; Hyde *et al.*, 2007). Along the same line, the amino acid transporter LAT1 is known to be regulated in activated T cells via the AP-1 and NF-κB pathways (Hayashi *et al.*, 2013). Finally, considering the amino acid intake at the level of the small intestine, B°AT1 has been shown to be regulated by glutamine and leptin in isolated rat everted gut sacs both at the mRNA and protein level (Ducroc *et al.*, 2010). This finding complements a well-documented list of nutrient transporters regulated by leptin, i.e. MCT-1 (Buyse *et al.*, 2002), PepT1 (Buyse *et al.*, 2001), GLUT2, GLUT5 (Sakar *et al.*, 2009) and SGLT1 (Lostao *et al.*, 1998; Ducroc *et al.*, 2005). The leptin response involves both the MAPK pathway as well as JAK2 (Morris & Rui, 2009) and experiments performed in *X. laevis* oocytes suggest a possible regulation of B°AT1 function by JAK2 (Bhavsar *et al.*, 2011).

In our case, we aimed at understanding the regulation of LAT4 through phosphorylation at a specific serine 274 residue, which has been described in a large phosphoproteomic screening by Feric *et al.* (Feric *et al.*, 2011). We approached this issue by mutagenizing the target serine residue in an alanine residue (S274A), which cannot be phosphorylated, or a glutamate residue (S274E), which should on the other hand chemically mimic a phosphorylated serine. Preliminary data in *X. laevis* oocytes clearly indicated that the different mutants possessed difference in LAT4 function independently on the days of expression (Fig. 5.9). Subsequent transduction in MDCK cells confirmed these findings, but, interestingly, the different mutant constructs revealed a remarkable difference in total protein expression (Fig. 5.10). The pattern of protein expression was also not directly correlating with LAT4 function, since the S274E displayed the highest protein expression but the lowest function in MDCK cells and *X. laevis* oocytes. This raised the possibility of a different degree of LAT4 surface expression in the different mutants; but, unfortunately, we encountered technical problems with the surface biotinylation (Fig. 5.12) and analysis of LAT4 distribution with laser confocal microscope scanning did not reveal a major difference between the different mutants (Fig. 5.14). This observation highlights the possibility that the serine phosphorylation is not essentially influencing LAT4 intracellular distribution but rather its function at the membrane. This may involve on one side a direct influence of the negatively charged phosphate group on the protein structure and thereby rendering the amino acid binding site less accessible, or, on the other side, the binding of an inhibitory protein to the phosphorylated serine residue. To investigate this issue, future experiments should be aimed at identifying and comparing the LAT4-interacting proteins in the different cell lines by performing for instance co-immunoprecipitation studies. In this sense, the candidate protein for the inhibitory function should be highly enriched in the co-immunoprecipitated fraction of the S274E mutant; whereas, it should be absent or present in low concentration in the fraction of the S274A mutant. To finally prove the involvement of the candidate protein, specific knock-down studies in MDCK should be performed to see if the reduced LAT4 function in the S274E mutant can be reverted.

In addition to investigating signaling pathways downstream of the phosphorylation step, the identification of the responsible kinase represents as well a very important issue. Interestingly, analysis of the sequence surrounding the predicted phosphorylated serine

residue (VGRRLS^{274}) revealed a consensus sequence (VXRXXS) for the serine/threonine protein kinases D (PKDs). These kinases are downstream effectors of protein kinase C (PKC) and diacylglycerol (DAG) that mediate the actions of growth factors, hormones and neurotransmitters. Activated PKDs are known to be involved in different cellular mechanisms such as oxidative stress, cell motility, Golgi vesicle dynamics, transcription regulation and innate immunity (Fu & Rubin, 2011). To address the possible involvement of PKDs in LAT4 phosphorylation, preliminary studies should aim at clarifying the interaction between the kinases and the transporter with co-immunoprecipitation and co-immunofluorescence. In order to prove the functional implication of PKDs in LAT4 phosphorylation, a pivotal tool to establish is a phospho-specific anti LAT4 antibody, which could be used to quantify the amount of phosphorylated LAT4 in co-expression with different PKD isoforms in cell culture models. As a complement to these studies, one should also consider the use of PKD inhibitors (e.g. Gö6976) or siRNA-mediated knockdown of PKDs that would be expected to reduce the amount of phosphorylated LAT4.

Beyond the investigation of the cellular mechanisms leading to LAT4 phosphorylation, an essential point to elucidate is the physiological relevance and the implication of LAT4 regulation. In particular, experiments should be devoted to the specific identification of the physiological triggers (e.g. growth factors, hormones or other paracrine substances) and the functional consequences of LAT4 phosphorylation in the context of the whole body amino acid homestasis. Moreover, it is important to highlight, that some of the LAT4 substrates (i.e. branched-chain amino acids) represent important signaling molecules for the mTORC1-dependent pathway, which is known to play a central role in cell growth and division. Therefore, it is reasonable to hypothesize a functional cross-talk between mTORC1 and branched-chain amino acids, where LAT4 might play an important role.

7. References

Alberts B, Johnson A, Lewis J, Raff M, Roberts K & Walter P. (2002). *Molecular Biology of the Cell*. Garland Science, New York.

Alpern RJ, Caplan MJ & Moe OW. (2013). *Seldin and Giebisch's The Kidney*. London.

Babu E, Kanai Y, Chairoungdua A, Kim DK, Iribe Y, Tangtrongsup S, Jutabha P, Li Y, Ahmed N, Sakamoto S, Anzai N, Nagamori S & Endou H. (2003). Identification of a novel system L amino acid transporter structurally distinct from heterodimeric amino acid transporters. *J Biol Chem* **278,** 43838-43845.

Bannai S, Christensen HN, Vadgama JV, Ellory JC, Englesberg E, Guidotti GG, Gazzola GC, Kilberg MS, Lajtha A, Sacktor B & et al. (1984). Amino acid transport systems. *Nature* **311,** 308.

Barker G & Simmons NL. (1981). Identification of two strains of cultured canine renal epithelial cells (MDCK cells) which display entirely different physiological properties. *Q J Exp Physiol* **66,** 61-72.

Bauch C, Forster N, Loffing-Cueni D, Summa V & Verrey F. (2003). Functional cooperation of epithelial heteromeric amino acid transporters expressed in madin-darby canine kidney cells. *J Biol Chem* **278,** 1316-1322.

Bedford JJ & Leader JP. (1993). Response of tissues of the rat to anisosmolality in vivo. *Am J Physiol* **264,** R1164-1179.

Bello-Reuss E & Weber MR. (1986). Electrophysiological studies on primary cultures of proximal tubule cells. *Am J Physiol* **251,** F490-498.

Bertran J, Werner A, Stange G, Markovich D, Biber J, Testar X, Zorzano A, Palacin M & Murer H. (1992). Expression of Na(+)-independent amino acid transport in Xenopus laevis oocytes by injection of rabbit kidney cortex mRNA. *Biochem J* **281 (Pt 3),** 717-723.

Bhavsar SK, Hosseinzadeh Z, Merches K, Gu S, Broer S & Lang F. (2011). Stimulation of the amino acid transporter SLC6A19 by JAK2. *Biochem Biophys Res Commun* **414,** 456-461.

Biber J, Stieger B, Haase W & Murer H. (1981). A high yield preparation for rat kidney brush border membranes. Different behaviour of lysosomal markers. *Biochim Biophys Acta* **647,** 169-176.

Bodoy S, Fotiadis D, Stoeger C, Kanai Y & Palacin M. (2013). The small SLC43 family: facilitator system l amino acid transporters and the orphan EEG1. *Mol Aspects Med* **34,** 638-645.

Bodoy S, Martin L, Zorzano A, Palacin M, Estevez R & Bertran J. (2005). Identification of LAT4, a novel amino acid transporter with system L activity. *J Biol Chem* **280,** 12002-12011.

Bogatikov E, Munoz C, Pakladok T, Alesutan I, Shojaiefard M, Seebohm G, Foller M, Palmada M, Bohmer C, Broer S & Lang F. (2012). Up-regulation of amino acid transporter SLC6A19 activity and surface protein abundance by PKB/Akt and PIKfyve. *Cell Physiol Biochem* **30,** 1538-1546.

Bohmer C, Broer A, Munzinger M, Kowalczuk S, Rasko JE, Lang F & Broer S. (2005). Characterization of mouse amino acid transporter B0AT1 (slc6a19). *Biochem J* **389,** 745-751.

Boron WF & Boulpaep EL. (2005). *Medical Physiology*. Elsevier, Philadelphia.

Broer A, Klingel K, Kowalczuk S, Rasko JE, Cavanaugh J & Broer S. (2004). Molecular cloning of mouse amino acid transport system B0, a neutral amino acid transporter related to Hartnup disorder. *J Biol Chem* **279,** 24467-24476.

Broer S. (2008). Amino acid transport across mammalian intestinal and renal epithelia. *Physiol Rev* **88,** 249-286.

Broer S, Broer A & Hamprecht B. (1995). The 4F2hc surface antigen is necessary for expression of system L-like neutral amino acid-transport activity in C6-BU-1 rat glioma cells: evidence from expression studies in Xenopus laevis oocytes. *Biochem J* **312 (Pt 3),** 863-870.

Brosnan JT. (2003). Interorgan amino acid transport and its regulation. *J Nutr* **133,** 2068S-2072S.

Buyse M, Berlioz F, Guilmeau S, Tsocas A, Voisin T, Peranzi G, Merlin D, Laburthe M, Lewin MJ, Roze C & Bado A. (2001). PepT1-mediated epithelial transport of dipeptides and cephalexin is enhanced by luminal leptin in the small intestine. *J Clin Invest* **108,** 1483-1494.

Buyse M, Sitaraman SV, Liu X, Bado A & Merlin D. (2002). Luminal leptin enhances CD147/MCT-1-mediated uptake of butyrate in the human intestinal cell line Caco2-BBE. *J Biol Chem* **277,** 28182-28190.

Camargo SM, Makrides V, Virkki LV, Forster IC & Verrey F. (2005). Steady-state kinetic characterization of the mouse B(0)AT1 sodium-dependent neutral amino acid transporter. *Pflugers Arch* **451,** 338-348.

Camargo SM, Singer D, Makrides V, Huggel K, Pos KM, Wagner CA, Kuba K, Danilczyk U, Skovby F, Kleta R, Penninger JM & Verrey F. (2009). Tissue-specific amino acid transporter partners ACE2 and collectrin differentially interact with hartnup mutations. *Gastroenterology* **136,** 872-882.

Catterall WA. (1995). Structure and function of voltage-gated ion channels. *Annu Rev Biochem* **64,** 493-531.

Cheval L, Pierrat F, Dossat C, Genete M, Imbert-Teboul M, Duong Van Huyen JP, Poulain J, Wincker P, Weissenbach J, Piquemal D & Doucet A. (2011). Atlas of gene expression in the mouse kidney: new features of glomerular parietal cells. *Physiol Genomics* **43,** 161-173.

Christensen HN. (1989). Distinguishing amino acid transport systems of a given cell or tissue. *Methods Enzymol* **173,** 576-616.

Christensen HN. (1990). Role of amino acid transport and countertransport in nutrition and metabolism. *Physiol Rev* **70,** 43-77.

Christensen HN & Oxender DL. (1960). Transport of amino acids into and across cells. *Am J Clin Nutr***,** 131-136.

Cleal JK, Glazier JD, Ntani G, Crozier SR, Day PE, Harvey NC, Robinson SM, Cooper C, Godfrey KM, Hanson MA & Lewis RM. Facilitated transporters mediate net efflux of amino acids to the fetus across the basal membrane of the placental syncytiotrophoblast. *J Physiol* **589,** 987-997.

Clugston SL, Sieber SA, Marahiel MA & Walsh CT. (2003). Chirality of peptide bond-forming condensation domains in nonribosomal peptide synthetases: the C5 domain of tyrocidine synthetase is a (D)C(L) catalyst. *Biochemistry* **42,** 12095-12104.

Costa CC, de Almeida IT, Jakobs C, Poll-The BT & Duran M. (1999). Dynamic changes of plasma acylcarnitine levels induced by fasting and sunflower oil challenge test in children. *Pediatr Res* **46,** 440-444.

Cutillas PR, Biber J, Marks J, Jacob R, Stieger B, Cramer R, Waterfield M, Burlingame AL & Unwin RJ. (2005). Proteomic analysis of plasma membrane vesicles isolated from the rat renal cortex. *Proteomics* **5,** 101-112.

Dall'Asta V, Franchi-Gazzola R, Bussolati O, Sala R, Rotoli BM, Rossi PA, Uggeri J, Belletti S, Visigalli R & Gazzola GC. (1996). Modulation of transport systems for neutral and anionic amino acids in mesenchymal cells. *Biochem Soc Trans* **24,** 864-869.

Dall'Asta V, Rossi PA, Bussolati O & Gazzola GC. (1994). Response of human fibroblasts to hypertonic stress. Cell shrinkage is counteracted by an enhanced active transport of neutral amino acids. *J Biol Chem* **269,** 10485-10491.

Danilczyk U, Sarao R, Remy C, Benabbas C, Stange G, Richter A, Arya S, Pospisilik JA, Singer D, Camargo SM, Makrides V, Ramadan T, Verrey F, Wagner CA & Penninger JM. (2006). Essential role for collectrin in renal amino acid transport. *Nature* **444,** 1088-1091.

Datta A, Bryant DM & Mostov KE. (2011). Molecular regulation of lumen morphogenesis. *Curr Biol* **21,** R126-136.

Dave MH, Schulz N, Zecevic M, Wagner CA & Verrey F. (2004). Expression of heteromeric amino acid transporters along the murine intestine. *J Physiol* **558,** 597-610.

DeLisle S, Blondel O, Longo FJ, Schnabel WE, Bell GI & Welsh MJ. (1996). Expression of inositol 1,4,5-trisphosphate receptors changes the Ca2+ signal of Xenopus oocytes. *Am J Physiol* **270,** C1255-1261.

DeLisle S, Marksberry EW, Bonnett C, Jenkins DJ, Potter BV, Takahashi M & Tanzawa K. (1997). Adenophostin A can stimulate Ca2+ influx without depleting the inositol 1,4,5-trisphosphate-sensitive Ca2+ stores in the Xenopus oocyte. *J Biol Chem* **272,** 9956-9961.

Deribe YL, Pawson T & Dikic I. Post-translational modifications in signal integration. *Nat Struct Mol Biol* **17,** 666-672.

Dewji GN. (1969). Kwashiorkor: a protein deficiency disease. *Nurs Times* **65,** 523-524.

Drummond MJ, Dreyer HC, Fry CS, Glynn EL & Rasmussen BB. (2009). Nutritional and contractile regulation of human skeletal muscle protein synthesis and mTORC1 signaling. *J Appl Physiol* **106,** 1374-1384.

Ducroc R, Guilmeau S, Akasbi K, Devaud H, Buyse M & Bado A. (2005). Luminal leptin induces rapid inhibition of active intestinal absorption of glucose mediated by sodium-glucose cotransporter 1. *Diabetes* **54,** 348-354.

Ducroc R, Sakar Y, Fanjul C, Barber A, Bado A & Lostao MP. (2010). Luminal leptin inhibits L-glutamine transport in rat small intestine: involvement of ASCT2 and B0AT1. *Am J Physiol Gastrointest Liver Physiol* **299,** G179-185.

Dumont JN. (1972). Oogenesis in Xenopus laevis (Daudin). I. Stages of oocyte development in laboratory maintained animals. *J Morphol* **136,** 153-179.

El-Kadi SW, Baldwin RLt, Sunny NE, Owens SL & Bequette BJ. (2006). Intestinal protein supply alters amino acid, but not glucose, metabolism by the sheep gastrointestinal tract. *J Nutr* **136,** 1261-1269.

Elliget KA & Trump BF. (1991). Primary cultures of normal rat kidney proximal tubule epithelial cells for studies of renal cell injury. *In Vitro Cell Dev Biol* **27A,** 739-748.

Evers J, Murer H & Kinne R. (1976). Phenylalanine uptake in isolated renal brush border vesicles. *Biochim Biophys Acta* **426,** 598-615.

Fehlmann M, Le Cam A & Freychet P. (1979). Insulin and glucagon stimulation of amino acid transport in isolated rat hepatocytes. Synthesis of a high affinity component of transport. *J Biol Chem* **254,** 10431-10437.

Feliubadalo L, Arbones ML, Manas S, Chillaron J, Visa J, Rodes M, Rousaud F, Zorzano A, Palacin M & Nunes V. (2003). Slc7a9-deficient mice develop cystinuria non-I and cystine urolithiasis. *Hum Mol Genet* **12,** 2097-2108.

Feric M, Zhao B, Hoffert JD, Pisitkun T & Knepper MA. (2011). Large-scale phosphoproteomic analysis of membrane proteins in renal proximal and distal tubule. *Am J Physiol Cell Physiol* **300,** C755-770.

Fernandez E, Torrents D, Chillaron J, Martin Del Rio R, Zorzano A & Palacin M. (2003). Basolateral LAT-2 has a major role in the transepithelial flux of L-cystine in the renal proximal tubule cell line OK. *J Am Soc Nephrol* **14,** 837-847.

Ferrell JE, Jr. (1999). Xenopus oocyte maturation: new lessons from a good egg. *Bioessays* **21,** 833-842.

Ferrell JE, Jr. & Machleder EM. (1998). The biochemical basis of an all-or-none cell fate switch in Xenopus oocytes. *Science* **280,** 895-898.

Fickert P, Zollner G, Fuchsbichler A, Stumptner C, Pojer C, Zenz R, Lammert F, Stieger B, Meier PJ, Zatloukal K, Denk H & Trauner M. (2001). Effects of ursodeoxycholic and cholic acid feeding on hepatocellular transporter expression in mouse liver. *Gastroenterology* **121,** 170-183.

Fincham DA, Mason DK & Young JD. (1985). Characterization of a novel Na+-independent amino acid transporter in horse erythrocytes. *Biochem J* **227,** 13-20.

Font-Llitjos M, Feliubadalo L, Espino M, Cleries R, Manas S, Frey IM, Puertas S, Colell G, Palomo S, Aranda J, Visa J, Palacin M & Nunes V. (2007). Slc7a9 knockout mouse is a good cystinuria model for antilithiasic pharmacological studies. *Am J Physiol Renal Physiol* **293,** F732-740.

Fu Y & Rubin CS. (2011). Protein kinase D: coupling extracellular stimuli to the regulation of cell physiology. *EMBO Rep* **12,** 785-796.

Fuchs BC & Bode BP. (2005). Amino acid transporters ASCT2 and LAT1 in cancer: partners in crime? *Semin Cancer Biol* **15,** 254-266.

Fukuhara D, Kanai Y, Chairoungdua A, Babu E, Bessho F, Kawano T, Akimoto Y, Endou H & Yan K. (2007). Protein characterization of NA+-independent system L amino acid transporter 3 in mice: a potential role in supply of branched-chain amino acids under nutrient starvation. *Am J Pathol* **170,** 888-898.

Furuse M, Furuse K, Sasaki H & Tsukita S. (2001). Conversion of zonulae occludentes from tight to leaky strand type by introducing claudin-2 into Madin-Darby canine kidney I cells. *J Cell Biol* **153,** 263-272.

Garlick PJ. (2005). The role of leucine in the regulation of protein metabolism. *J Nutr* **135,** 1553S-1556S.

Gleeson M. (2005). Interrelationship between physical activity and branched-chain amino acids. *J Nutr* **135,** 1591S-1595S.

Gomeza J, Ohno K, Hulsmann S, Armsen W, Eulenburg V, Richter DW, Laube B & Betz H. (2003). Deletion of the mouse glycine transporter 2 results in a hyperekplexia phenotype and postnatal lethality. *Neuron* **40,** 797-806.

Green IJ. (1962). Serial propagation of influenza B (Lee) virus in a transmissible line of canine kidney cells. *Science* **138,** 42-43.

Gropper SS, Smith JL & Groff JL. (2009). *Advanced nutrition and human metabolism*. Belmont.

Gurdon JB, Lane CD, Woodland HR & Marbaix G. (1971). Use of frog eggs and oocytes for the study of messenger RNA and its translation in living cells. *Nature* **233,** 177-182.

Halestrap AP & Meredith D. (2004). The SLC16 gene family-from monocarboxylate transporters (MCTs) to aromatic amino acid transporters and beyond. *Pflugers Arch* **447,** 619-628.

Hansson GC, Simons K & van Meer G. (1986). Two strains of the Madin-Darby canine kidney (MDCK) cell line have distinct glycosphingolipid compositions. *EMBO J* **5,** 483-489.

Hayashi K, Jutabha P, Endou H, Sagara H & Anzai N. (2013). LAT1 is a critical transporter of essential amino acids for immune reactions in activated human T cells. *J Immunol* **191,** 4080-4085.

Heck SD, Faraci WS, Kelbaugh PR, Saccomano NA, Thadeio PF & Volkmann RA. (1996). Posttranslational amino acid epimerization: enzyme-catalyzed isomerization of amino acid residues in peptide chains. *Proc Natl Acad Sci U S A* **93,** 4036-4039.

Hediger MA, Romero MF, Peng JB, Rolfs A, Takanaga H & Bruford EA. (2004). The ABCs of solute carriers: physiological, pathological and therapeutic implications of human membrane transport proteinsIntroduction. *Pflugers Arch* **447,** 465-468.

Hellsten U, Harland RM, Gilchrist MJ, Hendrix D, Jurka J, Kapitonov V, Ovcharenko I, Putnam NH, Shu S, Taher L, Blitz IL, Blumberg B, Dichmann DS, Dubchak I, Amaya E, Detter JC, Fletcher R, Gerhard DS, Goodstein D, Graves T, Grigoriev IV, Grimwood J, Kawashima T, Lindquist E, Lucas SM, Mead PE, Mitros T, Ogino H, Ohta Y, Poliakov AV, Pollet N, Robert J, Salamov A, Sater AK, Schmutz J, Terry A, Vize PD, Warren WC, Wells D, Wills A, Wilson RK, Zimmerman LB, Zorn AM, Grainger R, Grammer T, Khokha MK, Richardson PM & Rokhsar DS. (2010). The genome of the Western clawed frog Xenopus tropicalis. *Science* **328,** 633-636.

Hoffmann EK & Simonsen LO. (1989). Membrane mechanisms in volume and pH regulation in vertebrate cells. *Physiol Rev* **69,** 315-382.

Hu Y, Smith DE, Ma K, Jappar D, Thomas W & Hillgren KM. (2008). Targeted disruption of peptide transporter Pept1 gene in mice significantly reduces dipeptide absorption in intestine. *Mol Pharm* **5,** 1122-1130.

Huq F, Thompson M & Ruell P. (1993). Changes in serum amino acid concentrations during prolonged endurance running. *Jpn J Physiol* **43,** 797-807.

Husted RF, Welsh MJ & Stokes JB. (1986). Variability of functional characteristics of MDCK cells. *Am J Physiol* **250,** C214-221.

Hyde R, Cwiklinski EL, MacAulay K, Taylor PM & Hundal HS. (2007). Distinct sensor pathways in the hierarchical control of SNAT2, a putative amino acid transceptor, by amino acid availability. *J Biol Chem* **282,** 19788-19798.

Imai Y, Kuba K, Rao S, Huan Y, Guo F, Guan B, Yang P, Sarao R, Wada T, Leong-Poi H, Crackower MA, Fukamizu A, Hui CC, Hein L, Uhlig S, Slutsky AS, Jiang C & Penninger JM. (2005). Angiotensin-converting enzyme 2 protects from severe acute lung failure. *Nature* **436,** 112-116.

Ji LL, Miller RH, Nagle FJ, Lardy HA & Stratman FW. (1987). Amino acid metabolism during exercise in trained rats: the potential role of carnitine in the metabolic fate of branched-chain amino acids. *Metabolism* **36,** 748-752.

Kanai Y & Hediger MA. (1992). Primary structure and functional characterization of a high-affinity glutamate transporter. *Nature* **360,** 467-471.

Kaplan MR, Plotkin MD, Lee WS, Xu ZC, Lytton J & Hebert SC. (1996). Apical localization of the Na-K-Cl cotransporter, rBSC1, on rat thick ascending limbs. *Kidney Int* **49,** 40-47.

Kilberg MS, Handlogten ME & Christensen HN. (1980). Characteristics of an amino acid transport system in rat liver for glutamine, asparagine, histidine, and closely related analogs. *J Biol Chem* **255,** 4011-4019.

Kim DK, Kanai Y, Chairoungdua A, Matsuo H, Cha SH & Endou H. (2001). Expression cloning of a Na+-independent aromatic amino acid transporter with structural similarity to H+/monocarboxylate transporters. *J Biol Chem* **276,** 17221-17228.

Kleta R, Romeo E, Ristic Z, Ohura T, Stuart C, Arcos-Burgos M, Dave MH, Wagner CA, Camargo SR, Inoue S, Matsuura N, Helip-Wooley A, Bockenhauer D, Warth R, Bernardini I, Visser G, Eggermann T, Lee P, Chairoungdua A, Jutabha P, Babu E, Nilwarangkoon S, Anzai N, Kanai Y, Verrey F, Gahl WA & Koizumi A. (2004). Mutations in SLC6A19, encoding B0AT1, cause Hartnup disorder. *Nat Genet* **36,** 999-1002.

Konz D & Marahiel MA. (1999). How do peptide synthetases generate structural diversity? *Chem Biol* **6,** R39-48.

Kuba K, Imai Y, Rao S, Gao H, Guo F, Guan B, Huan Y, Yang P, Zhang Y, Deng W, Bao L, Zhang B, Liu G, Wang Z, Chappell M, Liu Y, Zheng D, Leibbrandt A, Wada T, Slutsky AS, Liu D, Qin C, Jiang C & Penninger JM. (2005). A crucial role of angiotensin converting enzyme 2 (ACE2) in SARS coronavirus-induced lung injury. *Nat Med* **11,** 875-879.

Lang F, Busch GL, Ritter M, Volkl H, Waldegger S, Gulbins E & Haussinger D. (1998). Functional significance of cell volume regulatory mechanisms. *Physiol Rev* **78,** 247-306.

Layman DK & Walker DA. (2006). Potential importance of leucine in treatment of obesity and the metabolic syndrome. *J Nutr* **136,** 319S-323S.

Lodish H, Berk A, Kaiser CA, Krieger M, Scott MP, Bretscher A, Ploegh H & Matsudaira P. (2008). *Molecular Cell Biology*. W.H. Freeman and Company, England.

Loffing J, Vallon V, Loffing-Cueni D, Aregger F, Richter K, Pietri L, Bloch-Faure M, Hoenderop JG, Shull GE, Meneton P & Kaissling B. (2004). Altered renal distal tubule structure and renal Na(+) and Ca(2+) handling in a mouse model for Gitelman's syndrome. *J Am Soc Nephrol* **15,** 2276-2288.

Lostao MP, Urdaneta E, Martinez-Anso E, Barber A & Martinez JA. (1998). Presence of leptin receptors in rat small intestine and leptin effect on sugar absorption. *FEBS Lett* **423,** 302-306.

Lynch CJ. (2001). Role of leucine in the regulation of mTOR by amino acids: revelations from structure-activity studies. *J Nutr* **131,** 861S-865S.

Makrides V, Simone, S.M.R., Verrey, F. . (2014). Transport of amino acids in the kidney. In *Comprehensive Physiology*, ed. Terjung R, pp. 367-403. John Wiley & Sons, Hoboken, NJ, USA.

Maller JL, Butcher FR & Krebs EG. (1979). Early effect of progesterone on levels of cyclic adenosine 3':5'-monophosphate in Xenopus oocytes. *J Biol Chem* **254,** 579-582.

Mann M & Jensen ON. (2003). Proteomic analysis of post-translational modifications. *Nat Biotechnol* **21,** 255-261.

Mariotta L, Ramadan T, Singer D, Guetg A, Herzog B, Stoeger C, Palacin M, Lahoutte T, Camargo SM & Verrey F. (2012). T-type amino acid transporter TAT1 (Slc16a10) is essential for extracellular aromatic amino acid homeostasis control. *J Physiol* **590,** 6413-6424.

Mastroberardino L, Spindler B, Pfeiffer R, Skelly PJ, Loffing J, Shoemaker CB & Verrey F. (1998). Amino-acid transport by heterodimers of 4F2hc/CD98 and members of a permease family. *Nature* **395,** 288-291.

Matthews DE, Marano MA & Campbell RG. (1993). Splanchnic bed utilization of glutamine and glutamic acid in humans. *Am J Physiol* **264,** E848-854.

Meier C, Ristic Z, Klauser S & Verrey F. (2002). Activation of system L heterodimeric amino acid exchangers by intracellular substrates. *EMBO J* **21,** 580-589.

Mishina M, Kurosaki T, Tobimatsu T, Morimoto Y, Noda M, Yamamoto T, Terao M, Lindstrom J, Takahashi T, Kuno M & et al. (1984). Expression of functional acetylcholine receptor from cloned cDNAs. *Nature* **307,** 604-608.

Moret C, Dave MH, Schulz N, Jiang JX, Verrey F & Wagner CA. (2007). Regulation of renal amino acid transporters during metabolic acidosis. *Am J Physiol Renal Physiol* **292,** F555-566.

Morris DL & Rui L. (2009). Recent advances in understanding leptin signaling and leptin resistance. *Am J Physiol Endocrinol Metab* **297,** E1247-1259.

Morris SM, Jr. (2006). Arginine: beyond protein. *Am J Clin Nutr* **83,** 508S-512S.

Nagasawa T, Kido T, Yoshizawa F, Ito Y & Nishizawa N. (2002). Rapid suppression of protein degradation in skeletal muscle after oral feeding of leucine in rats. *J Nutr Biochem* **13,** 121-127.

Naito M. (2008). Macrophage differentiation and function in health and disease. *Pathol Int* **58,** 143-155.

Nakamura E, Sato M, Yang H, Miyagawa F, Harasaki M, Tomita K, Matsuoka S, Noma A, Iwai K & Minato N. (1999). 4F2 (CD98) heavy chain is associated covalently with an amino acid transporter and controls intracellular trafficking and membrane topology of 4F2 heterodimer. *J Biol Chem* **274,** 3009-3016.

Nassl AM, Rubio-Aliaga I, Fenselau H, Marth MK, Kottra G & Daniel H. Amino acid absorption and homeostasis in mice lacking the intestinal peptide transporter PEPT1. *Am J Physiol Gastrointest Liver Physiol* **301,** G128-137.

Nicklin P, Bergman P, Zhang B, Triantafellow E, Wang H, Nyfeler B, Yang H, Hild M, Kung C, Wilson C, Myer VE, MacKeigan JP, Porter JA, Wang YK, Cantley LC, Finan PM & Murphy LO. (2009). Bidirectional transport of amino acids regulates mTOR and autophagy. *Cell* **136,** 521-534.

Nielsen S, Chou CL, Marples D, Christensen EI, Kishore BK & Knepper MA. (1995). Vasopressin increases water permeability of kidney collecting duct by inducing translocation of aquaporin-CD water channels to plasma membrane. *Proc Natl Acad Sci U S A* **92,** 1013-1017.

Nielsen S, Frokiaer J, Marples D, Kwon TH, Agre P & Knepper MA. (2002). Aquaporins in the kidney: from molecules to medicine. *Physiol Rev* **82,** 205-244.

Nishimura M & Naito S. (2005). Tissue-specific mRNA expression profiles of human ATP-binding cassette and solute carrier transporter superfamilies. *Drug Metab Pharmacokinet* **20,** 452-477.

Ogier de Baulny H & Saudubray JM. (2002). Branched-chain organic acidurias. *Semin Neonatol* **7,** 65-74.

Olson AL & Pessin JE. (1996). Structure, function, and regulation of the mammalian facilitative glucose transporter gene family. *Annu Rev Nutr* **16,** 235-256.

Oxender DL & Christensen HN. (1963). Distinct Mediating Systems for the Transport of Neutral Amino Acids by the Ehrlich Cell. *J Biol Chem* **238,** 3686-3699.

Palacin M, Estevez R, Bertran J & Zorzano A. (1998). Molecular biology of mammalian plasma membrane amino acid transporters. *Physiol Rev* **78,** 969-1054.

Parmacek MS, Karpinski BA, Gottesdiener KM, Thompson CB & Leiden JM. (1989). Structure, expression and regulation of the murine 4F2 heavy chain. *Nucleic Acids Res* **17,** 1915-1931.

Parys JB, Sernett SW, DeLisle S, Snyder PM, Welsh MJ & Campbell KP. (1992). Isolation, characterization, and localization of the inositol 1,4,5-trisphosphate receptor protein in Xenopus laevis oocytes. *J Biol Chem* **267,** 18776-18782.

Peghini P, Janzen J & Stoffel W. (1997). Glutamate transporter EAAC-1-deficient mice develop dicarboxylic aminoaciduria and behavioral abnormalities but no neurodegeneration. *EMBO J* **16,** 3822-3832.

Perkins CP, Mar V, Shutter JR, del Castillo J, Danilenko DM, Medlock ES, Ponting IL, Graham M, Stark KL, Zuo Y, Cunningham JM & Bosselman RA. (1997). Anemia and perinatal death result from loss of the murine ecotropic retrovirus receptor mCAT-1. *Genes Dev* **11,** 914-925.

Peters T, Thaete C, Wolf S, Popp A, Sedlmeier R, Grosse J, Nehls MC, Russ A & Schlueter V. (2003). A mouse model for cystinuria type I. *Hum Mol Genet* **12,** 2109-2120.

Pieczynski J & Margolis B. (2011). Protein complexes that control renal epithelial polarity. *Am J Physiol Renal Physiol* **300,** F589-601.

Pineda M, Fernandez E, Torrents D, Estevez R, Lopez C, Camps M, Lloberas J, Zorzano A & Palacin M. (1999). Identification of a membrane protein, LAT-2, that Co-expresses with 4F2 heavy chain, an L-type amino acid transport activity with broad specificity for small and large zwitterionic amino acids. *J Biol Chem* **274,** 19738-19744.

Puoti A, May A, Rossier BC & Horisberger JD. (1997). Novel isoforms of the beta and gamma subunits of the Xenopus epithelial Na channel provide information about the amiloride binding site and extracellular sodium sensing. *Proc Natl Acad Sci U S A* **94,** 5949-5954.

Ramadan T, Camargo SM, Herzog B, Bordin M, Pos KM & Verrey F. (2007). Recycling of aromatic amino acids via TAT1 allows efflux of neutral amino acids via LAT2-4F2hc exchanger. *Pflugers Arch* **454,** 507-516.

Ramadan T, Camargo SM, Summa V, Hunziker P, Chesnov S, Pos KM & Verrey F. (2006). Basolateral aromatic amino acid transporter TAT1 (Slc16a10) functions as an efflux pathway. *J Cell Physiol* **206,** 771-779.

Richardson JC, Scalera V & Simmons NL. (1981). Identification of two strains of MDCK cells which resemble separate nephron tubule segments. *Biochim Biophys Acta* **673,** 26-36.

Ristic Z, Camargo SM, Romeo E, Bodoy S, Bertran J, Palacin M, Makrides V, Furrer EM & Verrey F. (2006). Neutral amino acid transport mediated by ortholog of imino acid transporter SIT1/SLC6A20 in opossum kidney cells. *Am J Physiol Renal Physiol* **290,** F880-887.

Rossier G, Meier C, Bauch C, Summa V, Sordat B, Verrey F & Kuhn LC. (1999). LAT2, a new basolateral 4F2hc/CD98-associated amino acid transporter of kidney and intestine. *J Biol Chem* **274,** 34948-34954.

Rubio-Aliaga I, Frey I, Boll M, Groneberg DA, Eichinger HM, Balling R & Daniel H. (2003). Targeted disruption of the peptide transporter Pept2 gene in mice defines its physiological role in the kidney. *Mol Cell Biol* **23,** 3247-3252.

Rutter AR, Fradley RL, Garrett EM, Chapman KL, Lawrence JM, Rosahl TW & Patel S. (2007). Evidence from gene knockout studies implicates Asc-1 as the primary transporter mediating d-serine reuptake in the mouse CNS. *Eur J Neurosci* **25,** 1757-1766.

Sakar Y, Nazaret C, Letteron P, Ait Omar A, Avenati M, Viollet B, Ducroc R & Bado A. (2009). Positive regulatory control loop between gut leptin and intestinal GLUT2/GLUT5 transporters links to hepatic metabolic functions in rodents. *PLoS One* **4,** e7935.

Schimassek H & Gerok W. (1965). Control of the levels of free amino acids in plasma by the liver. *Biochem Z* **343,** 407-415.

Sheng M & Pak DT. (2000). Ligand-gated ion channel interactions with cytoskeletal and signaling proteins. *Annu Rev Physiol* **62,** 755-778.

Sheridan AM, Schwartz JH, Kroshian VM, Tercyak AM, Laraia J, Masino S & Lieberthal W. (1993). Renal mouse proximal tubular cells are more susceptible than MDCK cells to chemical anoxia. *Am J Physiol* **265,** F342-350.

Shigeoka T, Kawaichi M & Ishida Y. (2005). Suppression of nonsense-mediated mRNA decay permits unbiased gene trapping in mouse embryonic stem cells. *Nucleic Acids Res* **33,** e20.

Shoveller AK, Stoll B, Ball RO & Burrin DG. (2005). Nutritional and functional importance of intestinal sulfur amino acid metabolism. *J Nutr* **135,** 1609-1612.

Simmons NL. (1982). Cultured monolayers of MDCK cells: a novel model system for the study of epithelial development and function. *Gen Pharmacol* **13,** 287-291.

Sperandeo MP, Annunziata P, Bozzato A, Piccolo P, Maiuri L, D'Armiento M, Ballabio A, Corso G, Andria G, Borsani G & Sebastio G. (2007). Slc7a7 disruption causes fetal

growth retardation by downregulating Igf1 in the mouse model of lysinuric protein intolerance. *Am J Physiol Cell Physiol* **293,** C191-198.

Steed E, Balda MS & Matter K. (2010). Dynamics and functions of tight junctions. *Trends Cell Biol* **20,** 142-149.

Stevens BR, Ross HJ & Wright EM. (1982). Multiple transport pathways for neutral amino acids in rabbit jejunal brush border vesicles. *J Membr Biol* **66,** 213-225.

Stoll B, Henry J, Reeds PJ, Yu H, Jahoor F & Burrin DG. (1998). Catabolism dominates the first-pass intestinal metabolism of dietary essential amino acids in milk protein-fed piglets. *J Nutr* **128,** 606-614.

Strauss KA, Puffenberger EG & Morton DH. (1993). Maple Syrup Urine Disease.

Tamma G, Procino G, Mola MG, Svelto M & Valenti G. (2008). Functional involvement of Annexin-2 in cAMP induced AQP2 trafficking. *Pflugers Arch* **456,** 729-736.

Taylor MA & Smith LD. (1987). Accumulation of free amino acids in growing Xenopus laevis oocytes. *Dev Biol* **124,** 287-290.

Terryn S, Jouret F, Vandenabeele F, Smolders I, Moreels M, Devuyst O, Steels P & Van Kerkhove E. (2007). A primary culture of mouse proximal tubular cells, established on collagen-coated membranes. *Am J Physiol Renal Physiol* **293,** F476-485.

Tovar AR, Avila E, DeSantiago S & Torres N. (2000). Characterization of methylaminoisobutyric acid transport by system A in rat mammary gland. *Metabolism* **49,** 873-879.

Trinh-Trang-Tan MM, Bouby N, Kriz W & Bankir L. (1987). Functional adaptation of thick ascending limb and internephron heterogeneity to urine concentration. *Kidney Int* **31,** 549-555.

Tsumura H, Suzuki N, Saito H, Kawano M, Otake S, Kozuka Y, Komada H, Tsurudome M & Ito Y. (2003). The targeted disruption of the CD98 gene results in embryonic lethality. *Biochem Biophys Res Commun* **308,** 847-851.

Turk E, Martin MG & Wright EM. (1994). Structure of the human Na+/glucose cotransporter gene SGLT1. *J Biol Chem* **269,** 15204-15209.

Uezono Y, Bradley J, Min C, McCarty NA, Quick M, Riordan JR, Chavkin C, Zinn K, Lester HA & Davidson N. (1993). Receptors that couple to 2 classes of G proteins increase cAMP and activate CFTR expressed in Xenopus oocytes. *Receptors Channels* **1,** 233-241.

van de Poll MC, Soeters PB, Deutz NE, Fearon KC & Dejong CH. (2004). Renal metabolism of amino acids: its role in interorgan amino acid exchange. *Am J Clin Nutr* **79,** 185-197.

Van Slyke DD & Meyer GM. (1913). The fate of protein digestion products in the body. III. The absorption of amino acids from the blood by tissues. *The Journal of Biological Chemistry* **XVI**.

Varoqui H & Erickson JD. (2002). Selective up-regulation of system a transporter mRNA in diabetic liver. *Biochem Biophys Res Commun* **290,** 903-908.

Verrey F, Jack DL, Paulsen IT, Saier MH, Jr. & Pfeiffer R. (1999). New glycoprotein-associated amino acid transporters. *J Membr Biol* **172,** 181-192.

Voet D, Voet JG & Pratt CW. (2006). *Fundamentals of Biochemistry*. Wiley, Danvers.

Wada M, Tamura A, Takahashi N & Tsukita S. (2013). Loss of claudins 2 and 15 from mice causes defects in paracellular Na+ flow and nutrient transport in gut and leads to death from malnutrition. *Gastroenterology* **144,** 369-380.

Wagner CA, Ott M, Klingel K, Beck S, Melzig J, Friedrich B, Wild KN, Broer S, Moschen I, Albers A, Waldegger S, Tummler B, Egan ME, Geibel JP, Kandolf R & Lang F. (2001). Effects of the serine/threonine kinase SGK1 on the epithelial Na(+) channel (ENaC) and CFTR: implications for cystic fibrosis. *Cell Physiol Biochem* **11,** 209-218.

Wallace RA & Dumont JN. (1968). The induced synthesis and transport of yolk proteins and their accumulation by the oocyte in Xenopus laevis. *J Cell Physiol* **72,** Suppl 1:73-89.

Wallace RA & Jared DW. (1969). Studies on amphibian yolk. 8. The estrogen-induced hepatic synthesis of a serum lipophosphoprotein and its selective uptake by the ovary and trasformation into yolk platelet proteins in Xenopus laevis. *Dev Biol* **19,** 498-526.

Wells RG, Lee WS, Kanai Y, Leiden JM & Hediger MA. (1992). The 4F2 antigen heavy chain induces uptake of neutral and dibasic amino acids in Xenopus oocytes. *J Biol Chem* **267,** 15285-15288.

Williams CD, Oxon BM & Lond H. (2003). Kwashiorkor: a nutritional disease of children associated with a maize diet. 1935. *Bull World Health Organ* **81,** 912-913.

Wolfsdorf JI, Sadeghi-Nejad A & Senior B. (1982). Hypoalaninemia and ketotic hypoglycemia: cause or consequence? *Eur J Pediatr* **138,** 28-31.

Wu G. (2009). Amino acids: metabolism, functions, and nutrition. *Amino Acids* **37,** 1-17.

Xie X, Dumas T, Tang L, Brennan T, Reeder T, Thomas W, Klein RD, Flores J, O'Hara BF, Heller HC & Franken P. (2005). Lack of the alanine-serine-cysteine transporter 1 causes tremors, seizures, and early postnatal death in mice. *Brain Res* **1052,** 212-221.

Zimmer G, Lottspeich F, Maisner A, Klenk HD & Herrler G. (1997). Molecular characterization of gp40, a mucin-type glycoprotein from the apical plasma membrane of Madin-Darby canine kidney cells (type I). *Biochem J* **326 (Pt 1),** 99-108.

8. Curriculum vitae

PERSONAL INFORMATION

Adriano Guetg
adriano.guetg@gmail.com

Schaffhauserstrasse 374
8050 Zürich
+41 79 547 76 43

05.07.1986
Single
Swiss citizenship

EDUCATION

2010 – present **PhD studies in Integrative Molecular Medicine**, University of Zurich

- Title of the thesis: "Cooperation of basolateral amino acid transporters". Supervised by Prof. Dr. med. François Verrey.

2008 – 2009 **Master of Science in Biology**, University of Zurich

- Focus: Human Biology
- Title of the thesis: "Collagen glycosylation in adiponectin and mannose-binding lectin function". Supervised by Prof. Dr. Thierry Hennet.

2005 – 2008 **Bachelor of Science in Biology**, University of Zurich

LANGUAGES

Italian	mother language
German	advanced level, C1 (European standard)
English	advanced level, C1 (European standard)
French	basic level, B2 (European standard)

LABORATORY SKILLS

- Molecular biology (site-directed mutagenesis, cloning, DNA and RNA extraction, Taq-Man qPCR, *in vitro* RNA transcription)
- Biochemistry (expression and purification of proteins, Western blotting, SDS-PAGE, Immunocytochemistry, tracing assays with radioactive isotopes)
- Cell culture (HeLa, MDCK, HEK, Caco2, HepG2, 3T3-L1)
- *Xenopus laevis* oocytes expression system (oocytes sorting and RNA microinjection)
- Mouse models (FELASA Category B)

FELLOWSHIPS AND AWARDS

2012	Young investigator award of the Oetliker Foundation for Physiology for the best poster presentation
2011	Swiss Physiological Society travel grant

PUBLICATION LIST

- Torrente M, **Guetg A**, Arps L, Rückstuhl L, Camargo SM and Verrey F (2014). Mycoplasma-induced arginine depletion triggers GCN2-mediated gene regulation in MDCK cells. *PLOS One*. Submitted.
- **Guetg A**, Mariotta L, Bock L, Herzog B, Fingerhut R, Camargo SM and Verrey F (2014). Amino acid transporter Lat4 (*Slc43a2)* is essential for mice postnatal development. *J Physiol*. In revision.
- Mariotta L, Ramadan T, Singer D, **Guetg A**, Herzog B, Stöger C, Palacin M, Lahoutte T, Camargo SM and Verrey F (2012). T-type amino acid transporter TAT1 (Slc16a10) is essential for extracellular aromatic amino acid homeostasis control. *J Physiol*

9. Acknowledgements

First of all, I want to thank my supervisor Prof. Dr. François Verrey for giving me the possibility to work in his lab and providing new scientific inputs and ideas during our weekly “jour fixe”. Many thanks also to the other members of my PhD thesis committee, Prof. Dr. Olivier Devuyst and Prof. Dr. Bernard Thorens, for the scientific discussions and suggestions during these years.

I would like to thank Simone for always providing a patient ear for listening to my technical troubles and motivating me to be perseverant.

Many thanks to Brigitte for his help and support during experiments and for organizing great nourishment packages during my army services.

I particularly want to thank Marta for all the great chats and funny moments we shared during these years. I will always remember her for the endless help, support and her great laboratory skills that are secondary only to her outstanding cooking skills!

I also would like to sincerely thank the present and past members of the Verrey group: Luca for introducing and helping me with the mice work and for his constant help; Josua, for the great US trips and the scientific discussions we had together; Lukas, for being a superb apprentice; Carlos, for being a highly motivating gym-partner; Alok, for the constant paprika chips supply; Julia, for the nice time shared together and the help with german translations; Nadine, Tina, Raphael, Katja, Sandra, Chiara, Lorenz, Olga, Nicola, Monica, Stine, Ian, Vicky, Liviu, Sam, Elena, Emilia, Evelyne, Lalita, Eva, Helen and Laura for creating such a pleasant atmosphere during these years.

Special thanks to Christian Lutz for providing a great support especially at the beginning of my PhD and to Selene Araya for always be such a positive person and bringing some sunshine in the lab.

Thanks to Christoph Rutschmann for the precious advices in molecular cloning.

I would like to thank also my great friends from Ticino: especially, Claudio, Simone, Simona, Andrea, Bobby, Fabrizio, Raffael and Mateo for sharing funny week-ends that helped smoothing the stress accumulated during the week. Thanks a lot guys! I feel really lucky to be your friend.

I would like to express my greatest thanks to my family. Thanks to my father Doriano and my mother Giglia for their constant support and love. Thanks to my aunt and “vice-mother” Alba together with my uncle Piero for the beautiful discussions we shared and the great time in New York. Thanks to my brothers Fabio and Luca for being just as great as they are! Finally, a very special thanks to Iside for rendering my life as beautiful as it is!